Rocketdyne
North American Rockwell

6633 Canoga Avenue.
Canoga Park, California 91304

SER 1159/RS21/1001

MODIFIED RS2101 ROCKET ENGINE STUDY PROGRAM FINAL REPORT

This work was performed for the Jet Propulsion Laboratory, California Institute of Technology, sponsored by the National Aeronautics and Space Administration under Contract NAS7-100.

PREPARED BY

RS21 PROJECT ENGINEERING

APPROVED BY

R. S. Martinez
RS21 Project Engineer
Small Engines Division

F. E. Campagna
Program Manager
Advanced Programs

WJR:nw
NO. OF PAGES 122

REVISIONS

DATE 7 December 1971

DATE	REV. BY	PAGES AFFECTED	REMARKS

FORM R18-G REV. 5-69

CONTENTS

APPENDICES

TABLES

FIGURES

FIGURES - Cont'd.

FIGURES - Cont'd.

REFERENCES

1. Lewis, Jr.: Metallurgical Analysis, RS-21 V-Seals, Rocketdyne Report MPTR70-904, dated 21 July 1970.

2. Bauer, Paul: Investigation Of Leakage And Sealing Parameters, Technical Report AFRPL-TR-153, IIT Research Institute, August 1965.

3. Laniewski, J.P.: Advanced Leakage Tests. Volume III of Final Report Under Contract NA5 8-4012. Design Criteria For Zero Leakage Connectors For Launch Vehicles, G. E., Schenectady, N.Y., 20 July 1967.

4. McFarland, B. L. and N. Barsic: Advanced Experimental Thrust Chamber Program (Phases III and IV), Final Report, Report R-7281, Rocketdyne, 1968.

5. McFarland, B. L. and T. Finkelstein: Thermal Analysis Procedure for Interegen Thrust Chambers Using the Boundary Layer Cooling (BLC) Subroutine with the Thermal Analyzer Program (TAP), Report LAP 69-564, Rocketdyne, 1969.

6. Margin Limits Tests - JPL Report, C. Dodge, 15 March 1970.

7. McFarland, B.L.: Results of Nozzle Contour Study of 80% Bell 40:1 Nozzles for 300 Lb. Thrust Interegen Thrust Chambers, 28 February 1969.

8. McFarland, B.L.: Additional Discussion of 80% Bell, 40:1 Nozzles for 300 Lb. Thrust Interegen Thrust Chambers, 4 March 1969.

9. McFarland, B.L. and V. Jaqua: NAS 3-12071 Final Report, Space Storable Thruster Investigation, NASA CR72827, R-8415.

10. Minami, H. and S. Persselin: SR 8111-3002, Finite Element Stress Analysis of Two Dimensional Structures with Orthotropic Temperature - Dependent Material Properties, 12 August 1968.

11. Modified RS2101 Rocket Engine Study, Final Review, 12 May 1971.

INTRODUCTION

In accordance with JPL Contract 953066, a Modified RS2101 Rocket Engine Study Program was conducted at Rocketdyne.

The purpose of the program was to perform design studies and analyses to determine the effects of incorporating a 60:1 expansion area ratio nozzle extension, extended firing time, and modified operating conditions and environments on the MM'71 rocket engine assembly. Also, an injector-to-thrust chamber seal study was conducted to define potential solutions for leakage past this joint.

This report presents the results of, and recommendations evolving from, the engine thermal analyses, the injector-to-thrust chamber seal studies, and the nozzle extension joint stress analyses.

ABSTRACT

This report describes the results of the Modifed RS2101 Engine Study Program conducted at Rocketdyne. Included in the program were an injector-to-thrust chamber seal study, modified engine thermal analysis, and structural analysis including dynamic modeling of the engine. The modified engine requirements include, in addition to a 60:1 expansion area ratio nozzle extension, extended firing times and revised operating and environmental requirements.

SUMMARY OF RESULTS

This report describes the results of the modified RS2101 engine study conducted at Rocketdyne between 14 January 1971 and 29 April 1971. Modifications to the MM'71 engine include incorporation of a 60:1 area ratio nozzle extension and modified operational and environmental requirements. Figure 1 shows the relative size of the 40:1 and 60:1 nozzles. The program involved three primary areas of effort. These were, an injector-to-thrust chamber seal design study, modified engine thermal analysis, and a structural analysis including dynamic modeling of the engine.

The purpose of the seal study was to perform design and material analyses to define potential solutions for leakage past the injector-to-thrust chamber seals. Included were a weighted trade-off comparison between candidate seals and material compatibility and performance investigations. As a result of this program, a seal configuration was recommended to JPL to solve the RS2101 engine injector-to-thrust chamber seal leakage problem. Additionally, the seal study was supplemented by full-scale engine leakage tests using the primary seal configuration and leak test procedures recommended as a result of this program.

Thermal analyses were conducted to determine the effects of replacing the 40:1 nozzle extension with one of 60:1 area ratio and increasing the longest burn from 900 seconds to 3000 seconds.

Analyses were performed which led to characterization of the modified RS2101 engine thermally. This was accomplished by first calibrating the analytical models with existing test data to define the proper model input parameters, and then using these models to predict the operational behavior of the modified engine in the spacecraft. This report describes both the model calibration results and predictions for the operational behavior of the modified engine.

Structural analyses were performed to determine the effects of the 60:1 nozzle and changed environmental and mission requirements on the thrust chamber-to-nozzle joint. In addition, the effects of the new MDC and thermal requirements on the beryllium throat cyclic life were estimated. As a result of these analyses, recommendations were made for an improved nut finger design and torquing procedure.

Studies showed that the 60:1 nozzle defined by Rocketdyne drawing AP-216-003-00 did not have optimum wall thickness to prevent buckling. A new nozzle design (Rocketdyne drawing RS000622E003-00) minimizing this tendency was prepared.

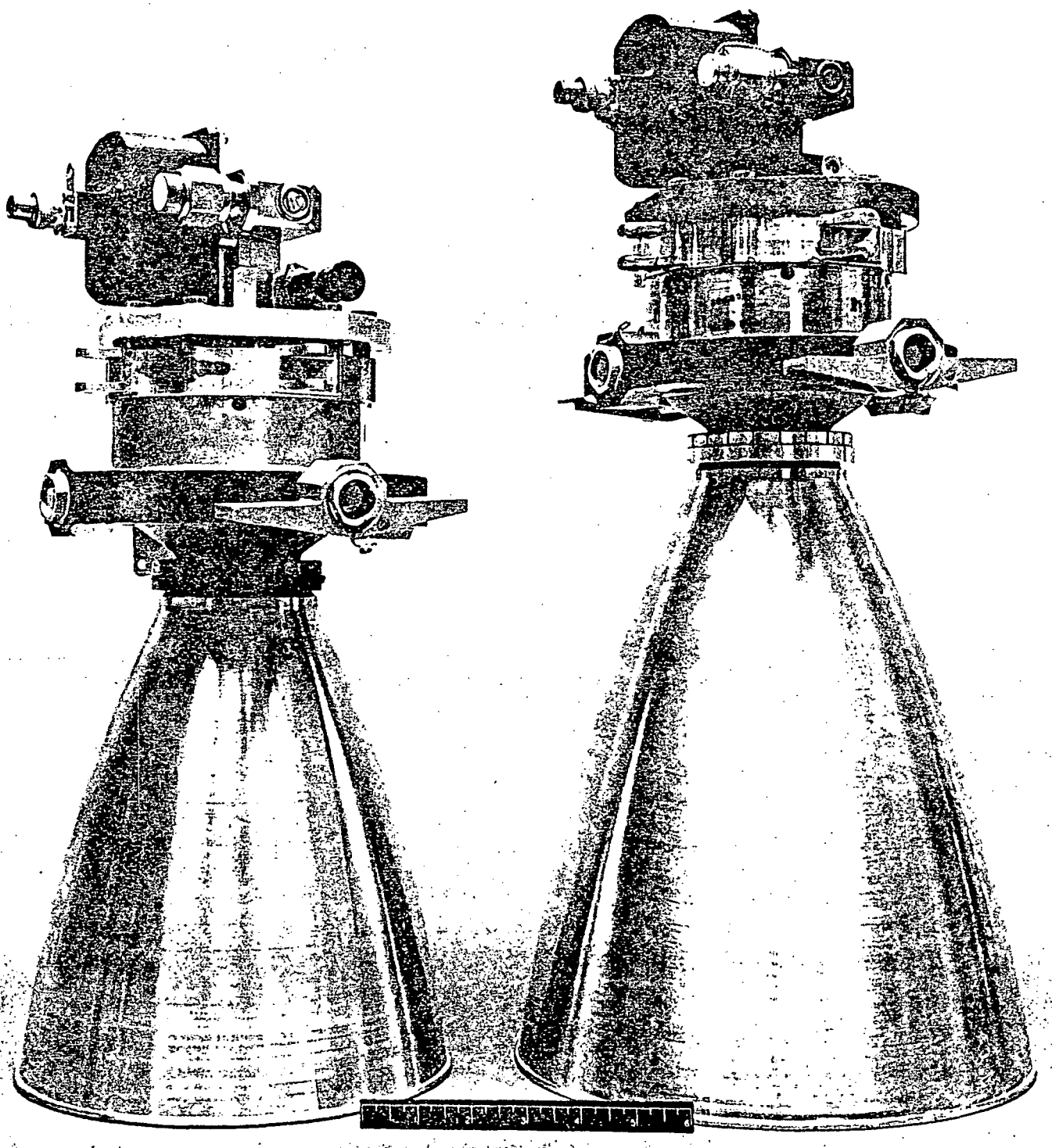

RS2101 AND MODIFIED RS2101 ENGINE COMPARISON

DISCUSSION

A Modified RS2101 Rocket Engine Study criteria was supplied by JPL as Exhibit 1 of Contract No. 953066. This criteria defined the engine operating conditions and requirements. The study criteria and the contract Statement of Work are attached to this report as Appendix A.

A mission duty cycle was supplied by JPL based on information available on 27 January 1971. JPL Interoffice Memo 384V0-71-181 "Engine Burn Time Requirements for the Modified RS2101 Thermal Study Contract # 953066" contained the following burn sequence.

Midcourse Correction #1	36 seconds
Midcourse Correction #2	15 seconds
Mars Orbit Insertion (MOI)	2700 seconds
Orbit Trim Pre Lander Separation #1	128 seconds
Orbit Trim Pre Lander Separation #2	24 seconds
Orbit Trim Pre Lander Separation #3	14 seconds
Orbit Trim Post Lander Separation #1	8 seconds
Orbit Trim Post Lander Separation #2	3 seconds
Orbit Trim Post Lander Separation #3	.4 seconds

Repeat the Orbit Trim Post Lander Separation Duty Cycle 8 times. All burn times except the last (.4 second) have been adjusted to whole seconds.

Performance Balance

Using the requirements of the study criteria and the performance history of the MM'71 engine, a performance balance was calculated for the modified RS2101 engine. This performance balance is presented in Table 1.

TABLE 1

MODIFIED RS2101 ENGINE

PERFORMANCE BALANCE

		60:1 ENGINE	MM'71
THRUST	LBF	300.0	300.0
SPECIFIC IMPULSE	LBF-SEC/LBM	291.1	287.4
CHAMBER PRESSURE-INJ END	PSIA	114.7	116.0
MIXTURE RATIO		1.55	1.57
PROPELLANT FLOWRATES			
OXIDIZER	LBM/SEC	0.6265	0.6377
FUEL	LBM/SEC	0.4041	0.4061
BLC (40%)	LBM/SEC	0.1616	0.1624
TOTAL	LBM/SEC	1.0306	1.0438
THRUST COEFFICIENT (INJ END)		1.812	1.792

Mass Properties

A complete mass properties analysis was performed on the modified RS2101 engine. The weight comparison between the MM'71 engine and the modified engine is as follows:

MM'71 Engine	17.1 Lb
40:1 Nozzle	1.52 Lb
60:1 Nozzle	2.40 Lb
Weight Change	+ .88 Lb
Modified Engine	18.0 $\pm$ .3 Lb

The Modified RS2101 Rocket Engine Mass Properties Report (SR 1112-4002) is attached in Appendix B.

Seals Design Study

The design studies and analyses of the RS2101 rocket engine injector-to-thrust chamber joint were performed to define potential solutions for leakage past this joint (Figure 2). Leakage was observed after mission duty cycle testing on several RS2101 engines including both of the Type Approval test engines. Post hot-fire leakage rates up to 300 cc/min GN_2 were observed past the primary seal when pressurized to 165 psig. This joint contains a gold plated Parker V-seal as the primary seal and a Viton O-ring as a secondary seal with both seals positioned between the chromic acid anodized 2219 aluminum alloy injector and the beryllium thrust chamber. Posttest examination disclosed local areas of a hard brittle gold-beryllium intermetallic phase on the gold plated sealing face. This suggested that posttest leaks occurred when the intermetallic material fractured. The failure analysis on these engines is contained in Reference 1.

Analysis was performed to evaluate alternates for both the primary and secondary seals since deterioration of the secondary seal was also evident on the TA engines. A joint trade-off study, material compatibility investigation (chemical and physical), and a study of the effects of seal-joint

Figure 2

MM'71 CONFIGURATION

INJECTOR-TO-THRUST CHAMBER JOINT

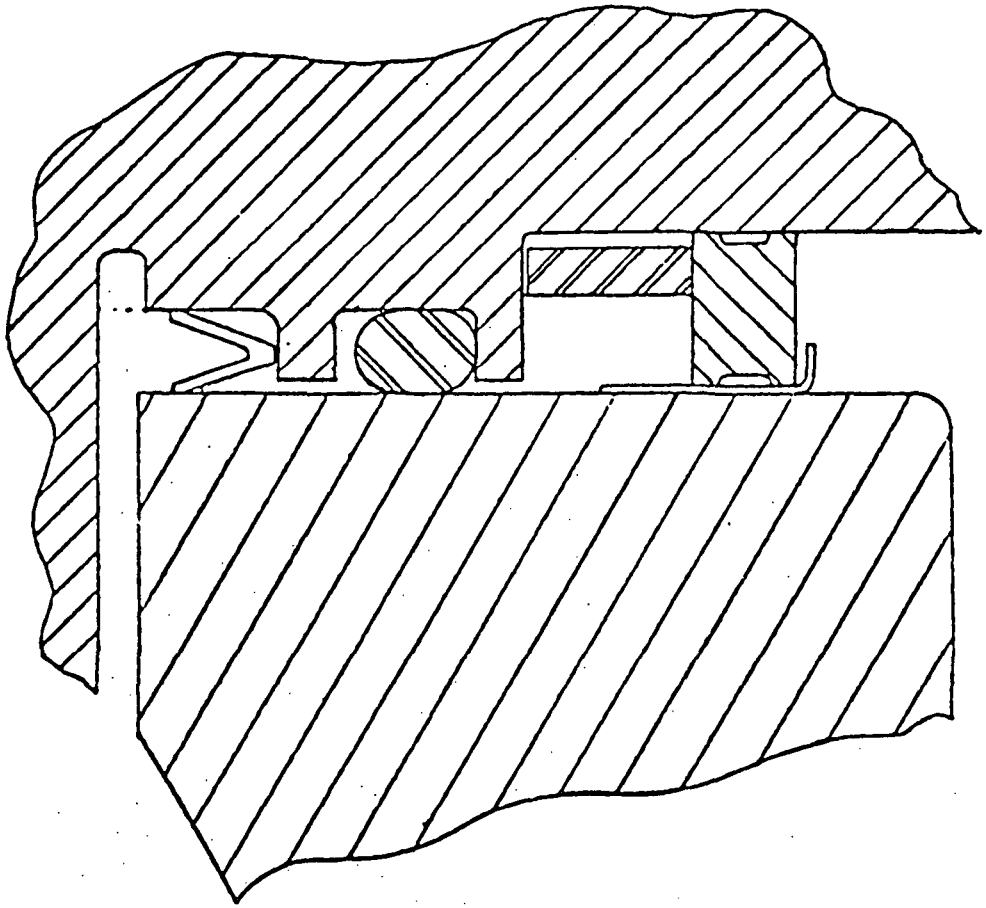

design changes on thermal management and the acoustic cavity were performed. Based on this analysis a solution to the leakage problem is proposed. Also, recommended leak test procedures are included.

Seal Study Constraints and Requirements

The following constraints and requirements on the joint and seals form a part of this study.

1. Joint Requirements

   a. A separable joint is required, i.e., no bonding, brazing, etc.

   b. The joint shall be capable of disassembly and re-assembly without reworking flange surfaces.

   c. Thermal management and acoustic chamber shall not change to the detriment of engine operation.

   d. Both primary and secondary seals shall be capable of being leak checked.

   e. Flange design changes should be limited so that engine operation and reliability have not been degraded.

   f. Particular emphasis shall be placed on minimal changes to the MM'71 engine configuration.

2. Operating Environment

   Primary Seal

   a. Exposure to MMH, NTO, and their combustion products.

   b. Maximum operating temperature estimated at 1000F.

   c. Nominal operating chamber pressure 115 psia.

Secondary Seal

a. Exposure to MMH, NTO, and their combustion products.

b. Temperature of 250F for 3000 seconds followed by a sharp soakout peak to 550F, and then a temperature decay.

c. Nominal operating pressure 115 psia.

3. Operating Requirements - three of the listed duty cycles after completion of flight acceptance testing.

   a. 3500 seconds operation per duty cycle.

   b. 35 starts per duty cycle.

   c. 3000 seconds longest single burn.

4. Leak Check Requirement - No leakage predicated on a 10 minute water displacement test using ambient temperature gaseous nitrogen at 150 psig.

Seals Requirement

The seal requirements for the injector-to-thrust chamber static joint include both a primary and secondary seal and a method of measuring leakage past each seal. The primary seal must be a metal seal to operate at the 1000F operating temperature. The secondary seal might be made of a metal, an elastomer or plastic material since the temperature is a maximum of 550F for less than 500 seconds per duty cycle.

The following seal configurations were considered as possible candidates for use in the subject joint. Seals marked with an asterisk were evaluated as secondary seals only since they are temperature limited.

Candidate Seals

Parker V-seal	*Teflon covered elastomer O-ring
Parker Mark II seal	*Omniseal
K-seal	*Rayco seal
Naflex seal	*Elastomer O-ring (If compound can
Bobbin seal	be found which is compatible with
Conoseal	the fluids)
Metal O-ring	*Titanium spacer with gold plated contact surfaces or gold shims.
C-seal	*Secondary seals only

To effect a seal with a metal seal requires either a load of sufficient magnitude to deform the interface between the seal and flange or micro finished flat surfaces. Sealing is best accomplished by using a soft material on the sealing surface which will plastically deform without damage to the mating flanges. Two government-sponsored technology programs, References 2 and 3, cover this theory in depth. A comparison matrix of the various metal static seals is shown in Table 2 and provides pertinent design and performance information for each seal. Table 3 contains a comparison rating matrix used for evaluating the primary seal configurations.

The Parker-V-seal was chosen as the primary seal with the Naflex and Parker Mark II as alternatives. This choice is not inconsistent with the present V-seal leakage problem at this joint. The V-seal apparently performs satisfactorily until it has been subjected to a high temperature thermal cycle(s) during engine operation. While at temperature diffusion occurs between the beryllium thrust chamber and the gold plating on the seal. The intermetallics formed, being hard and brittle, fracture during pressure decay and/or cool down, (Reference 1). One solution to this problem then would be to prevent the diffusion process. It would not be solved by using a different seal with the same gold plating.

TABLE 2

COMPARISON MATRIX OF PRIMARY SEAL DESIGN APPROACHES

CRITERIA	PARKER V SEAL	MATLOK	PARKER MARK II	K-SEAL	C-SEAL	METAL O-RING	BOBBIN SEAL	CO-CSEAL
LEAKAGE (1)	ACCEPTABLE	ACCEPTABLE	ACCEPTABLE	LOW SEAL-FLANGE LOAD INDICATES LESS SEALING ABILITY.	LOW SEAL-FLANGE LOAD INDICATES LESS SEALING ABILITY.	ACCEPTABLE BY ANALYSIS. HOWEVER, LAB TEST INDICATES HIGHER LEAKAGES, PROBABLY DUE TO LOW SPRING BACK.	ACCEPTABLE	ACCEPTABLE
SEAL-FLANGE LOAD	ACCEPTABLE	ACCEPTABLE	QUESTIONABLE	LOW TO ACHIEVE CONSISTENT SEAL.	LOW TO ACHIEVE CONSISTENT SEAL.	ACCEPTABLE	UNACCEPTABLE - NOTCHED SEAL GROOVE IS UNDESIRABLE ON BERYLLIUM T/C.	UNACCEPTABLE - NOTCHED SEAL GROOVE IS UNDESIRABLE ON BERYLLIUM T/C.
SEAL RECOVERY	ACCEPTABLE	ACCEPTABLE	ACCEPTABLE	ACCEPTABLE	SEAL RECOVERY LOW REDUCING SEALING ABILITY DUE TO THERMAL AND PRESSURE INDUCED DEFLECTION.	SEAL RECOVERY LOW REDUCING SEALING ASILITY DUE TO THERMAL AND PRESSURE INDUCED DEFLECTION.	ACCEPTABLE	ACCEPTABLE
LIFE	ACCEPTABLE	ACCEPTABLE	ACCEPTABLE	ACCEPTABLE	ACCEPTABLE	ACCEPTABLE	ACCEPTABLE	ACCEPTABLE
FLANGE REUSEABILITY	ACCEPTABLE	ACCEPTABLE	ACCEPTABLE	ACCEPTABLE	ACCEPTABLE	ACCEPTABLE	ACCEPTABLE	ACCEPTABLE
EXPERIENCE	ACCEPTABLE - ON RS14 AND RS301 EXCEPT FOR GOLD-BERYLLIUM DIFFUSION	GOOD EXPERIENCE ON F-1 & J-2 SATURN ENGINES. USED SILVER PLATED SEALS IN HOT GAS SYSTEMS. GOLD PLATING WILL PROVIDE COMPARABLE OPERATION.	LIMITED TO LAB DATA. DESIGN HAS BETTER RECOVERY CAPABILITY AND HIGHER SEALING LOAD THAN V-SEAL WHICH RESULTS IN IMPROVED SEALING OVER V-SEAL IN MORE CRITICAL APPLICATIONS.	LIMITED TO LAB DATA. RESULTS INDICATE HIGHER LEAKAGES THAN SEALS WITH HIGHER SEAL-FLANGE LOAD.	LIMITED LAB DATA. LOW SEAL SPRING BACK REDUCES RELIABILITY.	EXPERIENCE INDICATES THIS SEAL IS NOT AS RELIABLE AS PRESSURE ASSISTED SEALS.	LIMITED TO LAB DATA.	LIMITED AT ROCKETDYNE. HOWEVER, USED ON SATURN SIVB VEHICLE.
FLUID COMPATIBILITY	ACCEPTABLE	ACCEPTABLE	ACCEPTABLE	ACCEPTABLE	ACCEPTABLE	ACCEPTABLE	ACCEPTABLE	ACCEPTABLE
SEAL ENVELOPE	ACCEPTABLE - CURRENT SEAL	ACCEPTABLE - REQUIRES CHANGES TO SEAL GROOVE.	ACCEPTABLE - REQUIRES CHANGES TO SEAL GROOVE.	ACCEPTABLE - REQUIRES CHANGE TO SEAL GROOVE.	ACCEPTABLE - REQUIRES CHANGE TO SEAL GROOVE.	ACCEPTABLE - REQUIRES CHANGE TO SEAL GROOVE.	UNACCEPTABLE - GROOVE CONFIGURATION	UNACCEPTABLE - GROOVE CONFIGURATION
SEAL AVAILABILITY	ACCEPTABLE - CURRENT SEAL	ACCEPTABLE - ROCKETDYNE DESIGN AND FABRICATION AVAILABLE	ACCEPTABLE - PARTS MADE TO ORDER.	ACCEPTABLE - PARTS MADE TO ORDER.	ACCEPTABLE - PARTS MADE TO ORDER.	ACCEPTABLE - PARTS MADE TO ORDER.	UNACCEPTABLE - SOURCE NOT ESTABLISHED	ACCEPTABLE - PARTS MADE TO ORDER
THERMAL DISPLACEMENT	ACCEPTABLE	ACCEPTABLE	ACCEPTABLE	ACCEPTABLE	ACCEPTABLE	UNACCEPTABLE - HEAT PATH INCREASED	UNACCEPTABLE - HEAT PATH INCREASED	UNACCEPTABLE - HEAT PATH INCREASED
ACOUSTIC CAVITY	ACCEPTABLE	ACCEPTABLE	ACCEPTABLE - REQUIRES SEAL DIAMETER CHANGE	ACCEPTABLE	ACCEPTABLE - REQUIRES SEAL DIAMETER CHANGE	———	———	———
RATING	FIRST CHOICE	SECOND CHOICE	THIRD CHOICE	LOW RATINGS DUE TO GREATER POSSIBILITY OF LEAKAGE, LOWER SEAL RECOVERY, AND HIGH INSTALLATION LOAD ON METAL O-RING.			UNACCEPTABLE	UNACCEPTABLE

NOTE: (1) BASED ON GOLD PLATED SEALS WHICH MATE WITH FLANGES THAT HAVE EFFECTIVE DIFFUSION BARRIERS.

TABLE 3

PRIMARY STATIC SEAL SELECTION TRADE STUDY

SEAL TYPES	SEAL CRITERIA							JOINT CRITERIA				
	LEAKAGE RATE, SCC/SEC OF O_2 (BASED ON PRIMARY SEAL DIAMETER) (1)	SEAL FLANGE LOAD, LB/IN. CIRCUM.	SEAL RECOVERY, TOTAL, INCH	LIFE	ROCKET ENGINE EXPERIENCE	COMPATIBLE WITH ENGINE FLUIDS (2)	AVAILABILITY	ENVELOPE, IN. DEEP BY IN. RADIAL	REUSABLE FLANGE	FLANGE SURFACE FINISH, ARITHMETIC AVERAGE 10^{-6} IN. REF.	THERMAL MANAGEMENT	EFFECT ON ACOUSTIC CAVITY
PARKER V-SEAL	7.2×10^{-7}	200 – 300	.005	GOOD	USED ON RS14 AND RS21 ENGINES	YES	STANDARD DESIGN PARTS MADE TO ORDER.	.111 BY .125	YES	16	NOT AFFECTED	NOT AFFECTED
MARLOK SEAL	3.6×10^{-8}	250 – 300	.006	GOOD	EXTENSIVE USE ON F-1, J-2, AND J-2S ENGINE HOT GAS SYSTEMS	YES	STANDARD DESIGN PARTS MADE TO ORDER.	.165 BY .240	YES	16	NOT AFFECTED	NOT AFFECTED
PARKER SEAL MARK II SEAL	2.6×10^{-8}	300 – 400	.005	GOOD	SEAL DIAMETER MUST BE INCREASED TO RETAIN ACOUSTIC CAVITY FREQUENCY	YES	STANDARD DESIGN PARTS MADE TO ORDER.	.077 BY .122	YES	16	NOT AFFECTED	ACCEPTABLE – REQUIRES SEAL DIAMETER CHANGE
E-SEAL	$.41 \times 10^{-2}$	100 – 150	.004	GOOD	LIMITED TO LAB TEST DATA. REF.	YES	STANDARD DESIGN PARTS MADE TO ORDER.	.094 BY .145	YES	16	NOT AFFECTED	NOT AFFECTED
C-SEAL	1.2×10^{-3}	200	.002	GOOD	SEAL DIAMETER MUST BE INCREASED TO RETAIN ACOUSTIC CAVITY FREQUENCY	YES	STANDARD DESIGN PARTS MADE TO ORDER.	.113 BY .118	YES	16	NOT AFFECTED	ACCEPTABLE – REQUIRES SEAL DIAMETER CHANGE
METAL O-RING	$.14 \times 10^{-9}$	550	.002	GOOD	LIMITED USE AT ROCKETDYNE. LOW FLANGE SEPARATION CAPABILITY LIMITS USEAGE ON FLIGHT DESIGNS.	YES	STANDARD DESIGN PARTS MADE TO ORDER.	.150 BY .220	YES	16	UNACCEPTABLE	——
BOBBIN SEAL	1×10^{-9}	500	.005	GOOD	LIMITED TO TESTING PERFORMED BY BATTELLE MEMORIAL INSTITUTE. REF.	YES	PROPOSED MILITARY STANDARD. SOURCES NOT ESTABLISHED.	.737 BY .271	YES	32	UNACCEPTABLE	——
CONOSEAL	1.1×10^{-4}	500 – 600	.005	GOOD	LIMITED USE AT ROCKETDYNE. USED ON SATURN S-IVB VEHICLE.	YES	STANDARD DESIGN PARTS MADE TO ORDER.	.032 BY .275	YES	32	UNACCEPTABLE	——

(1) BASED ON ITRI ANALYSIS METHOD.

(2) ALL SEALS ARE MADE OF COMPATIBLE CRES OR INCONEL MATERIALS WITH GOLD PLATING.

Listed below are comments on the various rating criteria in Table 2.

1. Leakage - Leakage is acceptable if laboratory and/or hardware experience has indicated that zero leakage, based on water displacement, is obtainable with properly finished mating surfaces. Also, the leakage analysis based on the IITRI method (Reference 2) must indicate leakage of less than 1×10^{-6} scc/sec of nitrogen. Analysis in all cases is based on a gold plated seal.

2. Seal-Flange Load - Acceptable if the seat-flange contact load was of sufficient magnitude to effect a seal without damaging the flanges. Adequate joint bolt loading is available to deflect all seals during installation.

3. Flange Separation - The flanges and bolts are of sufficient rigidity and strength to keep deflections low, i.e., less than .001 inch under all conditions. However, even small flange separation on seals which have high yielding with low recovery results in significant loss of seal-flange loading.

4. Life - Acceptable when time, temperature, and environment do not cause deterioration of the seal or flanges within the acceptance test and MDC requirements of the engine.

5. Flange Reuseability - Acceptable when the seal has adequate load to provide the required seal during repeated thermal cycling without damaging the sealing surfaces so as to prevent seal replacement upon engine disassembly prior to firing.

6. Experience - Is based on both engine hardware and laboratory test experience at Rocketdyne and other aerospace companies.

7. Fluid Compatibility - Is based on available material compatibility information. Seal material and platings can be identical for all metal seals, therefore, this criterion does not influence the seal rating.

8. Seal Availability - Is based on existing or slightly modified seal configurations. Consideration was also given to established sources for fabrication of seals.

9. Thermal Management - Is based on maintaining or lowering the present heat transfer conditions between the thrust chamber and injector.

10. Acoustic Cavity - Acceptance is based on maintaining the same natural frequency of the acoustic cavity as on the MM'71 engine.

Secondary Seals - A comparison matrix of the various elastomer, plastic, and combination metal and plastic seals evaluated and a metal gasket is shown in Table 4. This table provides pertinent design and performance information for each seal. Table 5 contains a comparison rating matrix used for evaluating the seal configurations.

Based on this evaluation, a larger diameter V-seal similar to the primary seal was selected as first choice for the secondary seal. A resin-cured butyl O-ring was selected as a marginally acceptable second choice for the secondary seal. The V-seal was selected because it has good chemical compatibility with the fluids, and has adequate physical properties to perform under the environmental conditions.

The second choice elastomer O-ring, while one of the simplest and most reliable seals, at best is only marginally compatible with the fluids and environment. With an O-ring mating flange requirements are less stringent (i.e., surface finish roughness and lay, and flatness) than those required for plastic and metal seals.

The effects of high temperatures on the tensile properties of compounds made from Viton, resin cured butyl, ethylene propylene, and silicone elastomers are presented in Table 6. This data indicates that the ethylene propylene rubber is mechanically inferior to the Viton, resin cured butyl, and silicone compounds when tested at 400°F after 8 hours aging at that

TABLE 4

COMPARISON MATRIX OF SECONDARY SEAL DESIGN APPROACHES

CRITERIA	ELASTOMER O-RING BUTYL	ELASTOMER O-RING VITON	ELASTOMER O-RING TEFLON COVER	RACO SEAL	OMNISEAL	TITANIUM SPACER WITH GOLD PLATING	ARY SEAL CHOICE
LEAKAGE	ACCEPTABLE	ACCEPTABLE	ACCEPTABLE	ACCEPTABLE	QUESTIONABLE - SMALL JOINT DEFLECTIONS OR YIELDING OF JOINT COMPONENTS DURING THERMAL CYCLING REQUIRES TESTING FOR LEAKAGE VERIFICATION.	QUESTIONABLE - SMALL JOINT DEFLECTIONS OR YIELDING OF JOINT COMPONENTS DURING THERMAL CYCLING REQUIRES TESTING FOR LEAKAGE VERIFICATION.	ACCEPTABLE
SEAL - FLANGE LOAD	ACCEPTABLE	ACCEPTABLE	ACCEPTABLE	ACCEPTABLE	ACCEPTABLE	ACCEPTABLE WITH RESPECT TO PREVENTING DAMAGE; QUESTIONABLE IF LOAD IS ADEQUATE FOR SEALING REQUIREMENT.	ACCEPTABLE
SEAL RECOVERY	ACCEPTABLE	ACCEPTABLE	ACCEPTABLE	ACCEPTABLE	ACCEPTABLE	QUESTIONABLE - FLANGE LOADING DUE TO UNEVEN BOLT PATTERN AND OPERATIONAL CONDITIONS REQUIRE OPERATION LEAKAGE VERIFICATION.	ACCEPTABLE
LIFE	ACCEPTABLE	ACCEPTABLE	UNACCEPTABLE - 500 F SOAK BACK TEMPERATURE WILL CAUSE EXCESS TEFLON COLD FLOW.	UNACCEPTABLE - 500 F SOAK BACK TEMPERATURE WILL CAUSE EXCESS TEFLON COLD FLOW.	UNACCEPTABLE - 500 F SOAK BACK TEMPERATURE WILL CAUSE EXCESS TEFLON COLD FLOW.	QUESTIONABLE - THERMAL CYCLING MAY RESULT IN LOSS OF BOLT LOAD, WHICH COULD RESULT IN LEAKAGE.	ACCEPTABLE
FLANGE REUSEABILITY	ACCEPTABLE	ACCEPTABLE	ACCEPTABLE	ACCEPTABLE	ACCEPTABLE	ACCEPTABLE	ACCEPTABLE
EXPERIENCE	ACCEPTABLE	UNACCEPTABLE - NOT COMPATIBLE WITH PROPELLANTS	UNACCEPTABLE - DUE TO TEFLON COLD FLOW.	UNACCEPTABLE - DUE TO TEFLON COLD FLOW.	UNACCEPTABLE - DUE TO TEFLON COLD FLOW.	QUESTIONABLE - METAL GASKETS REQUIRE HIGH GASKET LOADS AND RIGID FLANGES TO EFFECT AND MAINTAIN A SEAL.	ACCEPTABLE BASED ON PRIMARY SEAL SERVICE ON RS14 AND RS2101 EXCEPT FOR GOLD-BERYLLIUM DIFFUSION
FLUID COMPATIBILITY	MARGINAL - LONG TERM COMPATIBILITY QUESTION.	UNACCEPTABLE - CHEMICAL REACTION BETWEEN ELASTOMER AND FLUIDS	ACCEPTABLE	ACCEPTABLE	ACCEPTABLE	ACCEPTABLE	ACCEPTABLE
SEAL ENVELOPE	ACCEPTABLE	ACCEPTABLE	ACCEPTABLE	ACCEPTABLE	ACCEPTABLE	ACCEPTABLE	ACCEPTABLE
SEAL AVAILABILITY	ACCEPTABLE - STANDARD PART	ACCEPTABLE - STANDARD PART	ACCEPTABLE - STANDARD COMMERCIAL PART	ACCEPTABLE - STANDARD COMMERCIAL PART	ACCEPTABLE - STANDARD COMMERCIAL PART	ACCEPTABLE - MODIFICATION OF TITANIUM SPACER TO INCLUDE GOLD PLATING	ACCEPTABLE
T[illegible] MANAGEMENT	ACCEPTABLE	ACCEPTABLE	ACCEPTABLE	ACCEPTABLE	ACCEPTABLE	ACCEPTABLE	ACCEPTABLE
ACOUSTIC CAVITY	NOT AFFECTED	NOT AFFECTED	NOT AFFECTED	NOT AFFECTED	NOT AFFECTED	NOT AFFECTED	ACCEPTABLE
RATING	SECOND CHOICE	UNACCEPTABLE	UNACCEPTABLE	UNACCEPTABLE	UNACCEPTABLE	UNACCEPTABLE	1ST CHOICE

TABLE 5

SECONDARY SEAL SELECTION TRADE STUDY

SEAL TYPES	SEAL CRITERIA								JOINT CRITERIA				
	LEAKAGE RATE, SCC/SEC OF O_2 (BASED ON SECONDARY SEAL DIA)	SEAL FLANGE LOAD, LB/IN. CIRCUM.	SEAL RECOVERY, TOTAL INCH	LIFE	FLANGE REUSEABLE	ROCKET ENGINE EXPERIENCE	COMPATIBLE WITH ENGINE FLUIDS	AVAILABILITY	ENVELOPE, IN. DEEP BY IN. RADIAL	REUSEABLE FLANGE	FLANGE SURFACE FINISH, ARITHMETIC AVERAGE 1×10^{-6} IN. REF.	THERMAL MANAGEMENT	EFFECT ON ACOUSTIC CAVITY
ELASTOMER O-RING BUTYL (RESIN CURED)	LESS THAN 1×10^{-4} BASED ON EXPERIENCE	17	.010	GOOD	YES	ACCEPTABLE	YES	STANDARD DESIGN, COMMERCIAL PART	.090 BY .142	YES	32	NOT AFFECTED	NOT AFFECTED
ELASTOMER O-RING VITON	LESS THAN 1×10^{-4} BASED ON EXPERIENCE	17	.010	GOOD	YES	UNACCEPTABLE. VITON ATTACKED BY FLUIDS WHICH LEAKED PAST PRIMARY SEAL ON RS2101	NOT COMPATIBLE WITH N_2O_4 OR MMH	STANDARD DESIGN, COMMERCIAL PART	.080 BY .142	YES	32	NOT AFFECTED	NOT AFFECTED
ELASTOMER O-RING + .015 IN. TEFLON COVER	LESS THAN 1×10^{-4} BASED ON EXPERIENCE ON RS2101	60	.010	TEMP. DURING OPERATION & SOAK BACK WILL CAUSE TEFLON FLOW.	YES	USED ON RS2101 FOR INITIAL LEAK CHECK AND HOT FIRE TEST	YES	STANDARD DESIGN, COMMERCIAL PART	.090 BY .180	YES	32	NOT AFFECTED	NOT AFFECTED
RADIAL SEAL (TEFLON JACKET - METAL V SPRING)	1.2×10^{-1} (LAB TEST RESULTS IN 1×10^{-3} TO 1×10^{-4} He RANGE REF.	80 - 130	.015	TEMP. DURING OPERATION & SOAK BACK WILL CAUSE TEFLON COLD FLOW	YES	GOOD SEALING TO 300 F. TEFLON COLD FLOWS AT HIGHER TEMPS.	YES	STANDARD DESIGN, PARTS MADE TO ORDER	.135 BY .156	YES	32	NOT AFFECTED	NOT AFFECTED
DEVI SEAL (TEFLON JACKET - METAL COIL SPRING)	2.6×10^{-1} (LAB TEST RESULTS IN 1×10^{-3} TO 1×10^{-4} He RANGE REF.	50 - 100	.020	TEMP. DURING OPERATION & SOAK BACK WILL CAUSE TEFLON COLD FLOW	YES	GOOD SEALING TO 350 F. TEFLON COLD FLOWS AT HIGHER TEMPS.	YES	STANDARD DESIGN, PARTS MADE TO ORDER	.123 BY .137	YES	32	NOT AFFECTED	NOT AFFECTED
TITANIUM SPACER WITH COLD PLATING	UNKNOWN	825 MINIMUM AVAILABLE LOAD	.600	GOOD IF THERMAL CYCLING DOES NOT DEFORM PLATING	YES WITH NEW SPACER FOR EACH INSTALLATION.	GASKETS HAVE BEEN FOUND UNACCEPTABLE BECAUSE OF HIGH BEARING LOADS AND RIGID FLANGE REQUIREMENTS.	YES	YES, MODIFICATION OF CURRENT SPACER DESIGN	.200 BY .135	YES	32 OR 8	NOT AFFECTED	NOT AFFECTED

TABLE 6

MECHANICAL PROPERTIES OF VARIOUS ELASTOMERIC TYPES *

PROPERTY	UNITS	MATERIAL TYPE VITON	RESIN CURED BUTYL	ETHYLENE PROPYLENE	SILICONE
Control Data					
Tensile Strength	psi	4330	2325	2050	1200
Elongation	%	560	570	430	300
Tests at 400F					
Tensile Strength	psi	695	720	340	270
Elongation	%	265	310	270	70
Tests at 500F					
Tensile Strength	psi	-	-	-	265
Elongation	%				75
400F after 8 hrs @ 400F					
Tensile Strength	psi	735	400	100	345
Elongation	%	170	180	60	80
500F after 8 hrs @ 500F					
Tensile Strength	psi	-	-	-	160
Elongation	%				45

* Data taken from AFML TR 56-331 parts IV, V, and VI, AFML TR 65-178, and AFML TR 67-440

temperature. At 500°F after aging 8 hours at 500°F, silicone is the only type compound available that has usable properties. After 8 hours at 400°F the Viton compound is better than the butyl, and the butyl is better than the silicone.

Compatibility

The resistance to NTO and MMH by the four types of elastomers considered for this study is presented below:

Viton - Viton compounds are resistant to chemical attack by NTO but are badly swollen and softened by contact with that oxidizer. They are severely attacked and embrittled by contact with any of the amine fuels. The rate of this deterioration is greatly accelerated by elevated temperatures.

Resin Cured Butyl - The resin cured butyl rubber compounds have the best overall resistance to NTO and MMH of any of the elastomeric types considered.

Many compounds have been developed that are extremely resistant to deterioration caused by exposure to amine fuels. This classification of compound also is the most resistant to deterioration by NTO of the commonly available elastomers.

Ethylene Propylene - Ethylene propylene rubber compounds have been developed that are very resistant to deterioration caused by exposure to amine fuels. However, they are rapidly attacked by exposure to NTO at temperatures in excess of 60°F.

Silicones - The silicone elastomers are considered to be incompatible with the storable oxidizers and the amine fuels. However, they are reasonably resistant to the amine fuels for short exposure durations, up to several days, at ambient temperatures.

Leakage Estimation

An estimate was made of the gaseous nitrogen leakage rate that can be expected from each candidate seal using the method developed by IIT Research Institute, Reference 2, and described below. These leakages, given in Tables 3 and 5, for gold plated metal seals and Teflon spring-loaded seals, were with the seals compressed to the manufacturer's specified value. The quoted leakages, while not absolute values, may be used for comparing the seal candidates. The leakage rates for combustion gases are essentially the same as for gaseous nitrogen.

A similar study using palladium plated seals (second choice plating) indicated that the expected leakage rates would be 10^4 times greater than that expected for the gold plated seals; less desirable condition. In order for the palladium plated V-seal to have the same leakage as a gold plated V-seal (using the IITRI analysis method) the unit loading would have to be increased from 250 lbs/inch to 465 lbs/inch of circumference. There is a high probability that this high loading would Brinell both the aluminum injector flange and the beryllium thrust chamber.

A leakage rate using the IITRI method could not be determined for the resin-cured butyl rubber O-ring as the equation is not applicable to elastomers or rubber compounds.

The leakage rate equation developed in Reference 2 considers the flow to be laminar, viscous, and compressible, and to be contained between two uniformly separated circular plates:

$$Q = \frac{\pi h^3 (r_o + r_i)(P_2^2 - P_1^2)}{12\mu(r_o - r_i) P_o} \left(1 + \frac{12.76\ \xi\ P_o \lambda_o}{(P_2 + P_1)h}\right) \qquad (1)$$

where

Q = Volume rate of flow at standard conditions (in.^{3}/sec)
h = Uniform channel clearance or conductance parameter (in.)
r_o = Outer radius of seal contact area (in.)
r_i = Inner radius of seal contact area (in.)
P_2 = Inlet fluid pressure (psia)
P_1 = Outlet fluid pressure (psia)
μ = Fluid viscosity (lb-sec/in.^{2})
P_o = Pressure at standard conditions (psia)
ξ = Correction factor: 0.9 for single gas; 0.66 for a mixture
λ_o = Molecular mean free path at standard conditions (in.)

The conductance parameter h^3 is obtained from curves in the reference as a function of surface finish and the modified stress ratio.

The modified stress ratio is defined by:

$$MSR = \frac{(P)^{2/N}}{\sigma_m\ A_A}$$

where

P = Applied load (lb/inch of circumference)
A_A = Interface area (in.^{2})
σ_m = Meyer hardness (KSI)
N = Meyer Index

The applied load P can be adjusted by addition of the pressure load on pressure-actuated seals, and by subtraction of any loss of load due to flange separation, material deformation, etc.

Metallic Material Analysis

The principal factors considered for the Parker V-seal and flanges are:

1. Hardness
2. Interaction between seal plating and flanges or flange overlay.
3. Fluid compatibility of platings and flange overlay.

Hardness - The seal plating should be soft in order to achieve plastic flow of the plating at a low seal load while still retaining mechanical properties over the specified temperature range. Based on data from Table 7, the order of plating preference from a hardness standpoint only is gold, silver, palladium, platinum, and copper. Palladium, platinum, and copper are considerably harder than gold and silver and would, therefore, require higher unit loading of the plating to effect a seal. The higher load presents the problem of Brinelling the aluminum and beryllium flanges.

Candidate flange overlay materials in order of preference from a hardness standpoint only are rhodium and beryllium oxide, nickel and chromium, tungsten, and molybdenum. Oxide films can be formed directly on the aluminum and beryllium surfaces by anodizing. The oxides are quite hard but are also brittle and may crack if the underlying material deforms plastically. Rhodium, nickel, and chromium can all be plated on beryllium; however, chromium and rhodium platings tend to have cracks which may provide leak paths. Chromium also has a low coefficient of thermal expansion which could cause separation between the plating and beryllium substrate. Electro-plating of chromium on beryllium has been performed by at least two different processes, Reference 5; however, these processes have not always successfully produced a crack-free plating. Nickel plating on beryllium has been tested against gold and has been found to be a good diffusion barrier.

TABLE 7

APPROXIMATE HARDNESS AND YIELD STRENGTH

CANDIDATE SEAL AND SEAT MATERIALS(1)

	HARDNESS		YIELD STRENGTH
	BHN	MEYER	KSI
BERYLLIUM	100	150	30 - 50
ALUMINUM (2219)	40 - 130	150 (est.)	11 - 27
NICKEL PLATE	100 - 600	427	15 - 100
CHROMIUM PLATE	120 - 1000	500	-
MOLYBDENUM	100 - 250	200	90 - 150
TITANIUM	100 - 300	200	20 - 80
TUNGSTEN	200 - 500	300	200
Al_2O_3	2000	1000	-
BE O	1200	600	-
GOLD	30 - 60	40	1 - 30
SILVER	25 - 70	50	10 - 40
COPPER	40 - 100	109	10 - 50
PALLADIUM	40 - 200	100	5 - 30
PLATINUM	40 - 300	100	5 - 30
RHODIUM	50 - 800	600	50 - 200

(1) Room-temperature values

Refractory metal coatings (molybdenum and tungsten) can be applied by gas plating and plasma spraying; however, porosity and the low coefficients of thermal expansions for the refractory materials could cause problems.

From a hardness standpoint, the choices for the soft seal coating are among gold, silver, palladium, platinum, and copper. The choices for the flange overlay material lie among chromium, rhodium, beryllium oxide, nickel and molybdenum.

Seal-Flange Material Compatibility - Table 8 is a summary of the interaction between various pairs of candidate seal and flange materials. In the absence of other experimental data, compatibility was judged "good" when the binary system showed a continuous solid solubility, and "fair" if intermetallic phases are present. Platinum shows a poorer compatibility than palladium. Since both are similar from a hardness standpoint, platinum for a seal coating was discarded. The flange candidates selected from a hardness standpoint (chromium, rhodium, beryllium oxide, nickel, and molybdenum) are all compatible with the seal materials (gold, silver, palladium, and copper) selected on the basis of hardness.

Propellant Compatibility - Table 9 presents the propellant compatibility of the candidate seal and flange materials. Gold and palladium are the prime candidates based on compatibility. Gold is compatible with all fluids. Palladium is compatible with MMH but insufficient data exist on NTO compatibility. Silver is incompatible with NTO while copper is incompatible with both propellants.

From a compatibility standpoint the choices for flange overlay coatings are chromium and rhodium. Molybdenum is incompatible with both propellants while the compatibility of tungsten is unknown.

TABLE 8

FLANGE INTERFACE SEAL AND MATERIALS COMPATIBILITY*

	SEAL MATERIALS				
SEAT MATERIALS	GOLD	SILVER	COPPER	PALLADIUM	PLATINUM
BERYLLIUM	P	F	F	P	P
ALUMINUM	F	F	F	F	P
NICKEL	G	G	G	G	P
CHROMIUM	(F)	G	G	(G)	P
MOLYBDENUM	G	G	G	G	P
TITANIUM	F	F	F	F	P
TUNGSTEN	G	G	G	G	P
Al_2O_3	G	G	G	G	G
Be O	G	G	G	G	G
RHODIUM	(G)	G	G	(G)	G

G = GOOD COMPATIBILITY

F = FAIR COMPATIBILITY

P = POOR COMPATIBILITY

* COMPATIBILITY JUDGED GOOD WHEN BINARY SYSTEM SHOWED A CONTINUOUS SOLID SOLUBILITY, FAIR IF INTERMETALLIC PHASES ARE PRESENT; AND POOR IF NUMEROUS INTERMETALLIC OR LOW TEMPERATURE MOLTEN PHASES PRESENT.

TABLE 9

PROPELLANT COMPATIBILITY

CANDIDATE SEAL AND FLANGE INTERFACE MATERIAL DETERIORATION

	MMH	NTO
NICKEL	I	C
CHROMIUM	(C)	(C)
MOLYBDENUM	I	I
TITANIUM	C	I
Be O	Q	Q
GOLD	(C)	(C)
SILVER	C	I
COPPER	I	I
PALLADIUM	(C)	(Q)
PLATINUM	C	C
RHODIUM	(C)	(C)
ALUMINUM (2219)	C	C
BERYLLIUM	C	C

CODE: C = COMPATIBLE
I = INCOMPATIBLE
Q = QUESTIONABLE

Material Summary - In summary, the results of the material analysis did not provide a single, clear-cut acceptable material system for the primary seal-flange joint. The acceptable seal platings are gold and palladium. Flange overlays compatible with gold could not be selected with confidence without a supporting laboratory evaluation. Listed below, in order of preference, are three possible flange overlay materials with comments on compatibility, processing, and problem areas.

First Choice:

Chromium - Compatible with all fluids. Plating thickness of .0001 to .0003 inch should be adequate. Possible problems include microcracking in the plating which could provide leak paths and plating separation due to thermal expansion. Dense thin chrome will minimize the susceptability to microcracking.

Second Choice:

Rhodium - May act as a catalyst with the propellants. Microcracking similar to chromium may result in leak paths.

Third Choice:

BeO(Anodize) - Compatible with all fluids. Available beryllium anodized surfaces have poor abrasion resistance, which could lead to excessive wear during the large number of engine starts (thermal cycles) required.

Another approach to eliminate beryllium-gold diffusion is to plate a thin layer of rhodium on the gold-plated seal. This approach has been successful on silver-plated seals to prevent diffusion between Inconel 718 flanges and the silver plating.

Catalytic Effects of Metals on MMH

Attempts to locate reliable data on high temperature catalytic effects of metal on MMH were unsuccessful. Both a NASA Literature Search (No. 14901) and a Defense Documentation Center Search (No. 059425) in addition to a personal industry contact effort failed to locate any valid high temperature data. Some related data, however, were found in a current Stanford Research Institute Program (SRI Project 7982) and an unpublished setchkin aparatus test series conducted at Rocketdyne during the years 1966 - 1967. A summary of these data are shown in Table 10.

Nickel was considered a prime candidate as a diffusion barrier early in the program. It was learned, however, that Rocketdyne's test experience on nickel plated copper thrust chambers showed that MMH was catalytically decomposed at a temperature several hundred degrees below that in a beryllium thrust chamber. One of the decomposition products of MMH is ammonia which attacks nickel. It was found that on both 100 lb. thrust and 1000 lb. thrust engines that .005 inch nickel plate was removed in approximately 200 seconds at a temperature between 600°F and 800°F. Since the primary seal environment is very similar to that experienced on these tests, nickel was eliminated as a compatible material.

Additional Consideration

The Parker V-seal was selected as the first choice for both the primary and secondary seals. It is believed that this seal together with the first choice material selections of gold plate on the seal and thin dense chrome on the beryllium, will most nearly meet the sealing requirements of the modified RS2101 engine.

Structural analysis showed that the present engine configuration is adequate to support two V-seals. The loads developed are as follows:

TABLE 10

CATALYTIC EFFECTS OF METALS ON MMH

NOTE: VALID HIGH TEMPERATURE (300 - 700°F) TEST DATA ON MMH CATALYSTS NOT AVAILABLE.

1. CURRENT SRI TEST PROGRAM RESULTS (7 DAYS @ 100°C)

METAL	PERCENT DECOMP
Al	.25
Ti	.29
Cr	.29
Fe	.49
Mo	3.2
Ni	5.2
CONTROL (NO METAL)	.26

2. ROCKETDYNE TESTS CONDUCTED 1966 - 1967
(SETCHKIN APARATUS 700°F SAMPLE TEMPERATURE)

METAL	DELTA-T
SS-321	33
SS-347	18
A-NICKEL	53
COPPER	22
Pd ON COPPER	33
Rh ON COPPER	56
L-605	22

NOTE: ROCKETDYNE DATA NOT PUBLISHED DUE TO CERTAIN INCONSISTENCIES.

WHEN CONDUCTING TESTS WITH MMH, A PROGRESSIVE DECREASE IN CATALYTIC EFFECT WAS NOTED WITH A CORRESPONDING INCREASE IN CARBON DEPOSITION ON THE SAMPLE.

METAL	DELTA-T ON CONSECUTIVE TESTS
SS-321	33, 10, 2

Maximum Injector-To-Thrust Chamber Force	=	34,200 Lb.
Minimum Injector-To-Thrust Chamber Force	=	14,400 Lb.
Primary V-Seal @ 400 Lb/Inch	=	3300 Lb.
Secondary V-Seal @ 400 Lb/Inch	=	4100 Lb.

The bending loads on the injector resulting from the use of two seals, were found to be well within acceptable limits.

Thermal analyses performed on various engine configurations showed that the required temperature limits could be maintained with the 2 V-seal configuration, and further, that by modifying the seal plating and titanium spacer, that the 2 V-seal configuration would result in a lower thermal path between the injector and thrust chamber than on the MM'71 engine.

It was learned from the thermal analysis that the primary heat path through the V-seal is through the .0007 inch gold plating on the seal I.D., and that with the gold removed, two V-seals will conduct less heat than one seal with the I.D. plating. It was further learned, that by increasing the relief on both mating surfaces of the titanium spacer from .015 inch to .050 inch, the heat transfer through the member could be reduced by approximately 40%. The thermal analysis is covered in detail later in this report.

The recommended seals configuration for the modified RS2101 engine is shown in Figure 3.

Leak Test Procedure

One of the program requirements was to devise a leak test procedure to measure leakage past each and every injector-to-thrust chamber seal. Several techniques were considered, however, the following procedure is recommended.

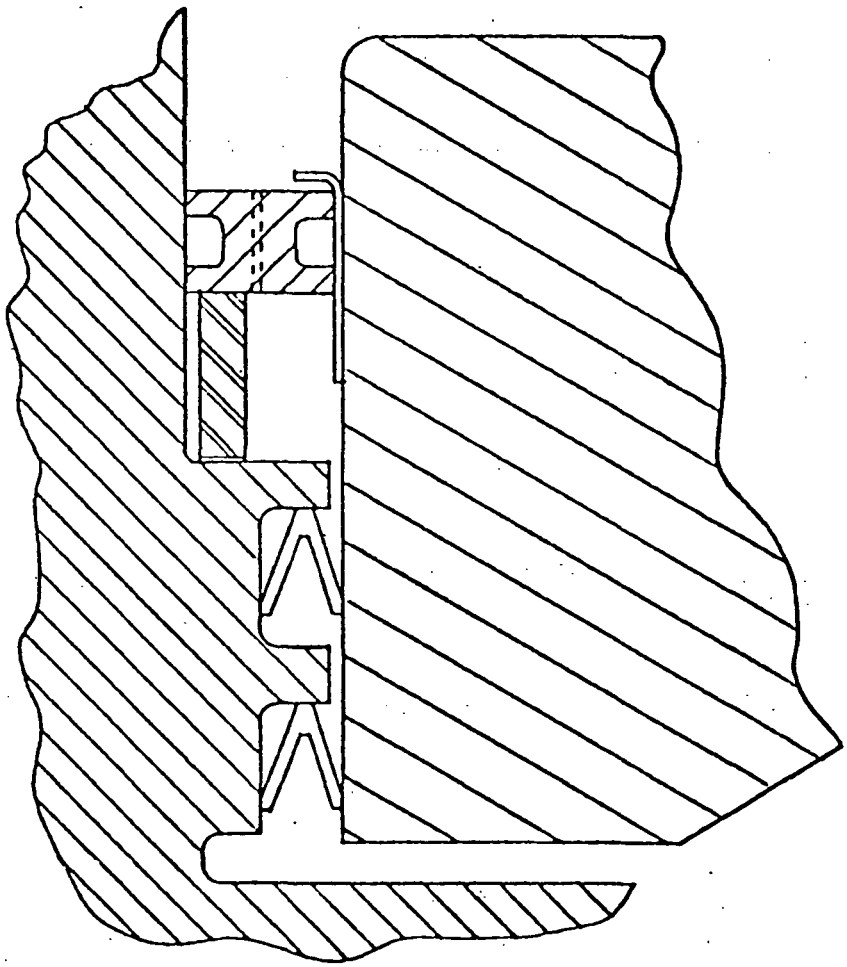

Figure 3
RECOMMENDED CONFIGURATION

1. Pressurize both the thrust chamber and the annulus between the primary and secondary seals to 150 psig with gaseous nitrogen at ambient temperature.

2. Apply soap type leak check solution (MIL-L-25567) to the titanium spacer, both top and bottom. Observe for ten minutes. No evidence of leakage is allowable.

3. Depressurize the annulus between the primary and secondary seals, and connect a positive water displacement leakage measuring device to the port provided. Monitor for ten minutes. No leakage is allowable.

4. Depressurize the thrust chamber and remove the pressurant lines.

5. Place the engine with all ports open in a vacuum oven that has been preheated to 160 $\pm$ 10 F. Maintain this temperature and ambient pressure for $\frac{1}{2}$ hour minimum. Then evacuate the oven and maintain the oven pressure at 1 psia or less and the temperature at 160 $\pm$ 10 F for a minimum period of three hours.

Laboratory Samples

A group of samples were subjected to laboratory testing and analysis in order to provide a reasonable basis for the full-scale hardware tests to follow. It was felt necessary to verify both the effectiveness of the diffusion barrier and the plating bond prior to hardware tests. Six test specimens were prepared by plating beryllium bars with the following materials: Specimens were prepared with each plating group.

PLATING GROUP		MATERIAL	SPECIFICATION
1.	.001	COPPER	CYANIDE COPPER PER MIL-C-14550
	.0001	CHROME	THIN DENSE CHROME PER QQ-C-320 CLASS II
	.0004	GOLD	PER MIL-G-45204
2.	.0005	COPPER	CYANIDE COPPER PER MIL-C-14550
	.0009	NICKEL	SULPHAMATE PER QQN-290
	.0001	CHROME	THIN DENSE CHROME PER QQ-C-320 CLASS II
	.0004	GOLD	PER MIL-G-45204
3.	.0002	CHROME	THIN DENSE CHROME PER QQ-C-320 CLASS II
	.0002	GOLD	PER MIL-G-45204

Each specimen was placed in an evacuated Vycor ampoule in preparation for elevated temperature testing. Specimens from each group were heated to both 800°F and 1000°F for one hour. Following this the ampoules were opened and the specimens were sectioned longitudinally for metallographic examination.

Examination of the mounts disclosed a significant variation in the plating groups with respect to diffusion barrier effectiveness and bond integrity. The test results for the three plating groups were:

1. The specimens from plating group 1 looked good. There was no evidence of plating bond separation or gold diffusion. A photomicrograph of this is shown in Figure 4.

2. The copper to chrome bond failed in several small areas on the samples from plating group 2. Apparently, the copper was too thin to support the differential thermal expansion with the copper-beryllium diffusion, which was apparent. Figure 5 is a photomicrograph of a non-failed area.

3. The thin chrome directly over beryllium did not result in an effective diffusion barrier. The beryllium-gold diffusion took place through the microcracks in the chrome. Figure 6 shows the diffusion through the microcracks.

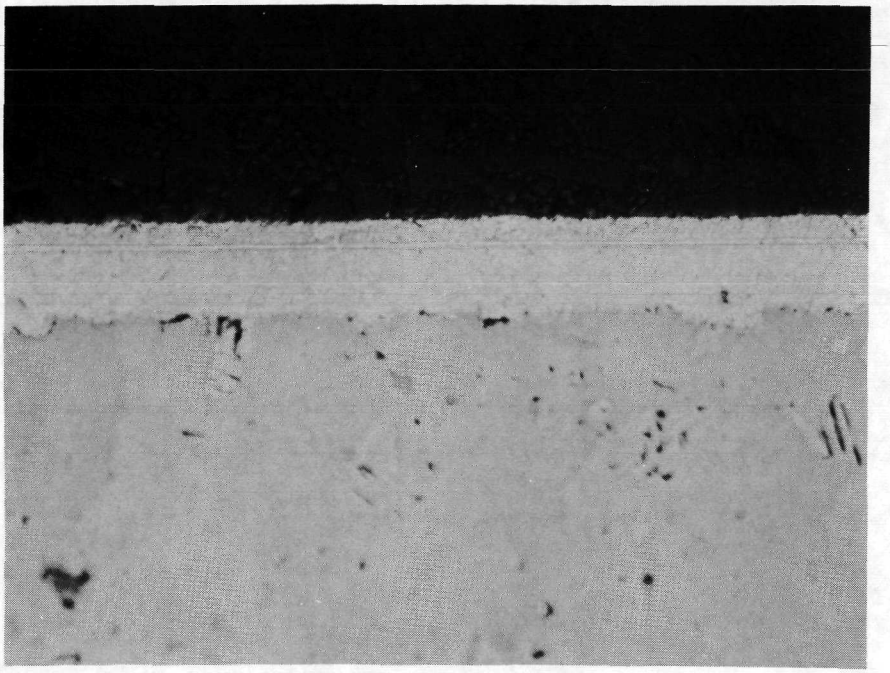

GOLD .0004 INCH
CHROME .0001 INCH
COPPER .001 INCH
800°F FOR 1 HOUR

PHOTOMICROGRAPH SHOWING CHROME OVER COPPER
AS A DIFFUSION BARRIER. 200X

FIGURE 4

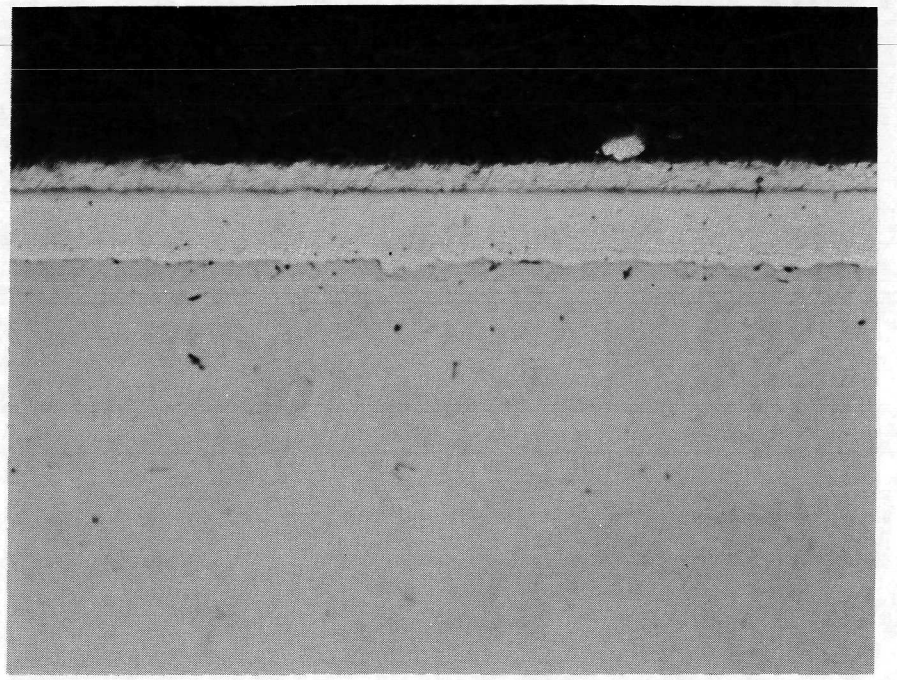

GOLD .0004 INCH
CHROME .0001 INCH
NICKEL .0009 INCH
COPPER .0005 INCH
1000°F FOR 1 HOUR

PHOTOMICROGRAPH SHOWING NON-FAILED AREA OF CHROME DIFFUSION BARRIER OVER A NICKEL-COPPER SUBSURFACE. 200X

FIGURE 5

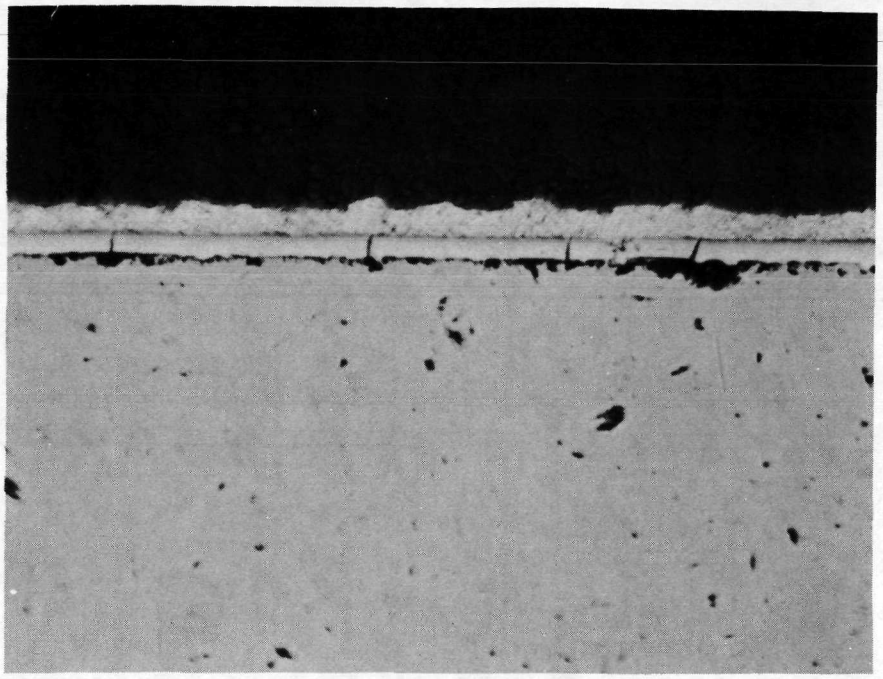

GOLD .0002 INCH
CHROME .0002 INCH
800°F FOR 1 HOUR

PHOTOMICROGRAPH SHOWING DIFFUSION OF GOLD INTO BERYLLIUM THROUGH MICROCRACKS IN CHROME PLATE. 200X

FIGURE 6

It was concluded from the laboratory tests, that chrome over copper had the best chance of success.

Full-Scale Hardware Tests

The decision was made, based on these results, to demonstrate the ability of a gold plated Parker V-seal to seal against chrome by plating a full size thrust chamber and performing a leak test. The following hardware was used:

Injector - New chromic acid anodized RS21 type injector (rejected earlier due to manufacturing discrepancies).

Thrust Chamber - Prepared as follows:

1. Hand lapped to a $\sqrt{16}_c$ finish as on MM'71.
2. Copper plated .002 inch and hand lapped $\sqrt{16}_c$.
3. Chrome plated .0002 inch.
4. Lapped on a carbide plate using 1 - 5 micron diamond dust.

Primary Seal - Standard Parker V-seal used on MM'71 engine.

Secondary Seal - Gold plated titanium spacer prepared by lapping flat to within .0001 inch and plating .001 inch temperex gold.

The test engine was assembled and leak tested. There was no leakage past the Primary V-seal at 150 psig GN_2 when tested for ten minutes. Leakage was measured by both the water displacement and soap check techniques. The gold plated titanium spacer, however, leaked 360^o around when subjected to a soap leak check with the annulars between the V-seal and spacer pressurized to 150 psig GN_2.

A second assembly was leak tested using a JPL supplied sulfamate nickel plated Parker V-seal. This assembly contained the following hardware:

Injector - A new chromic acid anodized RS21 type injector (rejected earlier due to manufacturing discrepancies).

Thrust Chamber - Normal beryllium surfaced hand lapped to a 16 c as on MM'71.

Primary Seal - Parker V-seal plated with sulfamate nickel per QQN-290.

Secondary Seal - Standard MM'71 O-ring.

The assembly was leak tested with 150 psig GN_2 for ten minutes and no leakage was found using the water displacement method.

Posttest Hardware Examination

After completion of the leak tests, the engines were disassembled and inspected to determine sealing surface condition. In neither case was the injector brinelled significantly. The thrust chambers, however, were both brinelled slightly. Figures 7 and 8 show the thrust chamber sealing surface conditions after disassembly. It is considered desirable to provide a configuration that will not brinell the thrust chamber surface. For this reason, a substrate harder than copper is recommended.

Recommendations

The recommended seal configuration is that shown in Figure 3. This consists of the following:

Primary Seal - Gold plated Parker V-seal with the gold in the seal area only.

Secondary Seal - Identical to the primary seal except the diameter is increased.

FIGURE 7

POST TEST THRUST CHAMBER SURFACE CONDITION

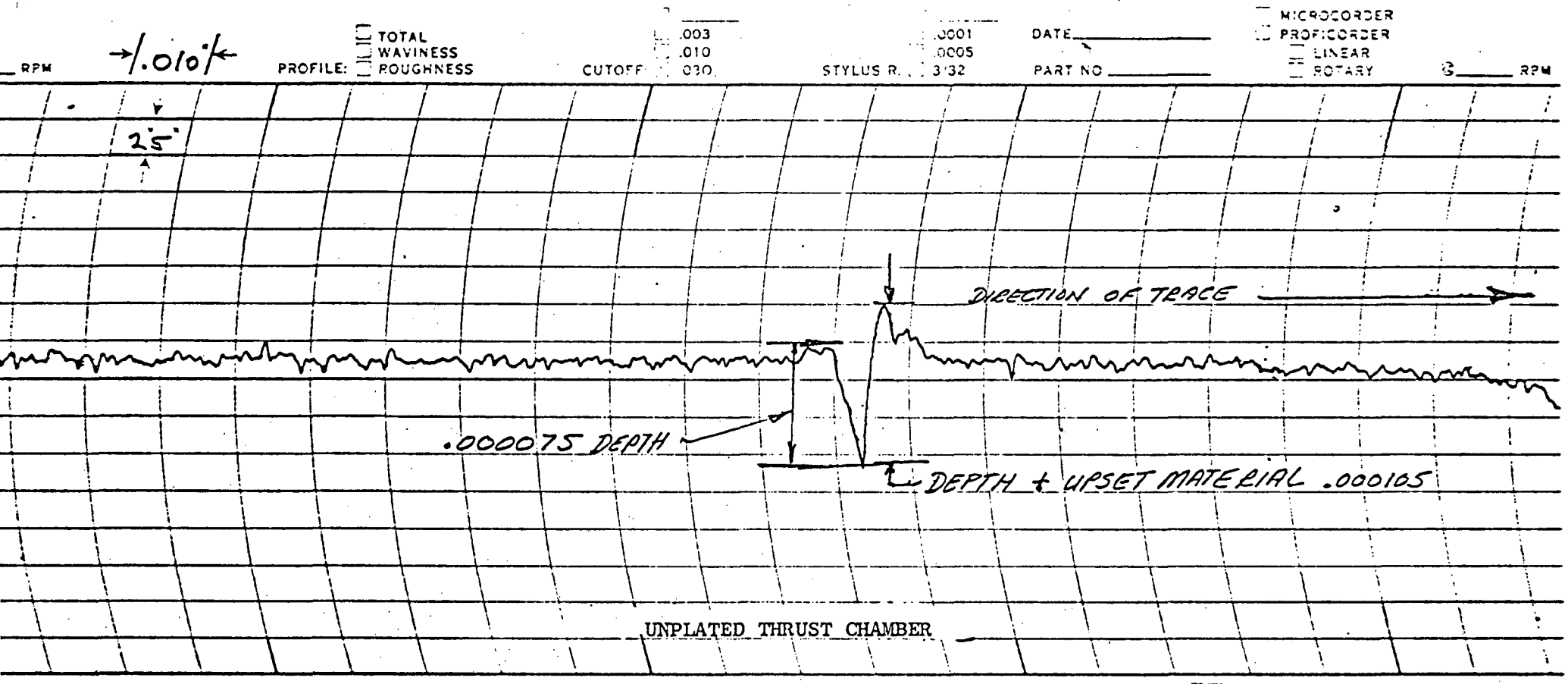

BRINELLED THRUST CHAMBER SURFACE

FIGURE 8

POST TEST THRUST CHAMBER SURFACE CONDITION

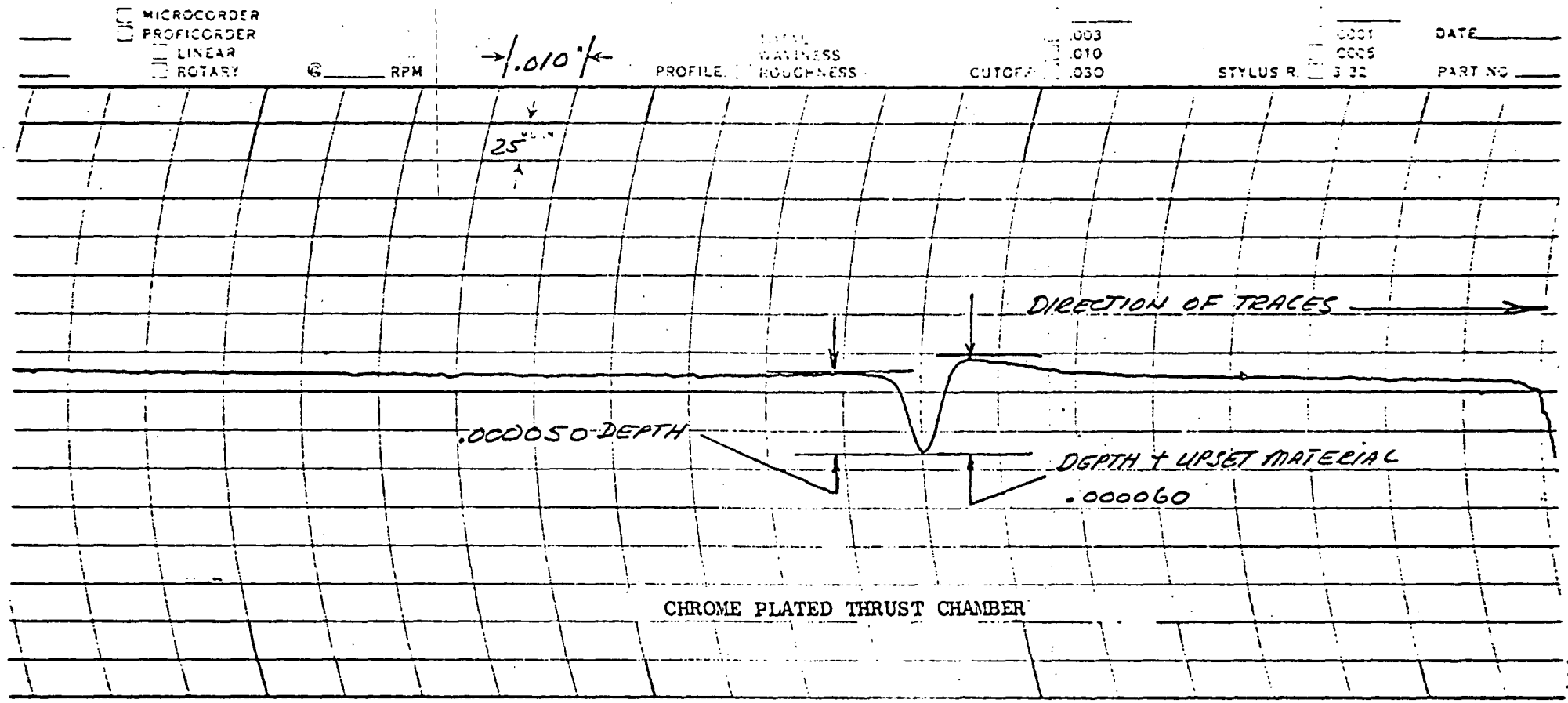

BRINELLED THRUST CHAMBER SURFACE

Titanium Spacer - Modified from that used on the MM'71 engine by increasing the annulus depth on both sides from .015 inch to .050 inch.

Injector Finish - Chromic acid anodized $\sqrt{8}_c$ finish in seal areas.

Thrust Chamber Finish - Thin dense chrome over a copper, or preferably harder subsurface. Lap to a $\sqrt{2}_c$ finish.

In order to provide a basis for plating an engine with the diffusion barrier, for testing at ETS, an additional effort was authorized to evaluate a plated surface that would minimize brinelling from the V-seal. It was believed that less brinelling would provide a better seal during repeated thermal cycling.

Laboratory Samples

It was felt that a harder, stronger underplate would reduce brinelling of the chromium under the V-seal seating pressure. Electroless nickel was selected for the chromium underplate to achieve this objective. Two beryllium test specimens were plated as follows:

.002 Electroless Nickel - Plating accomplished using a nickel sulphate/sodium hypophosphite bath.

.0002 Electrolytic "crack-free" chromium - This thin dense chromium was electrodeposited from a fluo-silicate catalyzed bath.

The two plated beryllium slabs were sliced into 1/2 X 3/4 X 3/16 inch segments. Each segment was sliced so that the diffusion barrier plate extended around the 3/16-wide perimeter, with both the 1/2 X 3/4 faces exposing freshly-cut nonplated beryllium. Each of the specimen slices was then electroplated all over with approximately .001 inch of gold.

Individual specimens were encapsulated in vycor ampoules, evacuated to a vacuum of about 10^{-5} mm Hg, and then sealed by tipping off. The ampoules were then inserted in a furnace for the desired time/temperature thermal treatment as shown below:

Specimen No.	Test Temperature °F	Test Exposure (Hours)
1	1000	0.5
2	1000	1.0
3	1000	3.0
4	900	1.0
5	1100	1.0

1. An as-plated specimen subjected to metallographic examination before thermal treatment showed the nickel to be mechanically bonded to the beryllium as seen in Figure 9.

2. The five test specimens exposed to thermal treatment showed progressive reaction between the gold and beryllium with increasing temperature and duration of exposures. This surface condition is compared in Figure 10 where the surfaces shown are those where the gold plate was in direct contact with the beryllium. The severest condition is noted in specimen #5 where diffusion has progressed to the point where the brittle intermetallic product spalled from the surface. In contrast, metallographic examination showed no evidence of formation of gold-beryllium intermetallic phase in those areas protected by the nickel/chromium protective barrier.

3. All specimens subjected to thermal treatment showed a diffusion zone at the nickel side of the nickel/beryllium interface which becomes more pronounced with increased temperature as shown in Figure 11.

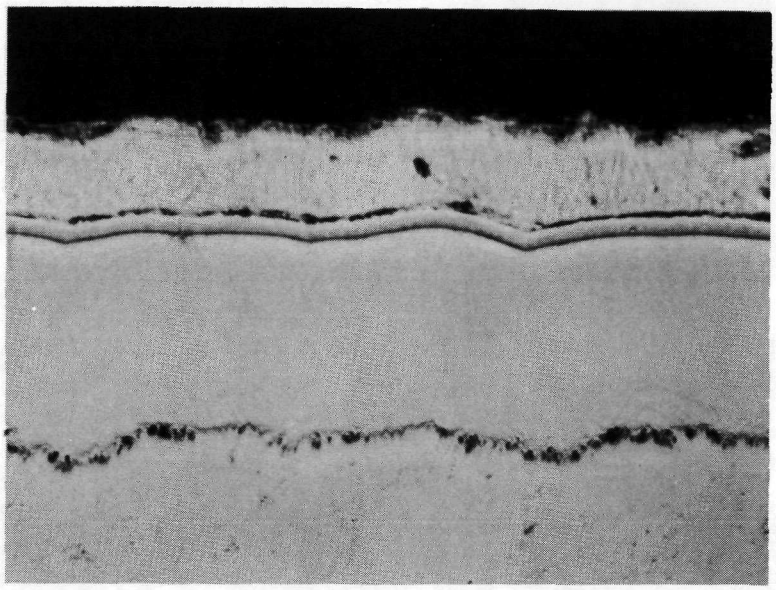

Mag. 500X

Figure 9 Cross-Section Through As-Plated Specimen, Showing Mechanical Bond Between Beryllium and Nickel Plate. Electrolytic Chromium Plate is Between Nickel and Gold Plate. Gold Plate is at the Top of Photomicrograph Beryllium at Bottom

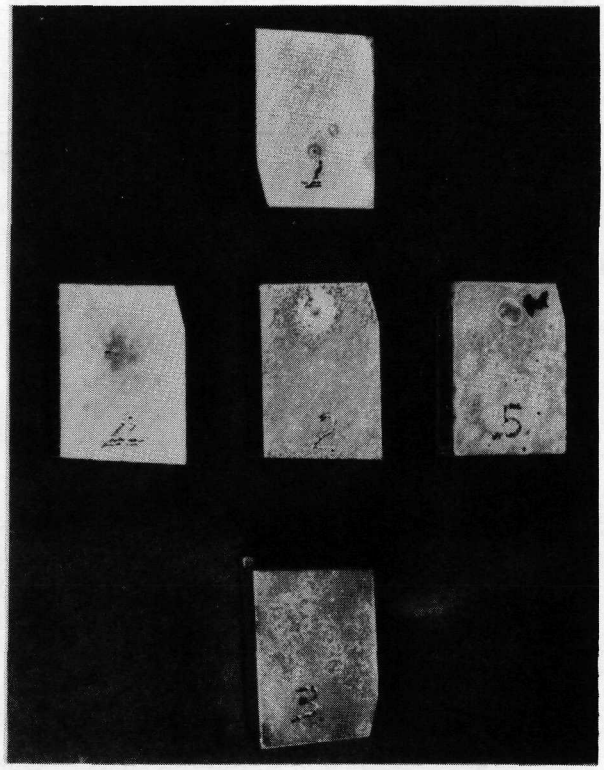

Mag. 1.5X

Figure 10 Appearance of Test Specimens After Thermal Treatment. Note Spalled Surface of Specimen #5. Specimen Numbers Correspond to Table I.

4. Small cracks in the electroless nickel/beryllium interface were observed in all specimens. This condition could have been the result of; a) thermal stresses during thermal treatment and/or during the water quench cooldown employed after treatment, b) during metallographic sectioning. The latter ties in with the high oxide content in the beryllium specimen which contributed to chipping and pull-out of the edges and interfaces during metallographic preparation of the specimen. Poor adherence may also be a contributing factor. This could result from possible formation of beryllium phosphide Be_3P_2 which decomposes quickly in moist air leaving voids and/or the inadvertent omission of a 375 degree F bake cycle immediately after plating. Both conditions would contribute to poor adherence of the electroless nickel to the beryllium.

5. Microcracks were present in the chromium plate as anticipated. The nickel plate itself was quite hard and brittle as evidenced by the cracks sustained during microhardness testing as seen in Figure 12.

It is concluded, from the results of these tests, that the electrolytic chrome plate over electroless nickel provides a good diffusion barrier between the beryllium and V-seal gold plate. However, the severity of cracking in the electroless nickel-plated specimens as compared to the electrolytic nickel and the copper-plated specimens tested previously indicates the latter substrate of copper should be retained. The desirable plated configuration should then consist of electrolytic copper followed by electroless nickel followed by electrolytic chromium.

Prototype Engine Seal Modification

The specimen test results clearly demonstrated the effectiveness of the plated surface as a diffusion barrier between beryllium and gold. Its effectiveness in preventing leakages, however, can best be ascertained by incorporation into an engine and exposing it to actual usage environment. A previously tested prototype configuration RS2101 engine S/N 4098603 was, therefore, selected to evaluate this seal configuration.

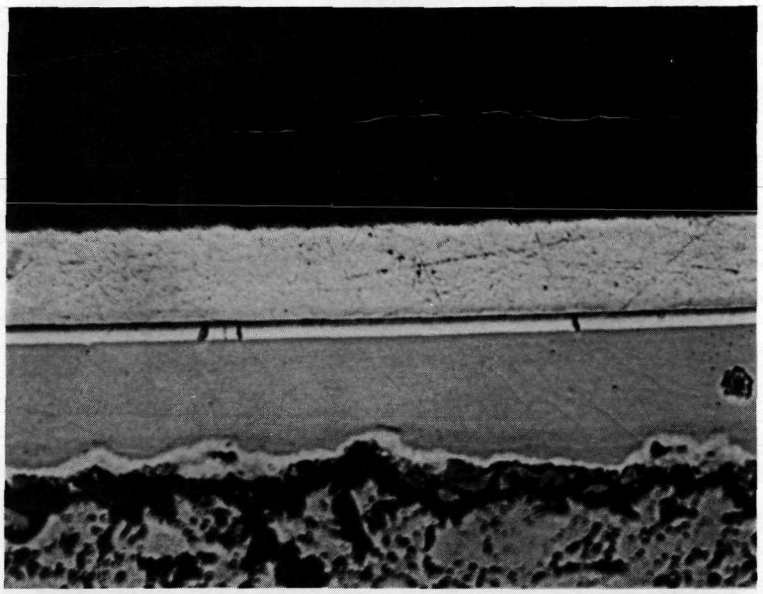

1100°F

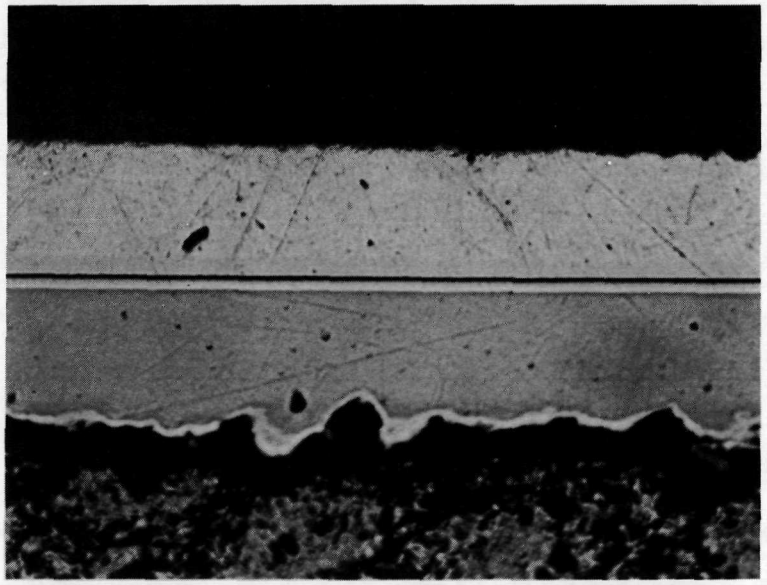

1000°F

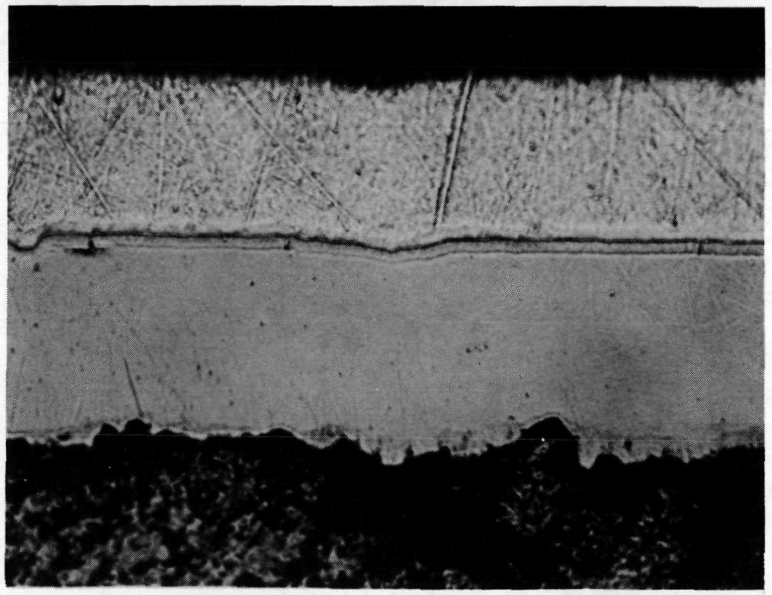

900°F

Figure 11 Microsections Through Gold/Chromium/Electroless Nickel/Beryllium Diffusion Specimens After 1 Hour Exposure. Gold is on the Top; Beryllium on the Bottom in Each Photograph. All at 500X Magnification.

The seal evaluation effort included the required seal modification by Rocketdyne, to the JPL furnished engine S/N 4098603, and delivery to JPL for eventual hot-testing at JPL's Edwards Test Site. The seal modification included beryllium surface plating and replacement of the secondary "O" ring with a V-seal for concurrent evaluation of the seal design of Figure 3 which was recommended from this study. The modified engine head end configuration is shown in Figure 13. It consists of the following:

Injector - Resurface seal surfaces, clean and brush anodize seal surfaces only.

Thrust Chamber - Prepared as follows:

1. Hand lapped to a $\sqrt{2}_c$ finish.
2. Electrolytic copper plated .002 - .003 inch and hand lapped to $\sqrt{2}_c$ finish.
3. Electroless nickel plated .002 - .003 inch and hand lapped to $\sqrt{2}_c$ finish.
4. Chrome plated .0002 - .0003 inch and hand lapped to $\sqrt{2}_c$ finish.

Primary Seal - Standard gold-plated Parker V-seal used on MM'71 engine, except some gold removed from the I.D.

Secondary Seal - V-seal with gold-plated sealing surface provided by JPL.

Spacer - Standard MM'71 spacer modified by increasing the undercut depth to .050 in.

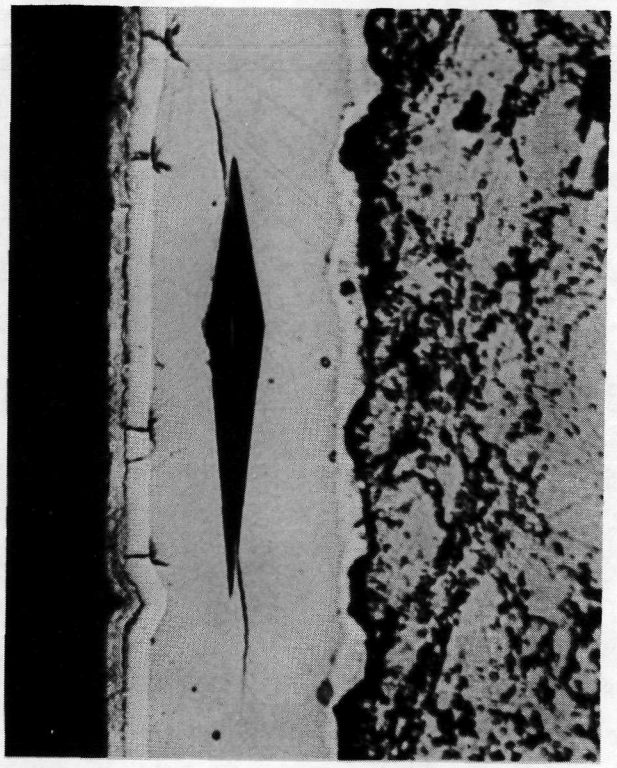

Mag. 500X

Figure 12 Microhardness Identation, Showing Crack in Electroless Nickel Plate. Specimen was exposed for 3 Hours at 1000°F.

The engine was assembled and leak tested. There was no leakage past the primary V-seal as measured by a positive water displacement method from a leak test port located in the annular cavity created by the two V-seals. The test pressure of 150 PSIG GN_2 was held for 10 minutes. The secondary V-seal and spacer was leaked tested by pressurizing the annulus between the two V-seals via the leak test port. No leakage was detected when a test pressure of 150 PSIG GN_2 was held for 10 minutes and leakage determined by applying leak test solution to the exterior surfaces of the spacer.

Disposition of Engine S/N 4098603

The subject engine was delivered to JPL for eventual hot-test evaluation of the seal configuration.

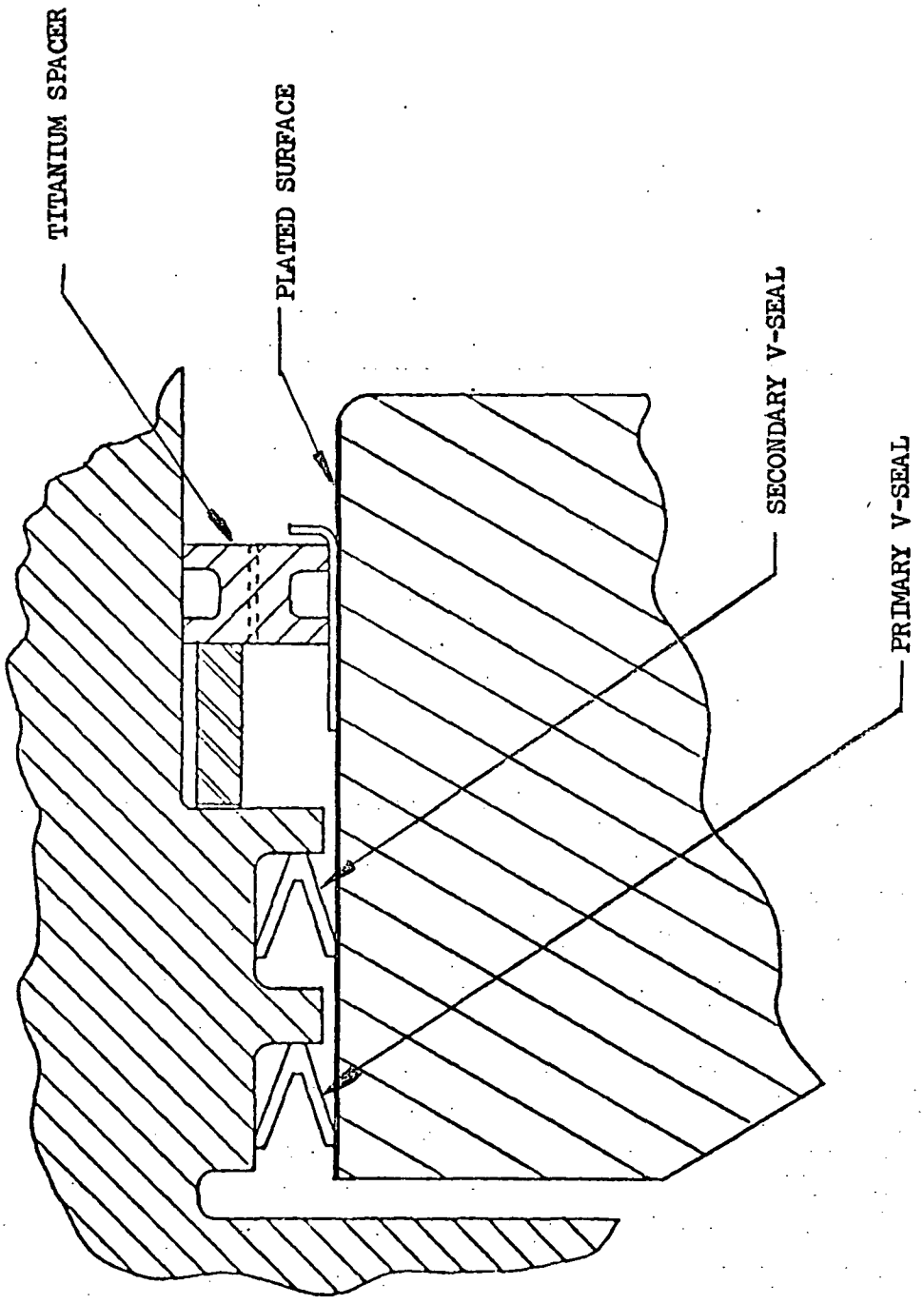

FIGURE 13 SEAL CONFIGURATION OF REA S/N 4098603

THERMAL ANALYSIS

An important portion of the work under this study contract was the thermal analysis of the operation of the Modified RS2101 Rocket Engine during both steady-state operation and during soakback, with emphasis on:

1. Analysis of the characteristics of heat soakback, with special emphasis on the effects of inductive heating and extended duration engine firing on the propellant valve seats.

2. Analyses of the engine thermal stability (Interegen) characteristics.

3. Definition of the engine thermal load to the spacecraft.

This section discusses the results of these analyses that have characterized the Modified RS2101 Rocket Engine thermally. The results were obtained by first calibrating the analytical models with existing test data to define the proper model input parameters, and then using these models to predict the operational behavior of the modified engine in the spacecraft. In the discussion that follows, the model calibration results are given first, for both the Interegen and the soakback models, and then followed by the predictions for the operational behavior of the modified engine.

Model Calibration

Internal Regenerative Cooling Model (Interegen)

In order for the modified RS2101 engine to operate successfully for a 3000-second firing, it is essential that true steady-state internal regenerative cooling of the engine be established. The nature of this type of cooling process and the analytical model to predict its behavior are discussed in detail in References 4 and 5 and will not be repeated here, except to emphasize that three different modes of operation are possible in these engines. The first and most desirable mode of operation occurs during

the starting transient of all Interegen cooled engines, and results in a complete blanketing of the combustion chamber by the coolant (liquid and vapor). When the proper conditions of energy feedback and absorption by the film coolant are met, the engine will operate entirely in this mode. If the energy feedback is excessive, the coolant cannot maintain this blanket and will recede to a new location, and cause the throat temperatures to rise significantly although the injector end temperatures will still remain low. This is the second mode of operation and is possible only when the energy feedback from the hot throat region does not exceed the allowable heat transfer capabilities of the liquid film. The third mode of operation occurs when the energy feedback is too large and "vapor binding" of the liquid film occurs. The film then becomes unstable and all temperatures in the thrust chamber rise to a new level, where radiation cooling is the predominant cooling mechanism.

These three modes of operation are important to this study, because the RS2101 design is such that either Mode I or Mode III operation will probably occur, and it was, therefore, necessary to accurately define the limits of operation in Mode I for the engine, since the high temperatures inherent in Mode III operation would cause excessive valve temperatures during soakback as well as increase the thermal strain damage to the thrust chamber.

Consequently, a critical review of the Interegen analytical model was made and all input parameters recalculated before attempting to match the available test data. As part of this review, the test data on the thermal diffusivity of beryllium, recently completed at Atomics International, was used to compute the material's conductivity for comparison with the values in use. The comparison is shown in Figure 14, and indicates a 15-percent lower thermal conductivity in the 500°F temperature range. These newer values are believed to be more representative of the beryllium used in fabricating the RS2101 engine and have been incorporated into the model. The inner and outer surface areas used in the model were also corrected to give a more accurate finite difference representation of the engine. Also, acoustic cavity heating was added to the model for a better repre-

FIGURE 14

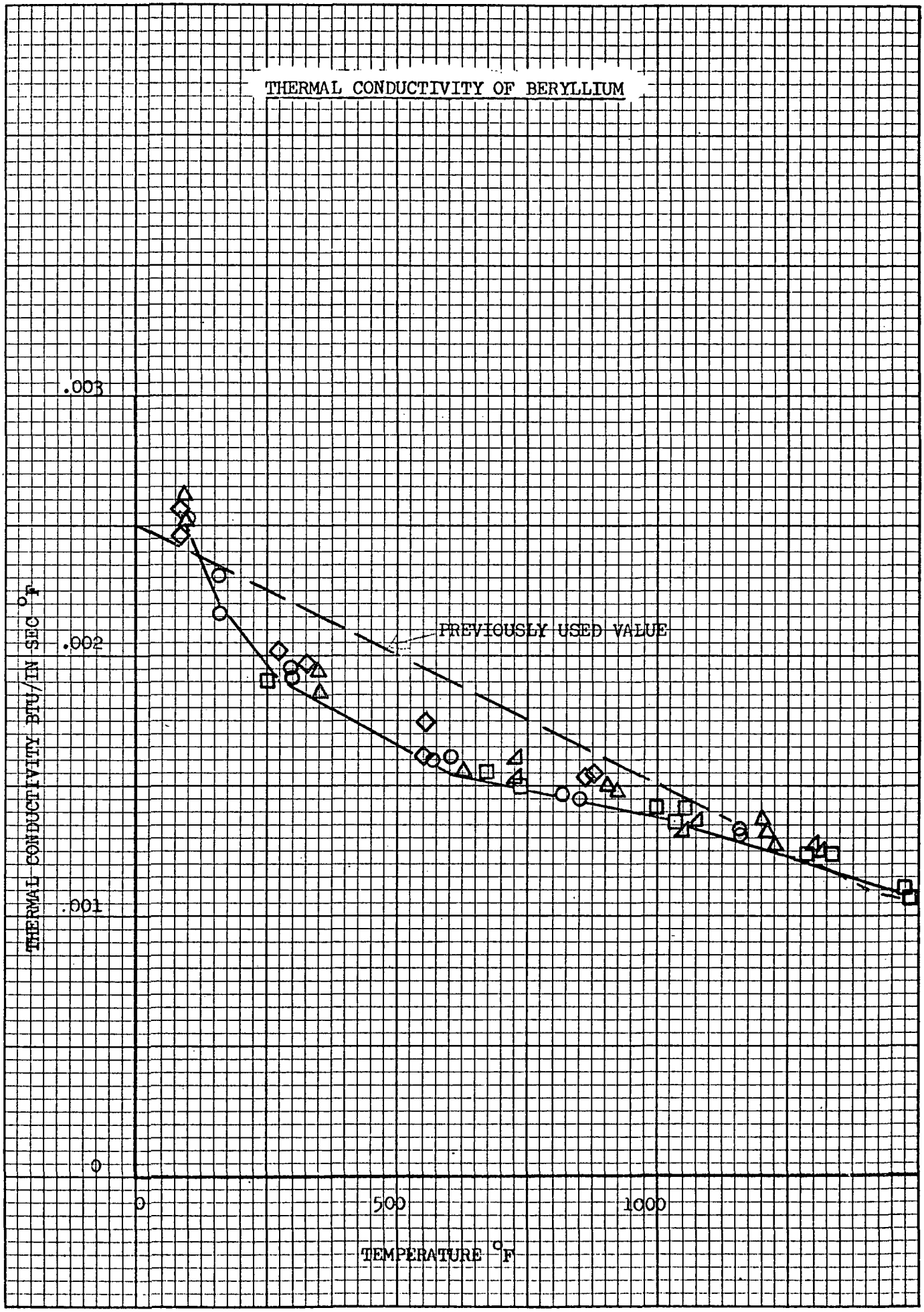

sentation of the actual operational conditions of the engine. The last addition made to the model was incorporation of convective cooling on the outside surfaces of the engine to better estimate the effect of test conditions on the transition points of the engine from Mode I operation.

The need for inclusion of convective cooling in the model was discovered during the evaluation of available test data for calibration of the model. Data were available from tests at CTL-4 at Rocketdyne and from the JPL Edwards facility. The steady-state nozzle temperatures measured during tests at CTL-4 were higher than temperatures measured during tests at the JPL facility, as shown in Table 11. The outside throat temperatures measured at Rocketdyne, however, were lower than throat temperatures measured at the JPL facility. To explain these differences, the original test data for Rocketdyne tests 870-030, 050, 331, 405 and 442 were compared with data from JPL tests DD-339, DV-370 & DD-391, using the Rocketdyne TEMP program to analyze the transient behavior of the nozzle thermocouples during the start and shutdown transients. This analysis considered radiation as well as convective heat transfer conditions. The results of these analyses, listed in Table 12 along with the values predicted by the Interegen analytical model, indicated that the convective losses in the JPL test cell were significant. The effects of the different environmental conditions on nozzle temperatures are shown in Figures 15 and 16, where the steady state operating temperatures predicted by the model are compared with data from the respective facilities. Figure 17 then gives the temperature profile predicted for the engine in a space environment. The difference in measured throat temperature was resolved by examination of chambers tested at Rocketdyne which showed that the throat thermocouples were attached 1/4" to 3/8" upstream of the throat location and, hence, measured a lower temperature.

After resolution of these apparent differences in the test data, the more extensive instrumentation of the beryllium body during the Margin Limits tests, Reference 6, led to the use of this data for the prototype engine

TABLE 11

STEADY STATE NOZZLE TEMPERATURES

O/B	FUEL TEMP	JPL DATA TEST NO./TEMP	RD DATA TEST NO./TEMP
JPL/RD	JPL/RD		
1.57/1.55	93/95	341/1660 F	442/1910 F
1.57/1.55	70/70	329/1640 F	331/1770 F
1.64/1.63	37/36	406/1750 F	405/1830 F

TABLE 12

ESTIMATED TEST CELL CONVECTIVE HEAT TRANSFER COEFFICIENTS

TEST NO.	TEST CELL H $Btu/in^2\text{-sec-F}$	$F\epsilon$	$F\epsilon$ max
405 (RD)	$.94 \times 10^{-6}$	.7	.75
442 (RD)	3.1×10^{-6}	.7	.85
AVERAGE	2×10^{-6}	.7	.8
370 (JPL)	1.47×10^{-5}	.7	>1.
370 (JPL)	1.42×10^{-5}	.7	>1.
339 (JPL)	$.72 \times 10^{-5}$	.7	>1.
AVERAGE	1.07×10^{-5}	.7	>1.

FIGURE 15

STEADY STATE OPERATING TEMPERATURES

ROCKETDYNE TEST CELL

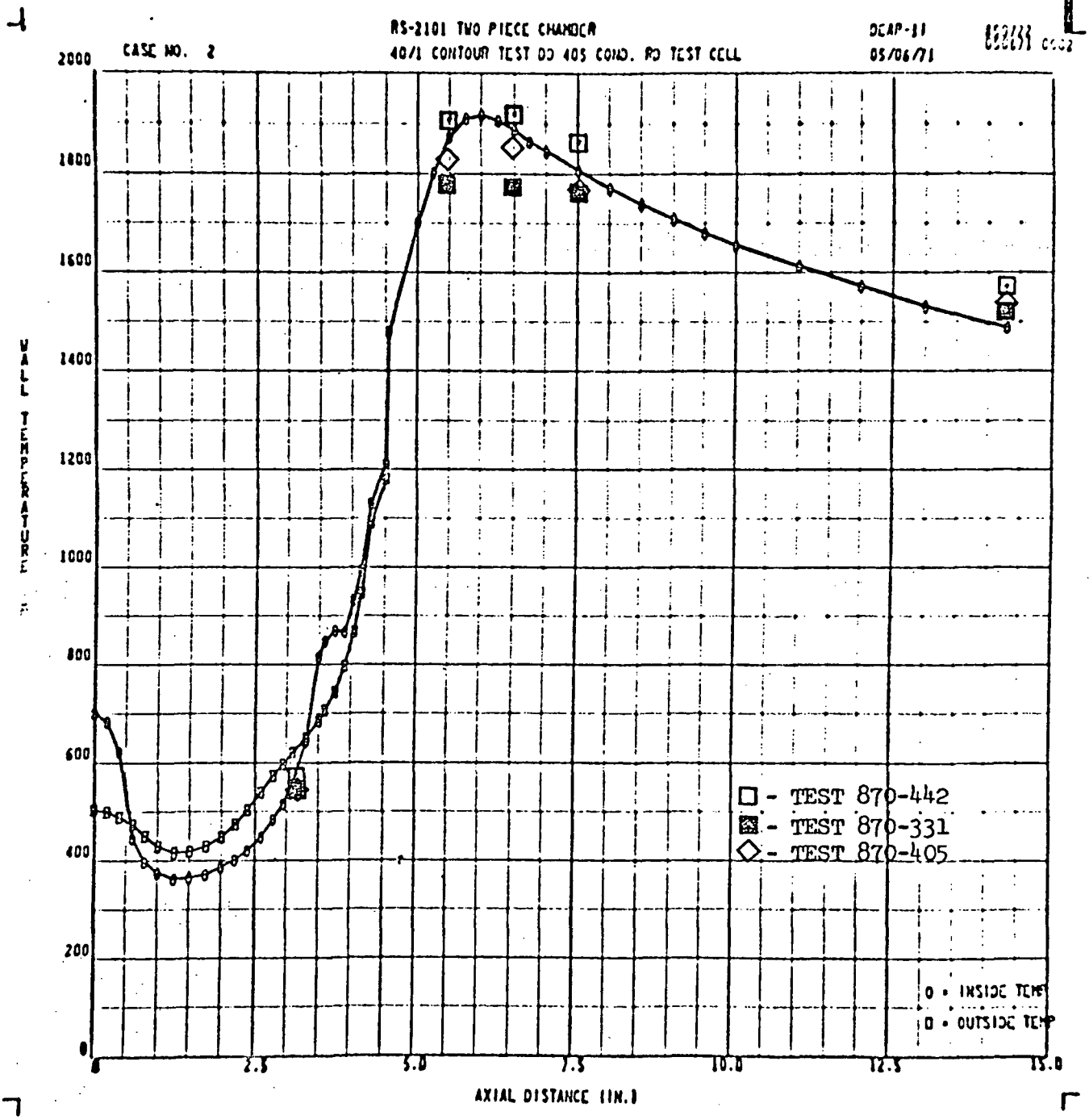

FIGURE 16

STEADY STATE OPERATING TEMPERATURES

JPL TEST CELL

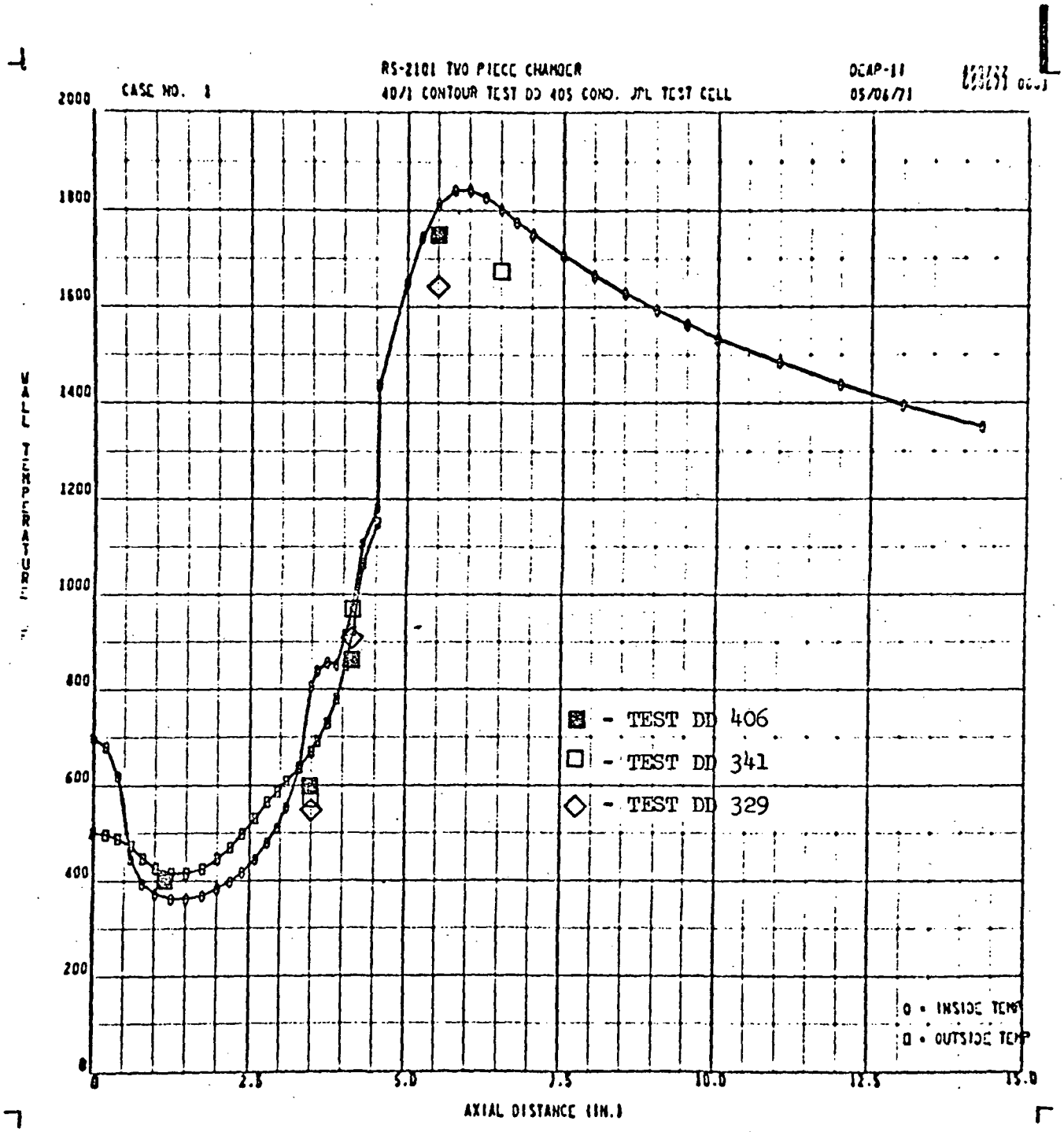

FIGURE 17

STEADY STATE OPERATING TEMPERATURES

SPACE CONDITIONS

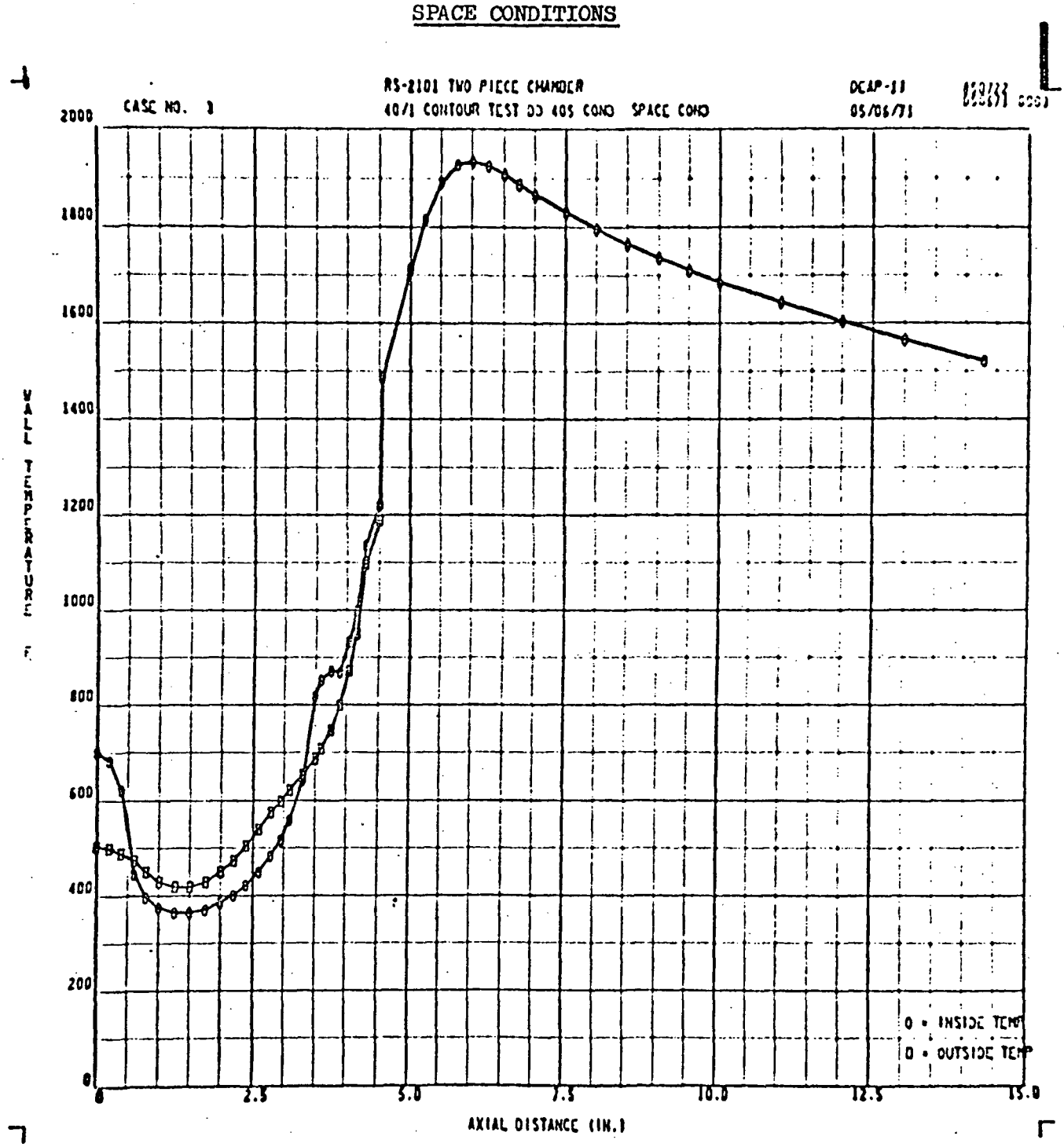

assembly to test the model after calibrating the model with data from Test DV370 for the S/N 4098604 engine. Test DV370 was chosen for model calibration primarily because the increase in measured temperatures after 700 seconds of firing (Figure 18) indicated that this test condition was close to the transition point from Mode I operation. The model was, therefore, adjusted to predict transition at this condition, while matching the transient and "steady-state" thermocouple data, as shown in Figure 19. It can be seen that excellent agreement was achieved for both the start transient, steady-state, and the shutdown transient periods. The calculation was then repeated using a reduced convective loss coefficient (80 percent of the expected value) to verify that transition from Mode I would occur. Figure 20 shows this comparison and predicts a transition from Mode I to occur at 700 seconds. These predictions also illustrate the sensitivity of the nozzle temperatures to the thermal losses to the test cell since the nozzle data and predictions shown in Figure 14 are in good agreement, but those shown in Figure 20 diverge during the nozzle cool-down with only a 20-percent change in the convective heat loss.

The calibrated analytical model was then tested using data from DD-405 to simulate nominal operating conditions, DD-413 for high propellant temperature, and DD-420 for high chamber pressure. These comparisons are shown in Figures 21, 22, and 23, and indicate excellent agreement between the data and the model prediction.

The comparison of the model predictions with data from DD-413 illustrates how well the model simulates the transition from Mode I operation for the high propellant temperature condition. Since the model accurately predicts the engine behavior under high mixture ratio, high chamber pressure and high propellant temperature conditions as well as the nominal operational condition, predictions for the modified RS2101 configuration could now be made with a high degree of confidence.

FIGURE 18

TEMPERATURE RISE DURING JPL TEST 370

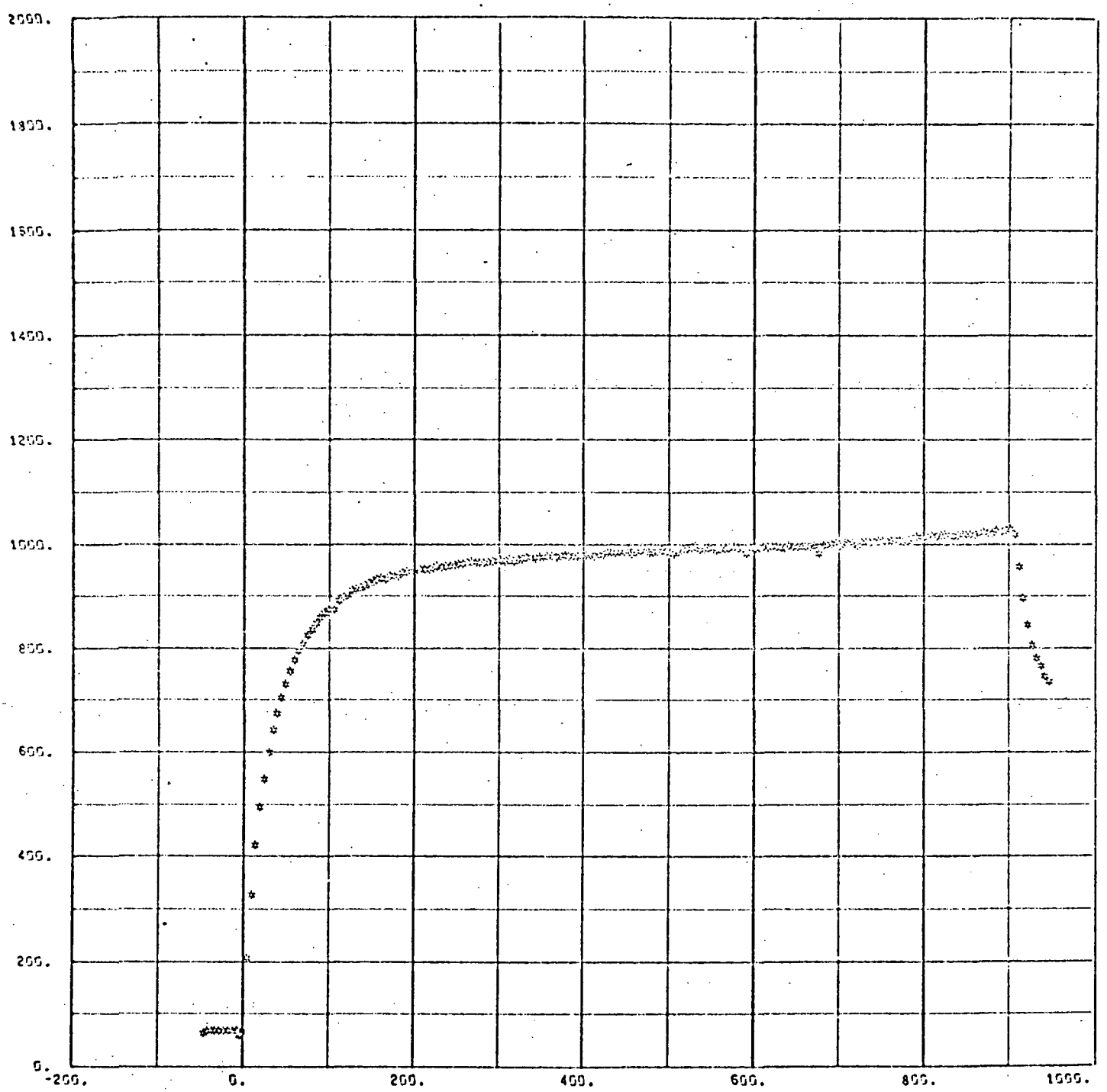

FIGURE 19

COMPARISON OF PREDICTED AND EXPERIMENTAL DATA FOR TEST DV370

TEST CELL H = 9×10^{-5} BTU $IN^2 SEC^{\circ}F$

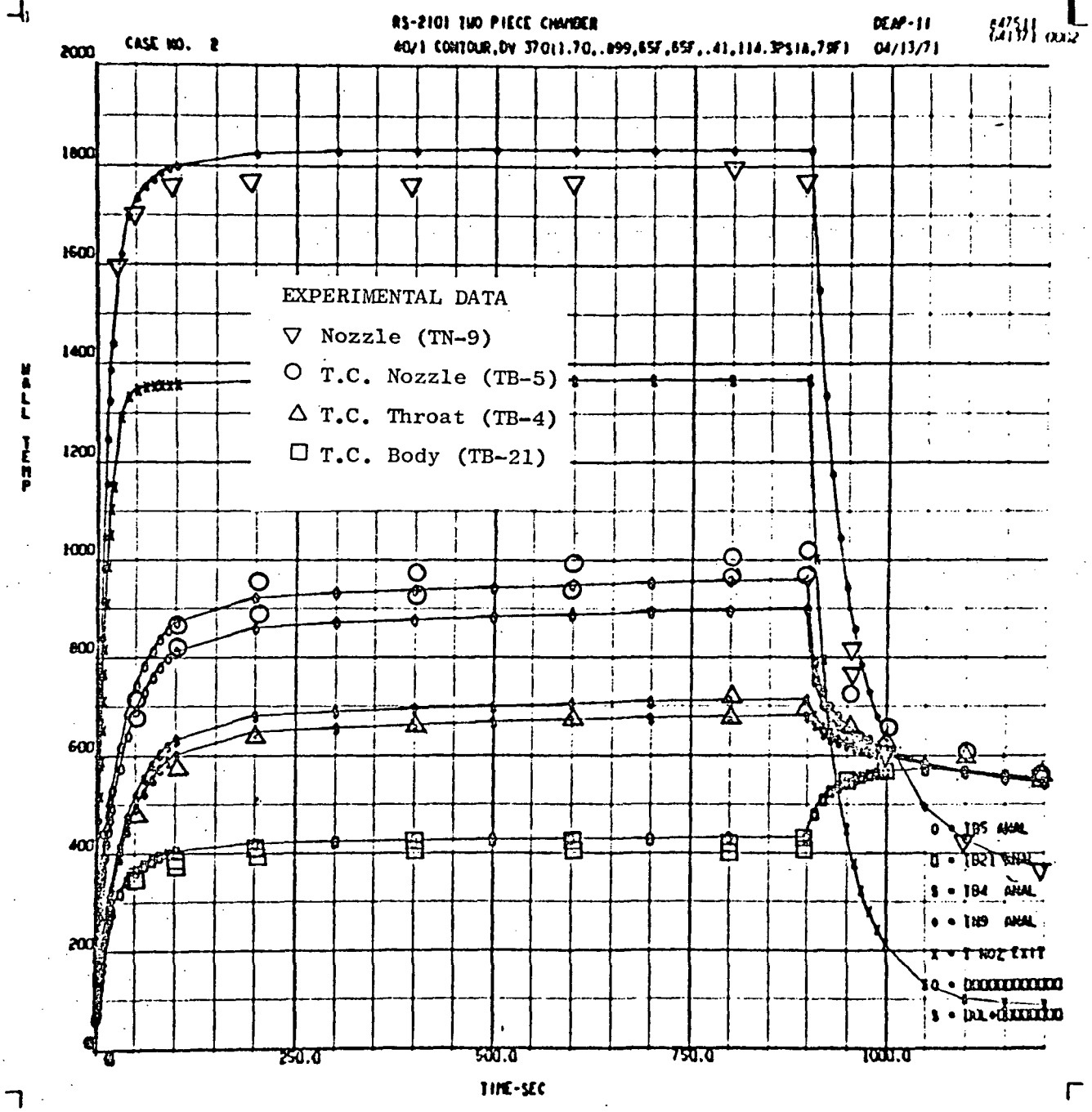

FIGURE 20

COMPARISON OF PREDICTED AND EXPERIMENTAL DATA FOR TEST DV370

TEST CELL H = 8×10^{-6} BTU $IN^2 SEC^{\circ}F$

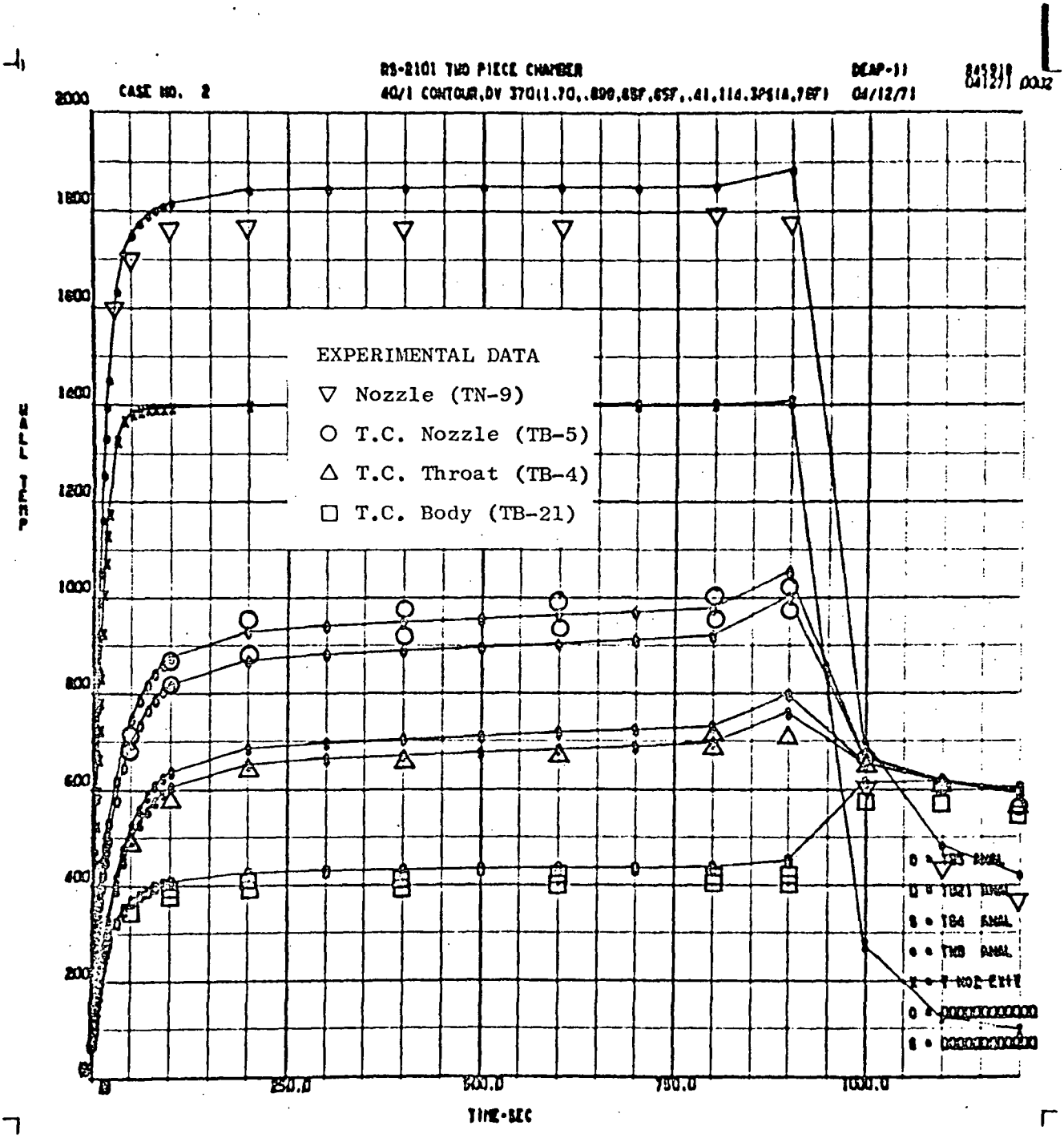

FIGURE 21

COMPARISON OF PREDICTED AND EXPERIMENTAL DATA FOR TEST DD405

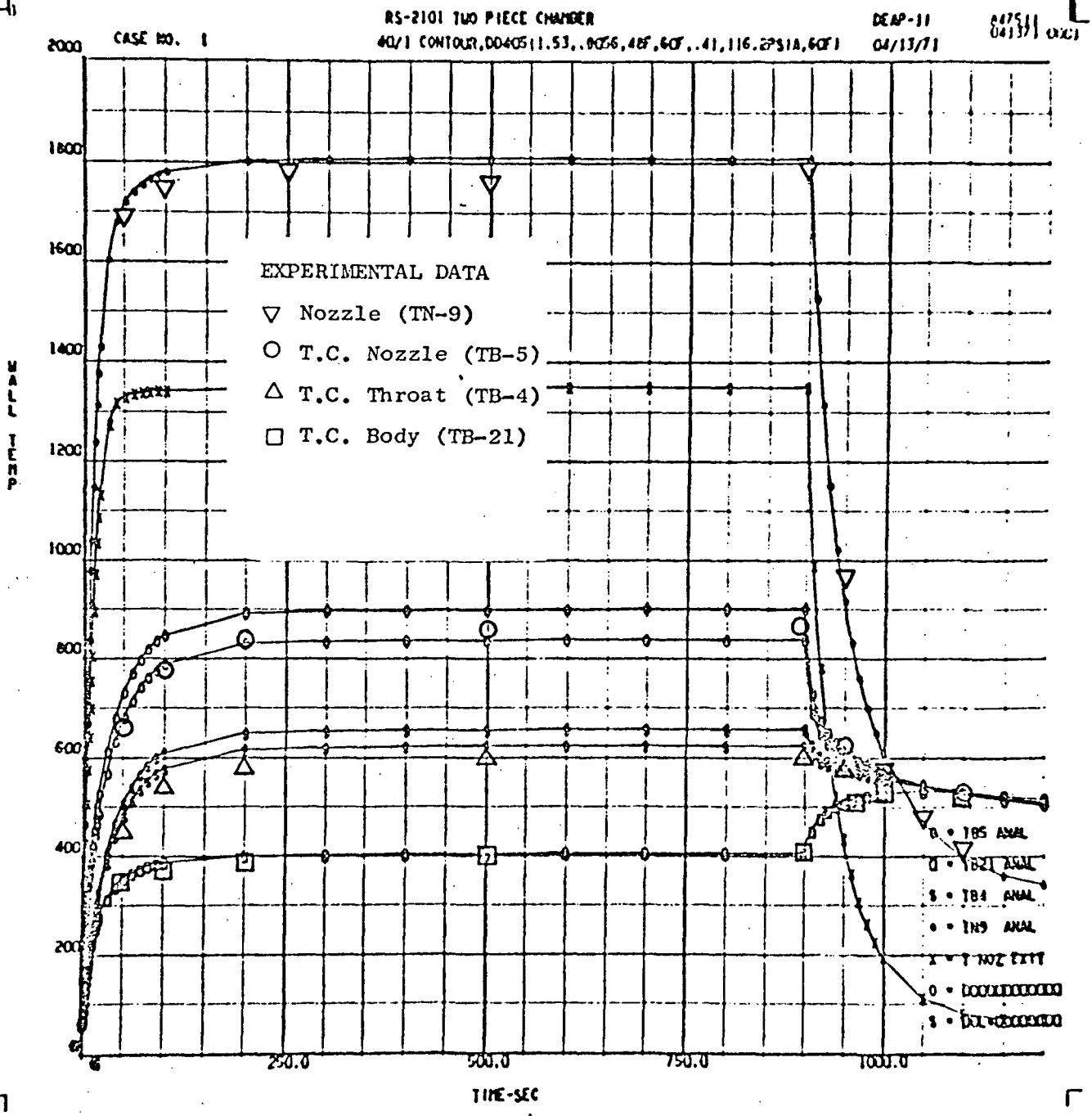

FIGURE 22

COMPARISON OF PREDICTED AND EXPERIMENTAL DATA FOR TEST DD413

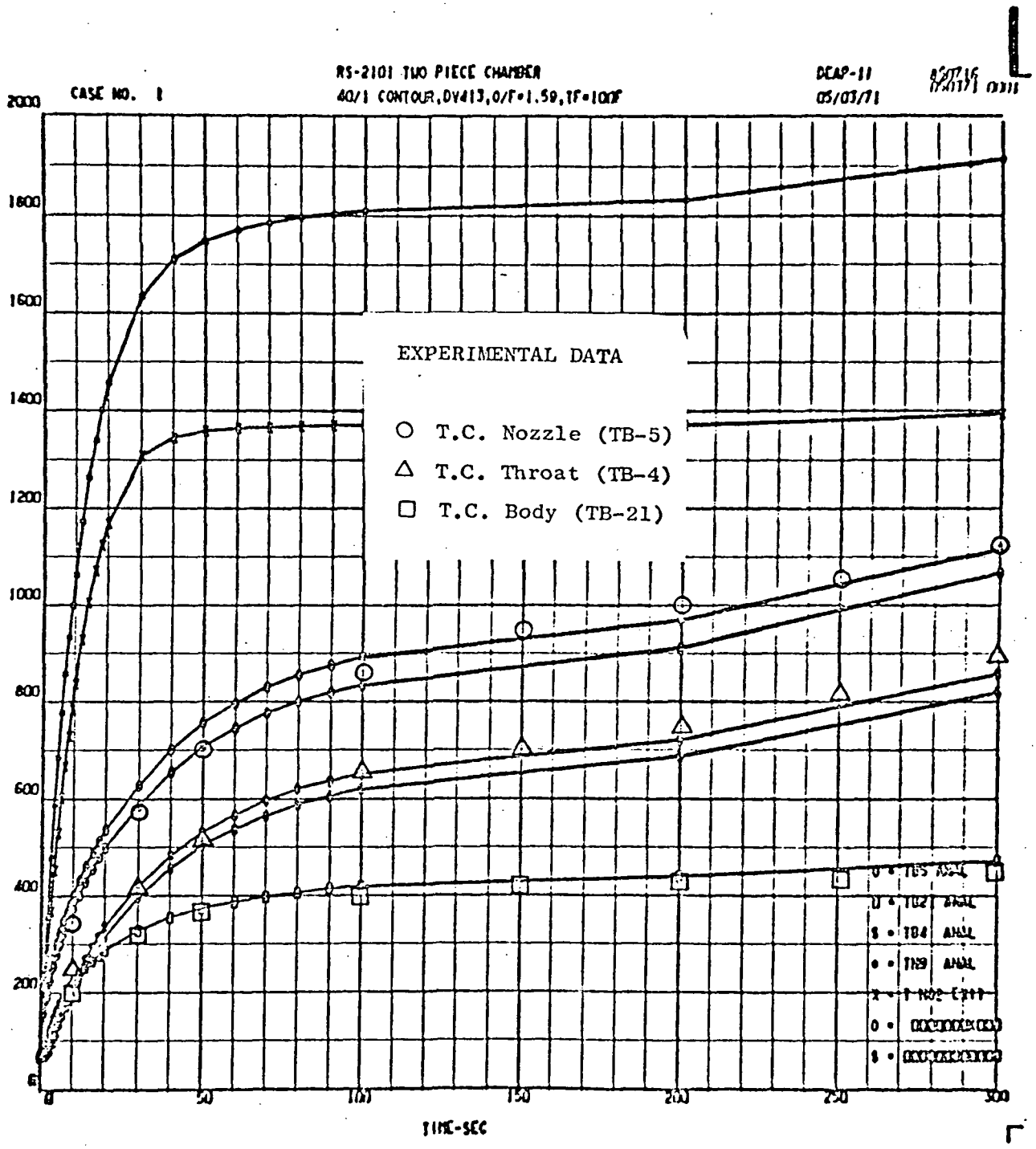

FIGURE 23

COMPARISON OF PREDICTED AND EXPERIMENTAL DATA FOR TEST DD420

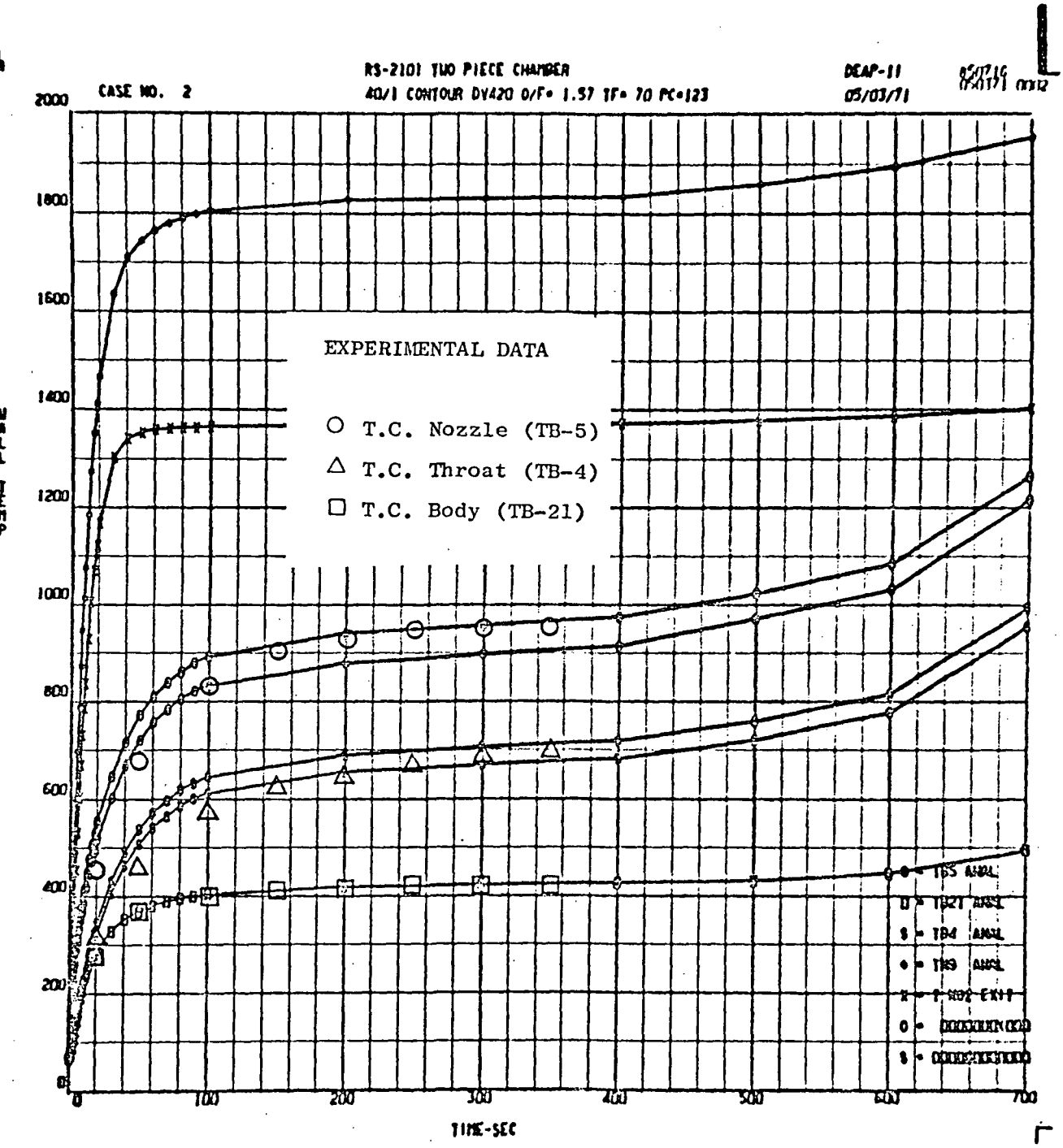

Soakback Model Calibration

The computer model used to predict soakback temperatures for the RS2101 engine uses 34 nodes to represent the engine during engine-off periods for evaluation of the thermal interactions of the various engine and system components with the beryllium thrust chamber body. Data from the interegen model discussed previously is used to reproduce engine-on operation, but the interegen analysis model is not used directly in the soakback model.

The most important parameters in the soakback model are the thermal conductances between components since the energy flowrates are low during soakback and gradients within the components are generally small. The values for these conductances between components are difficult to calculate analytically since contact resistance is usually a factor in direct connections and view factors for radiant heat transfer can only be estimated.

The procedure followed during this study was to establish a model that included all significant heat flow paths with analytical estimates of the conductances for these paths. Comparisons with test data were then used to define view factors and contact resistances that allowed predictions to match the test data. JPL Test DD405 was used for this purpose as the most complete as well as representative of available soakback data. It was also necessary to evaluate the thermal conductance between the valve coil and the valve body in order to predict coil temperatures before comparisons with data could be made. For this purpose, transient coil temperature data from a Freon bench test on an RS2101 valve was used to determine the effective coil to body conductance and check the effective thermal capacity of the coil. These data are shown in Figure 24 along with the rise rates used to calculate the coil capacitance and conductance values. Using these values in the model gave further verification of their correctness by the good agreement between predicted and experimental temperatures right after engine shutdown before energy input from the injector became significant. During the calibration of the model, it was found that the

FIGURE 24

VALVE COIL TEMPERATURE

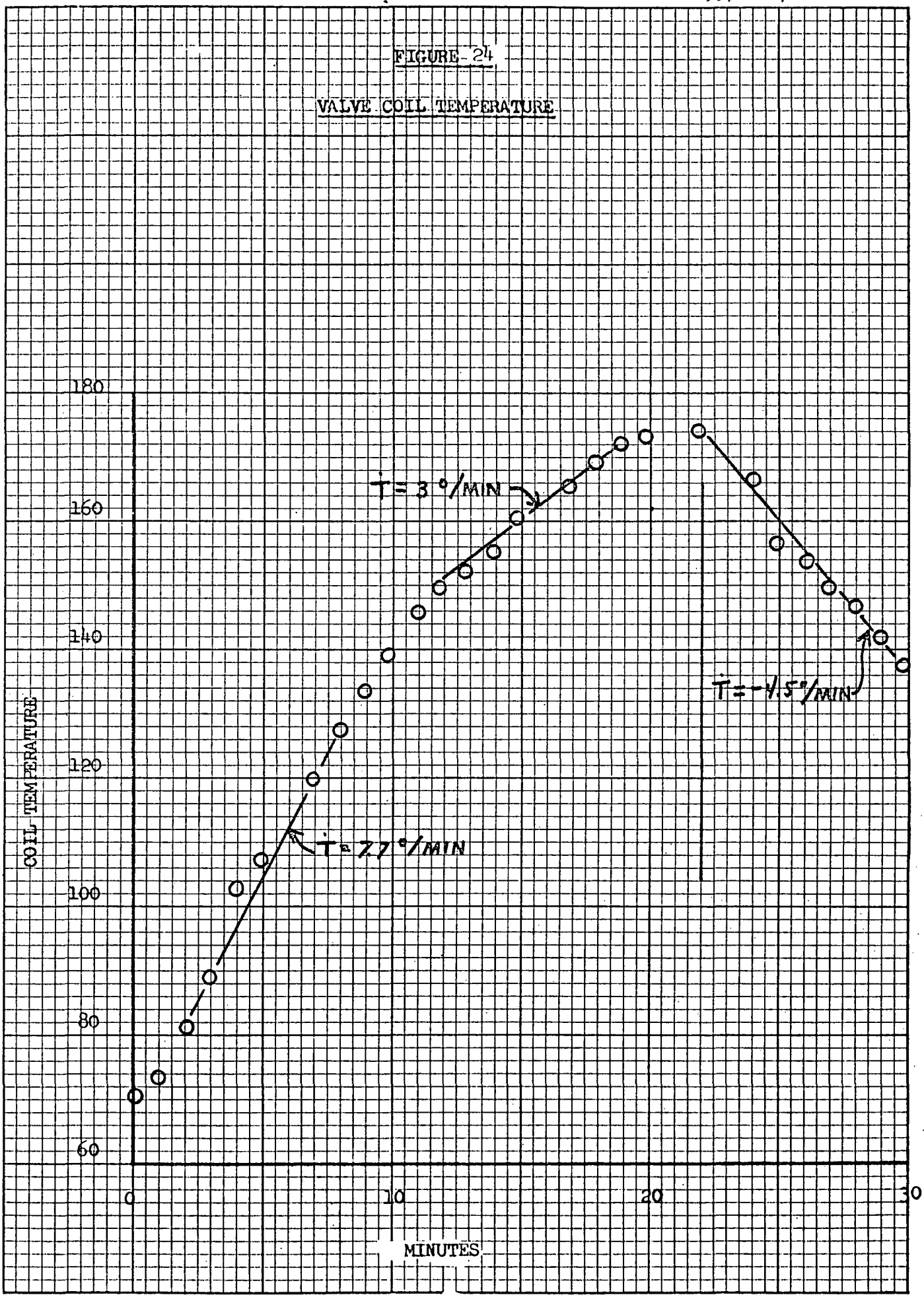

thrust mount temperatures were strongly influenced by radiation from the nozzle extension even though the view factor was very small. This is the primary cause for the almost constant rate of rise of the thrust mount temperatures and indicates that the steady state thrust mount temperatures will be considerably above the values measured thus far.

The overall agreement between the calibrated soakback model and experimental temperatures from JPL Test DD405 is shown in Figures 25 and 26. These predictions include the convective losses discussed earlier and match the peak temperatures for all components well. The transient predictions also agree with the test data except for the valve and nozzle temperatures. The predicted valve temperatures rise slower then the test data during the time period when energy from the injector is the dominant factor, but then agree with the peak temperature values, and the cooldown following this peak. This behavior is believed to be caused by the small number of nodes representing the valve and is not felt to be a serious discrepancy. As shown in Figure 26, the cooldown of the nozzle is poorly represented by the model. This is partially caused by the small number of nodes (See Figures 19 and 20 for a better prediction from the interegen model) but also indicates that the test cell walls were heated to temperatures between 150 and 200F during the engine operation as evidenced by the slow cooldown rate between 3000 and 6000 seconds.

The agreement between the soakback model predictions and test data is felt to be more than adequate and lends further substantiation to the estimated convective losses discussed earlier. Figure 27 shows the prediction for the 40:1 RS2101 configuration in a space environment to demonstrate the effects of the extra thermal losses during testing. The most significant effect is an increase of 25F in the predicted valve seat temperature.

After calibration of both analytical models was completed, the models were modified to the 60:1 configuration and used to predict the space environment performance of the modified RS2101 engine.

FIGURE 25

COMPARISON BETWEEN PREDICTED AND EXPERIMENTAL

SOAKBACK TEMPERATURES FOR TEST DD405

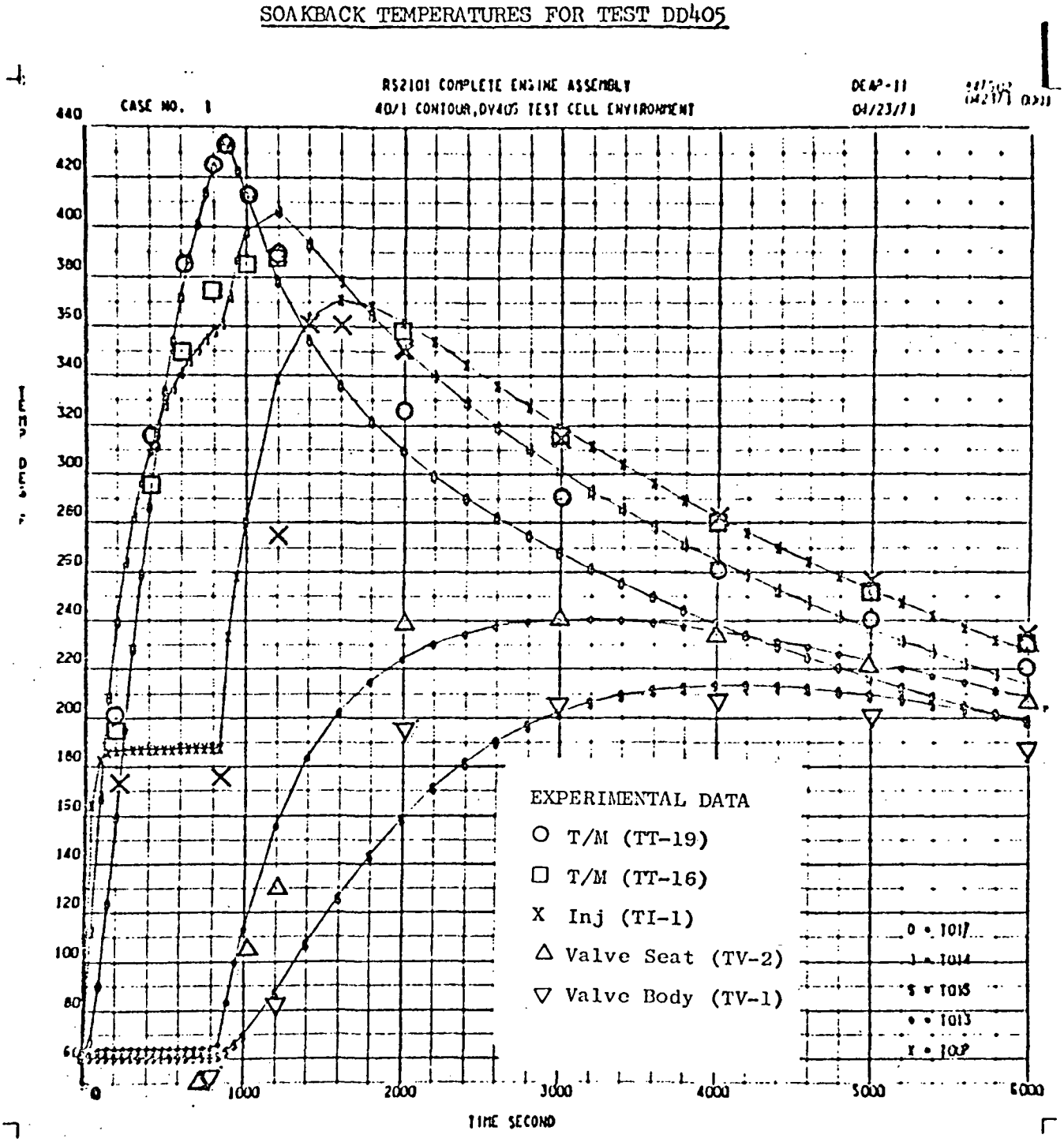

FIGURE 26

COMPARISON BETWEEN PREDICTED AND EXPERIMENTAL

SOAKBACK TEMPERATURES FOR TEST DD405

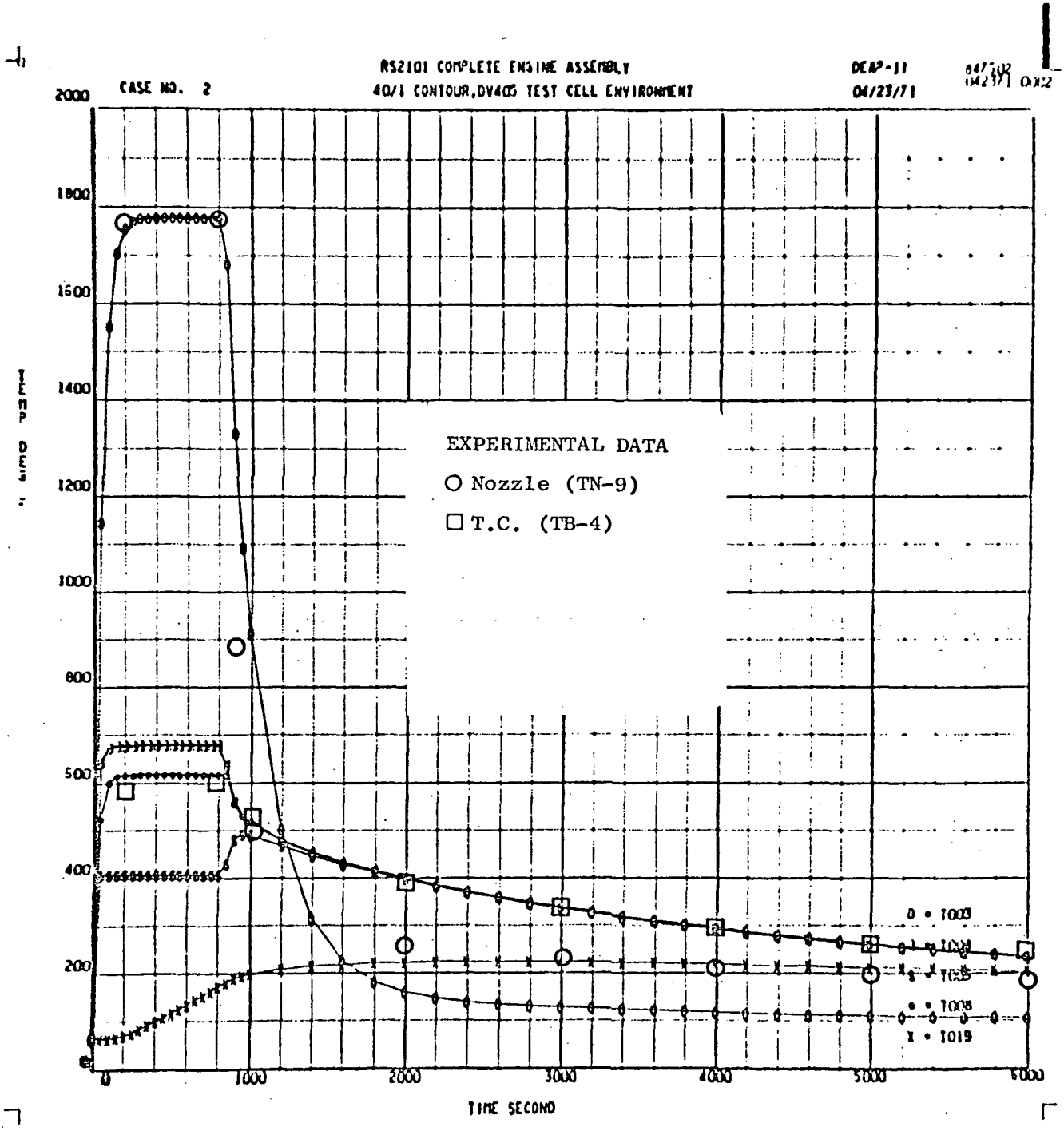

FIGURE 27

PREDICTED SOAKBACK TEMPERATURES FOR 40:1 NOZZLE

IN A SPACE ENVIRONMENT

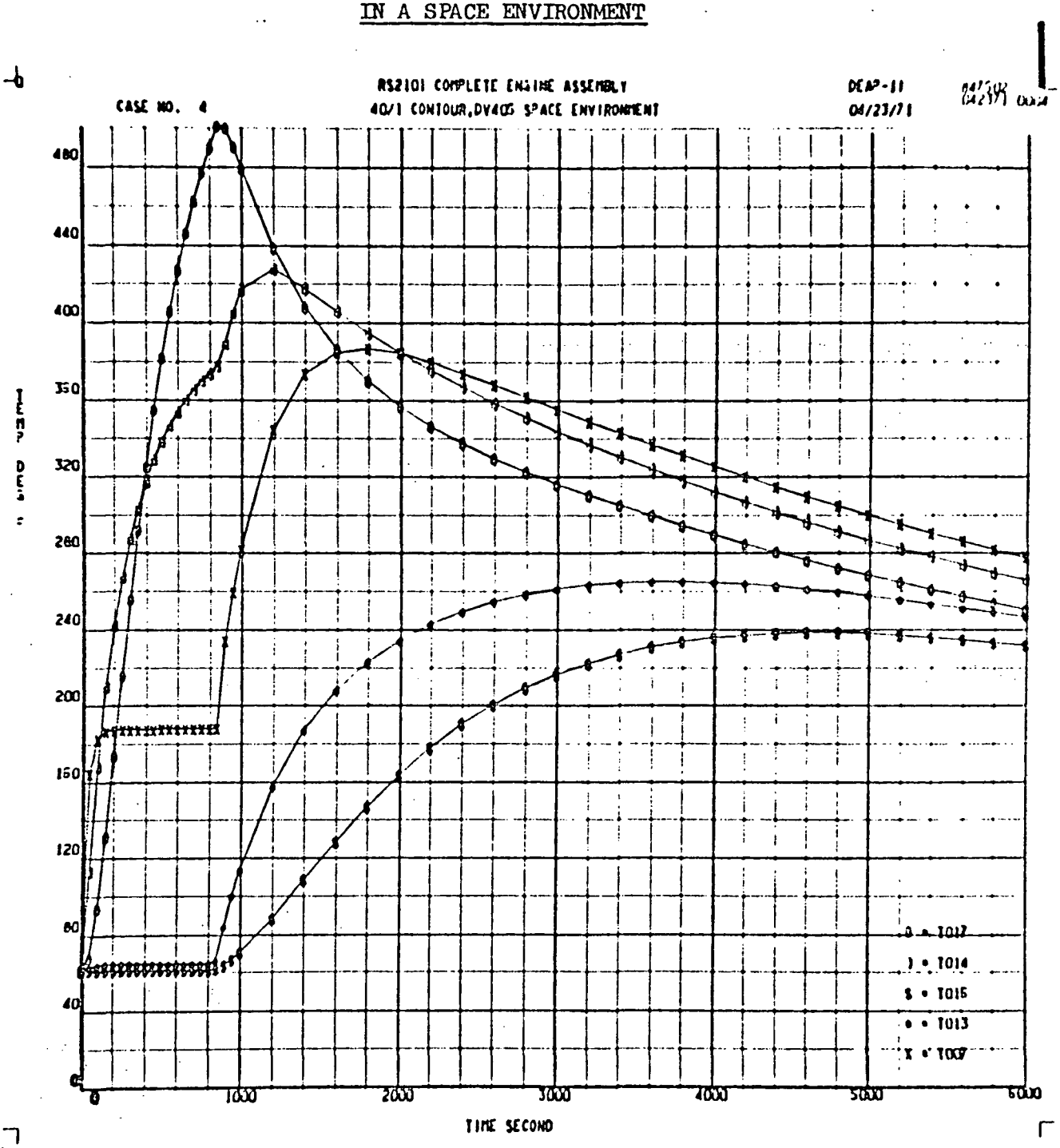

Analysis Results

The major modifications to the RS2101 engine evaluated in this study consist of:

1) A 60:1 80 percent bell L-605 nozzle extension in place of the 40:1 extension.

2) A low emissivity (.05) polished aluminum motor shield in place of the gold plated titanium shield.

3) A high emissivity (.85) thrust box enclosing the engine components to reduce the heat load to the propellant tanks.

Minor modifications to the design in terms of 1) Cat-a-lac paint applied to various surfaces and 2) a conductive ground strap (3 Watts/50F temperature differential) attached to various points on the engine were also studied to define the configuration having the best overall behavior.

The operational requirements for the modified RS2101 engine of 35 starts for 3500 seconds total burn with a 3000 second maximum burn duration are more severe than the 1971 mission requirements primarily because of the requirement for a 3000 second steady state firing capability. This duration is long enough to negate the high heat capacity of the beryllium in the case of transition from Mode I operation, and limits operation of the modified engine to those conditions where Mode I operation can be maintained.

The soakback requirements of a 250F maximum valve seat temperature and a 450F actuator clevis temperature are also restrictive on the design and preclude operation of the engine with a high temperature beryllium body.

Because of these restraints, the operational behavior of the modified design was characterized with the analytical model to define the effects of propellant temperature, mixture ratio, chamber pressure, performance level, and percent film coolant on the interegen capabilities of the design. The results of these calculations are shown in Figures 28 and 29 in terms of the beryllium thrust chamber forward end thermocouple reading and the throat station thermocouple reading. Figure 28 also shows approximate maximum forward end temperature to maintain interegen operation for the full 3000 seconds. Operation at conditions beyond these limits is of course possible, but will result in a transition from Mode I operation of the engine. While the engine will still run for at least 1000 seconds under these conditions, the much higher beryllium body temperatures that result will cause valve overheating during soakout, compromising subsequent firings.

The predicted nominal behavior of the modified RS2101 engine in space is shown in Figure 30 were true steady state interegen operation is predicted to occur after about 1000 seconds of firing.

The predicted soakback conditions for the modified engine following a 3000 second firing are shown in Figures 31 (for the nominal design) and 32 (for the best configuration evaluated). The predicted maximum temperature for the various critical components are listed in Table 13 for a number of minor design modifications which were examined in order to improve the soakback characteristic of the design.

Of the configurations considered, the modifiecations producing the most improvement in soakback characteristics were 1) use of Cat-a-lac paint on the thrust mount O.D. 2) use of a ground strap attached from the valve seat block to the thrust box and 3) use of two stripped V-seals with a modified titanium H-spacer.

The configuration incorporating all three of these changes is predicted to stay within the design limits for all components following a long duration firing of the engine (Figure 32) where Mode I operation is maintained.

FIGURE 28

THERMAL CHARACTERIZATION OF THE MODIFIED RS2101 ENGINE

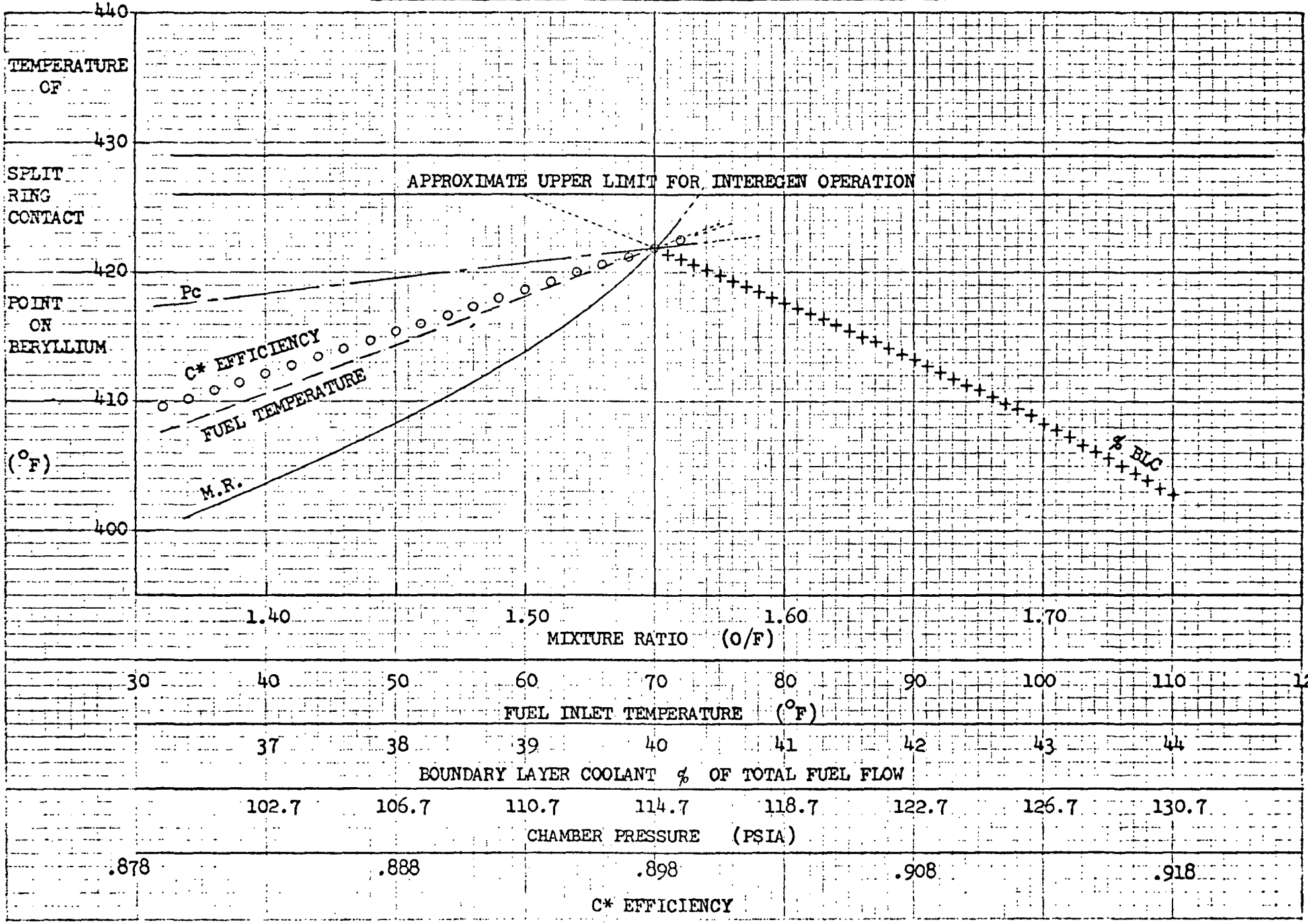

SEK LTV/RS2T/1001

FIGURE 29

THERMAL CHARACTERIZATION OF THE MODIFIED RS2101 ENGINE

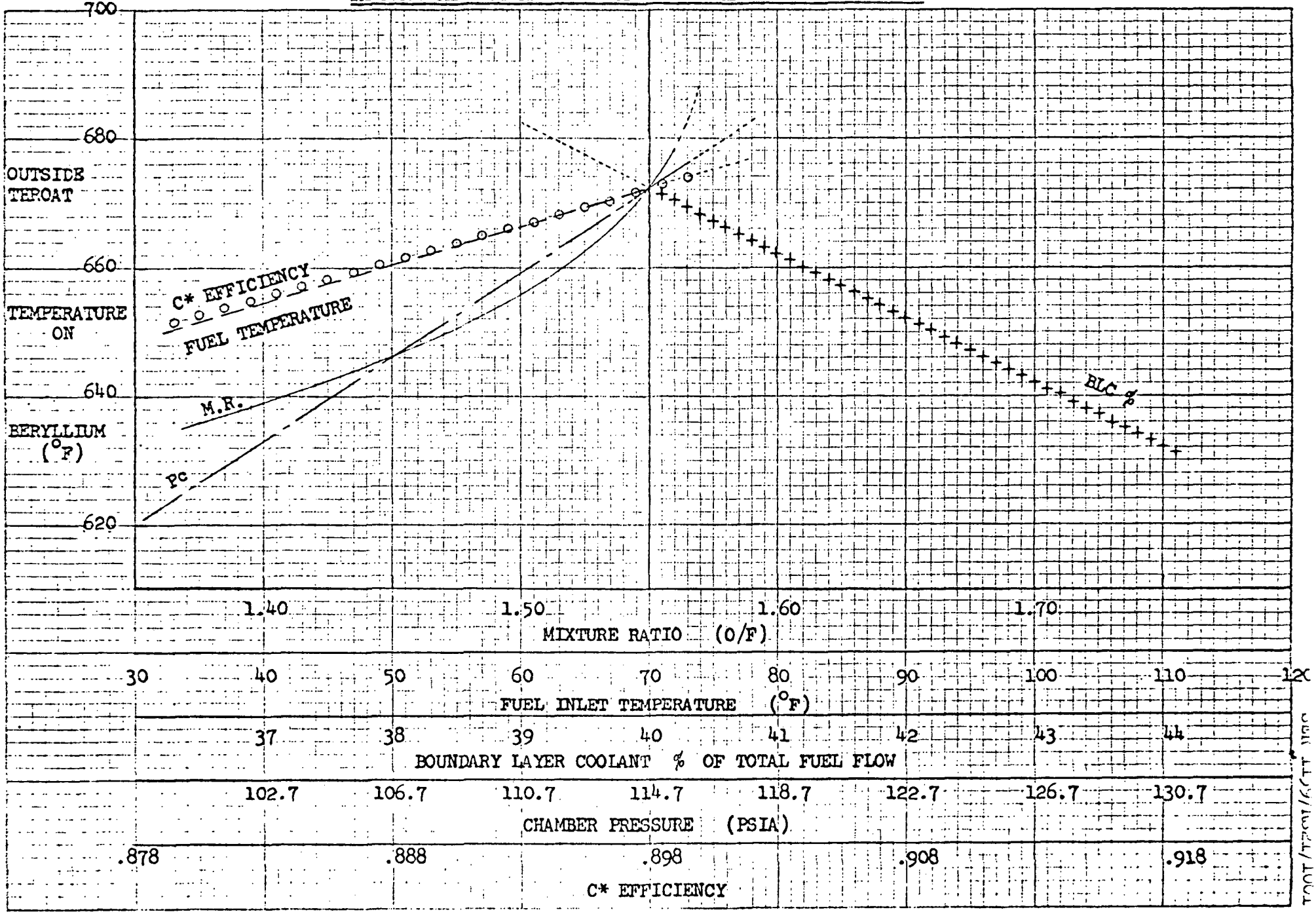

FIGURE 30

PREDICTED TEMPERATURES, MODIFIED RS2101 ENGINE

IN SPACE ENVIRONMENT

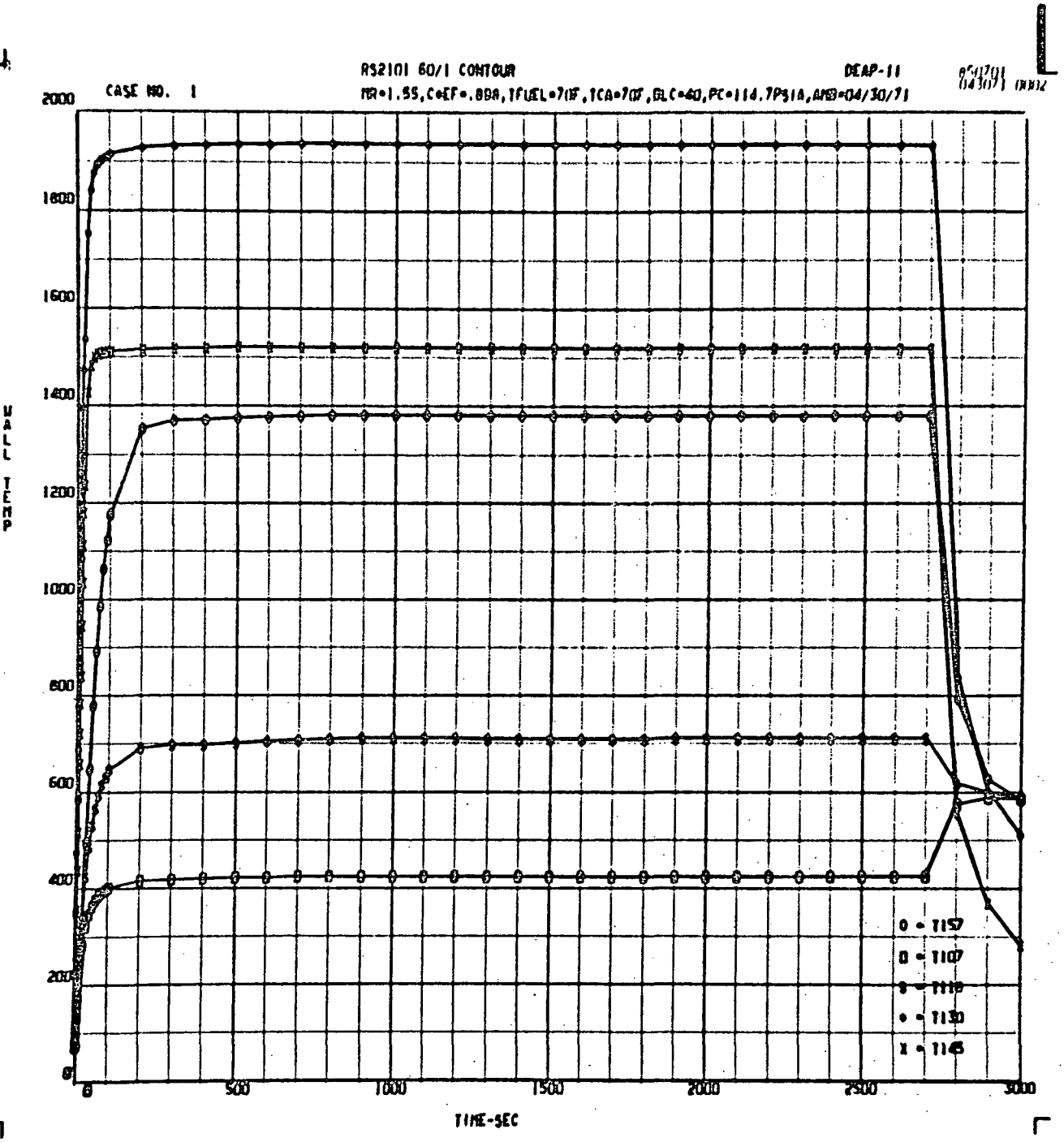

FIGURE 31

PREDICTED TEMPERATURES, MODIFIED RS2101 ENGINE

IN SPACE ENVIRONMENT (NOMINAL DESIGN)

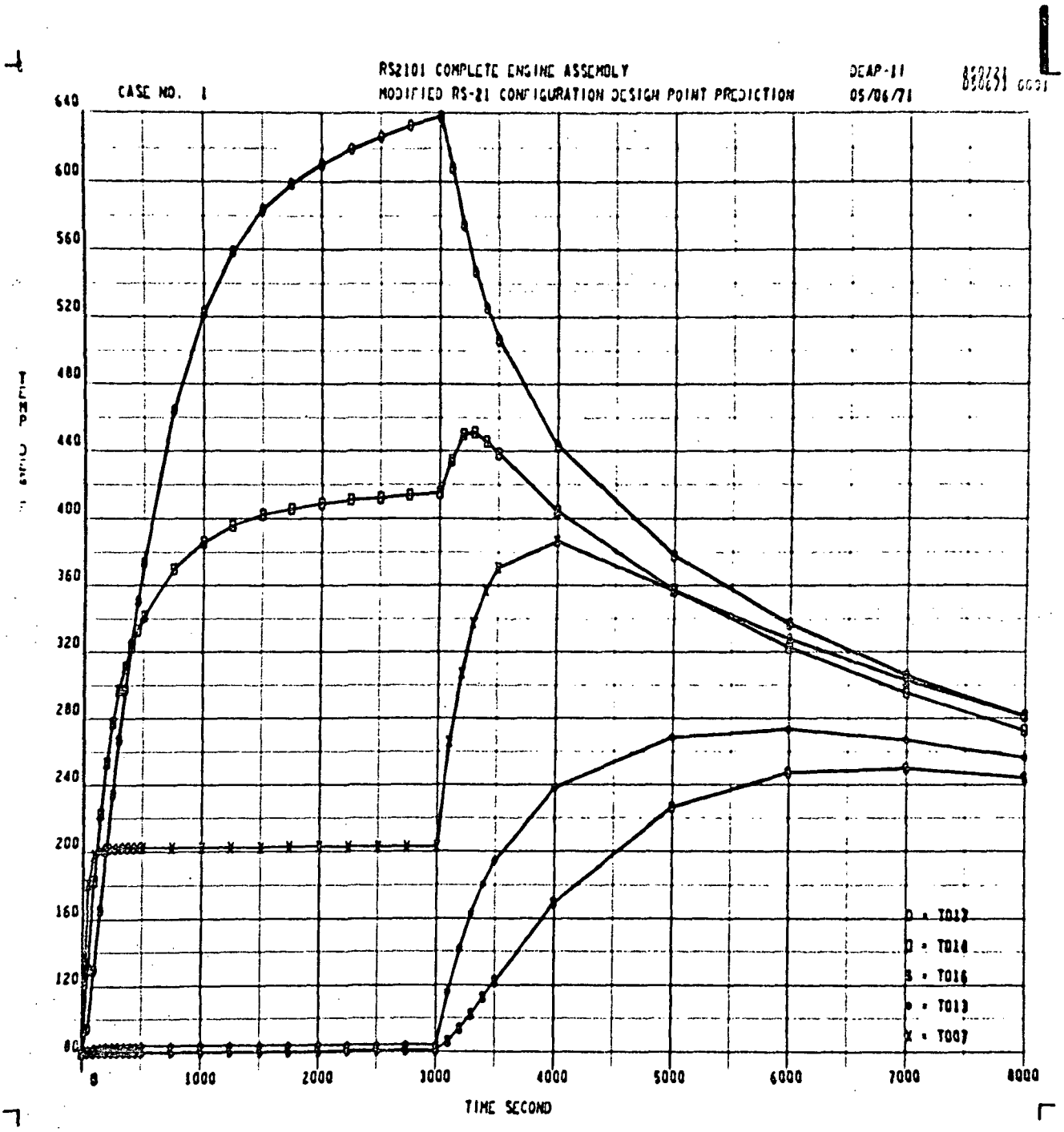

FIGURE 32

PREDICTED TEMPERATURES, MODIFIED RS2101 ENGINE

IN SPACE ENVIRONMENT (BEST CONFIGURATION EVALUATED)

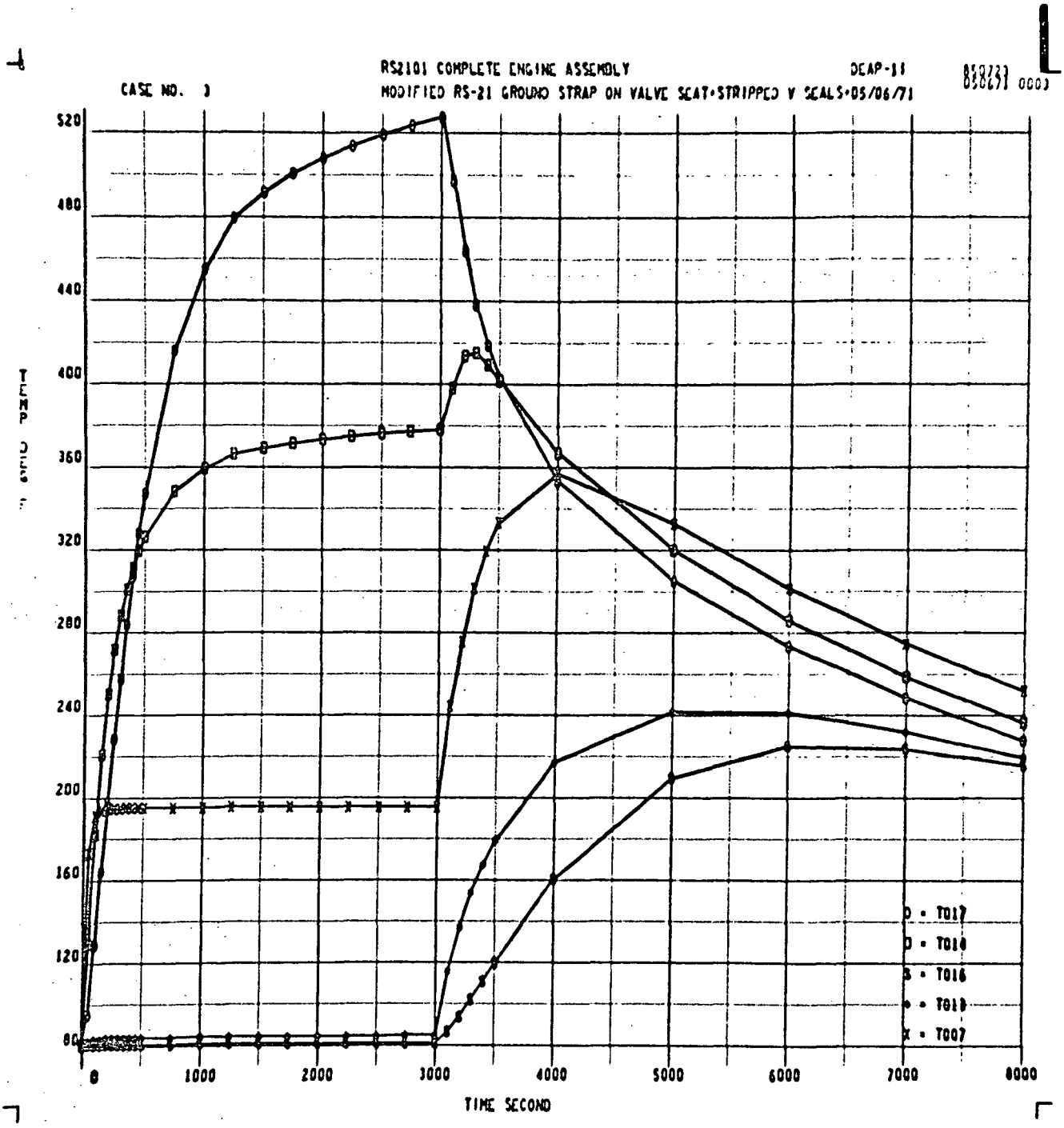

TABLE 13
MODIFIED RS-21 SOAKBACK STUDY RESULTS

MODIFICATION	MAXIMUM PREDICTED TEMPERATURES					
	VALVE SEAT	CLEVIS	THRUST MOUNT	THRUST BOX	NOZZLE	GIMBAL
NOMINAL (60/1 NOZZLE)	273	451	637	124	1862	553
Hi-E NOZZLE COATING	265	436	561	119	1679	448
Hi-E O.D. T/M	265	411	527	141	1862	526
Hi-E T/M (BOTH SIDES)	264	412	529	141	1862	527
GROUND STRAP (VALVE BODY)	265	451	637	125	1862	544
GROUND STRAP (VALVE SEAT)	254	451	637	126	1862	544
2 STRIPPED V-SEALS, MODIFIED Ti SPACER	267	455	637	124	1862	544
SAME PLUS GROUND STRAP (V. SEAT)	248	455	637	125	1862	544
SAME PLUS Hi-E O.D. T/M	242	415	526	140	1862	526
Hi-E O.D. T/M PLUS GROUND STRAP (INJECTOR)	258	411	527	145	1862	526
	HOT CHAMBER CASES					
NOMINAL	290	490	675	130	1863	553
2 STRIPPED V-SEALS, MODIFIED Ti SPACER Hi-E O.D. T/M, GROUND STRAP ON VALVE SEAT	257	448	548	148	1862	532

If a hot beryllium thrust chamber body temperature occurs, the valve temperature will exceed the 250F limit as listed in Table 13.

The heat load to the spacecraft during engine operation was predicted to be within the allowable limits for all cases considered. The heat rejection rate to a constant spacecraft sink temperature from the thrust box for the nominal case was 400 BTU for the 8000 second period analyzed and was about 2/3 of the allowable load.

Thermal Analysis Conclusions

The modified RS2101 design is capable of meeting all requirements for the engine at the nominal operating point, but has little tolerance to variations in operating conditions such as might be expected during the actual mission. To achieve a design capable of meeting the specified thermal requirements over a reasonable operating range (the specific limits desired have not yet been specified) will require either a change in the nominal operating point (and limits) or a design change to the engine that will reduce the average beryllium body temperature about 50F. This can be achieved by increasing the amount of film coolant, and/or decreasing the operating mixture ratio.

A simple design change to achieve this reduction in body temperature would be to recontour the nozzle from the present configuration to a rapid expansion 60:1 80 percent bell nozzle by increasing the initial overturning angle from 31.6 degrees to 40 degrees. This change in contour is shown in Figure 33 and was studied previously (Ref. 7 and 8) as a means to improve the operation of 300 lb thrust interegen engines.

These studies indicated a reduction of 150F in throat temperatures, 75F in average body temperature, and 50F in maximum nozzle temperature could be achieved by this recontouring with less than a 0.5 percent decrease in performance relative to the optimum 80 percent bell configuration. For the modified RS2101 design the performance loss should be less than 0.3 percent. This type of nozzle contour was used under NAS3-12071, Ref. 9, and gave experimental temperatures in agreement with the analytical predictions as shown in Figure 34.

FIGURE 33

60:1 NOZZLE CONTOUR COMPARISON

NEAR NOZZLE ATTACH POINT

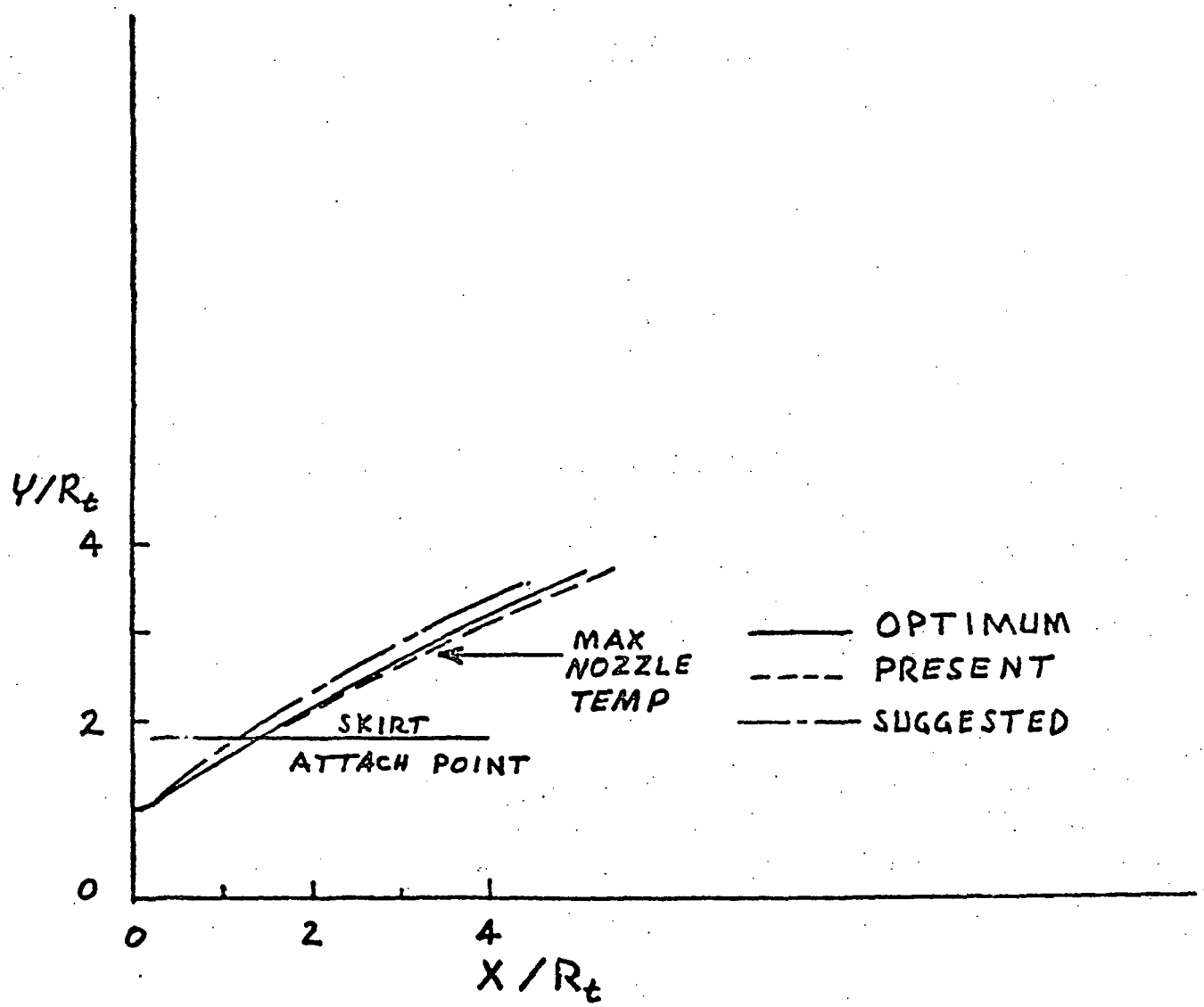

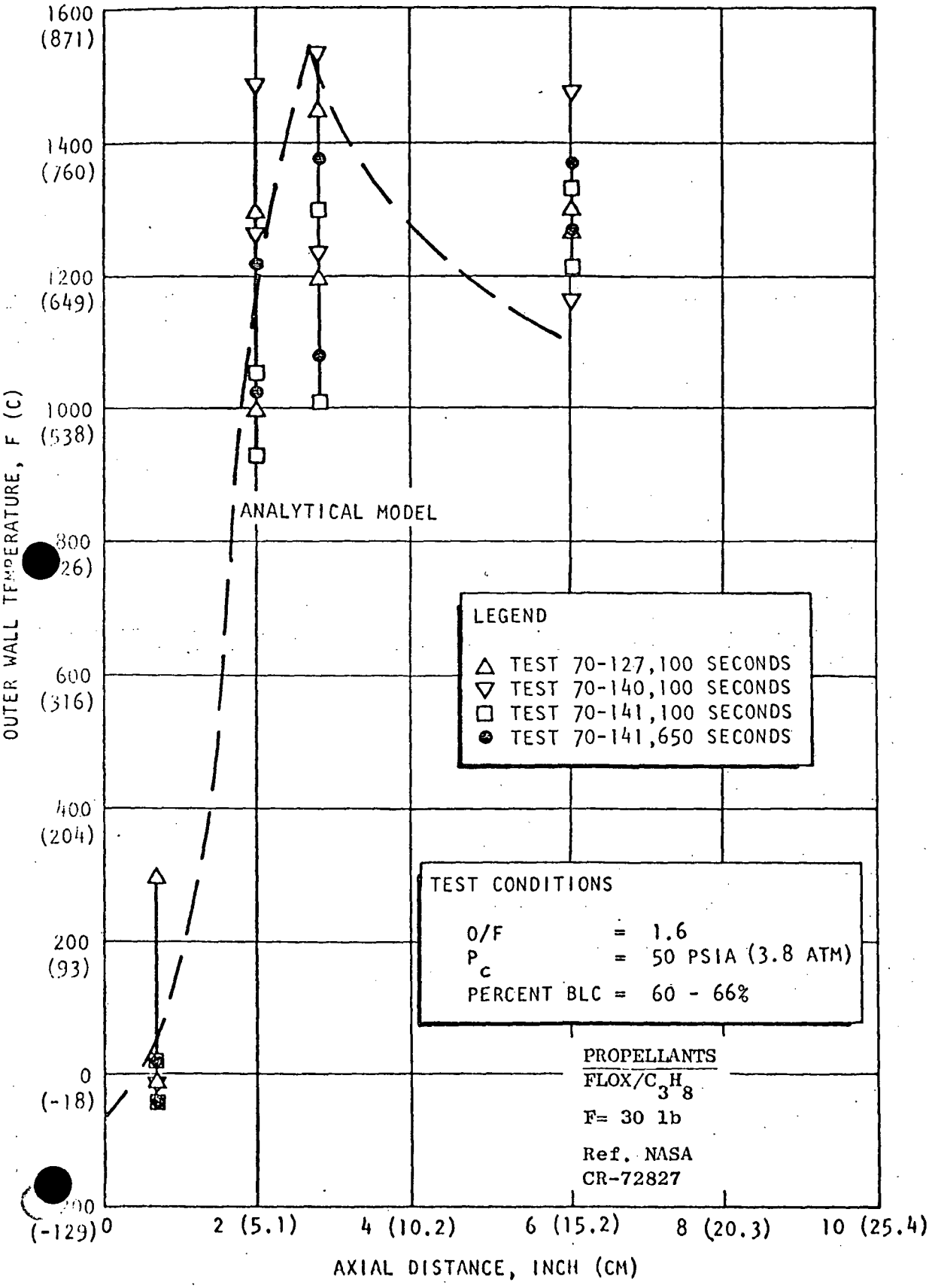

Figure 34 Comparison of Predicted and Experimental Steady-State

STRUCTURAL ANALYSIS

Detailed structural analyses were conducted to determine the effects of replacing the RS2101 engine 40:1 nozzle extension with a 60:1 extension in light of new operating and environmental requirements. The analysis considered the structural limitations imposed on the nozzle joint and the adjacent thrust chamber and nozzle extension during both operational and non-operational environments.

Thrust Chamber Damage Analysis

A finite element elastic-plastic computer program (Ref. 10) was used to determine the state of stress and strain in the thrust chamber. The thrust chamber cross section is divided into a series of ring elements and the computer program solves for the compatible forces and moments and the resulting stresses and strains due to the temperature environment. The computer adjusts the secant modulus for each element strained beyond the yield point and, using an iterative solution process, obtains a plastic solution. The computer model used for the analysis (Figure 35) consisted of 651 ring elements.

Once the strains are calculated a damage analysis can be performed for any location in the thrust chamber. This analysis was restricted to the thrust chamber throat inner diameter, which was subjected to the most severe operating environment. Computer solutions were obtained for the Acceptance Test and Mission Duty Cycle (MDC) engine firing requirements shown in Table 14. The plastic strain was calculated for each firing by subtracting the elastic strain from the total strain values calculated. Figure 36 shows beryllium typical and minimum tensile yield strength versus temperature used to calculate plastic strain.

The damage analysis uses Miner's rule which defines damage as

$$\text{Damage} = \frac{\text{number of applied cycles } (n)}{\text{number of cycles to failure } (N)}$$

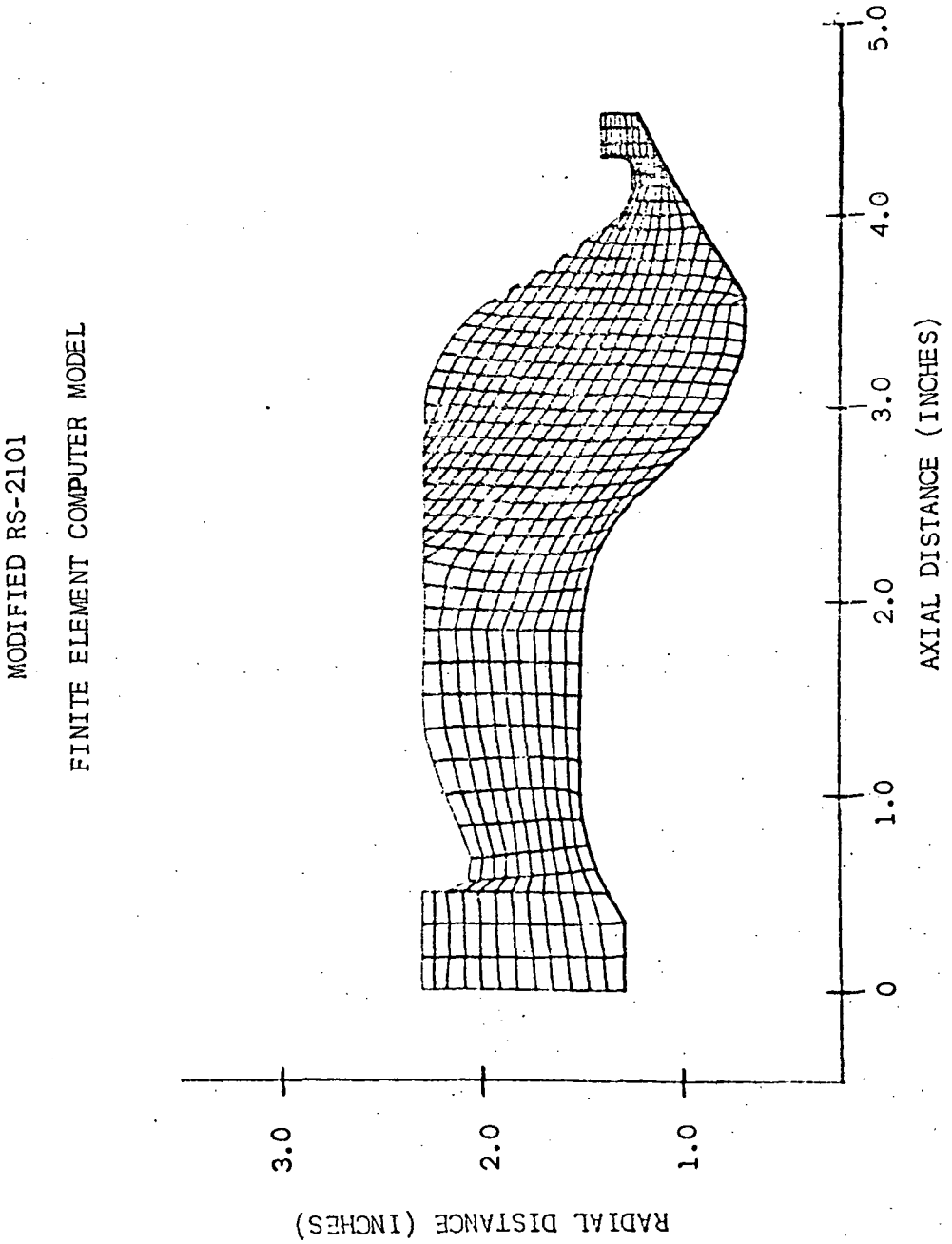
MODIFIED RS-2101
FINITE ELEMENT COMPUTER MODEL
AXIAL DISTANCE (INCHES)
0
1.0
2.0
3.0
4.0
5.0
RADIAL DISTANCE (INCHES)
1.0
2.0
3.0

FIGURE 35

MODIFIED RS-2101

ENGINE OPERATION REQUIREMENTS

EVENT	DURATION (SEC)	NUMBER OF CYCLES
ACCEPTANCE TESTING	10 2700	4 1
MISSION DUTY CYCLE	36 15 2700 128 24 14 8 3 .4	1 1 1 1 1 1 8 8 8

TABLE 14

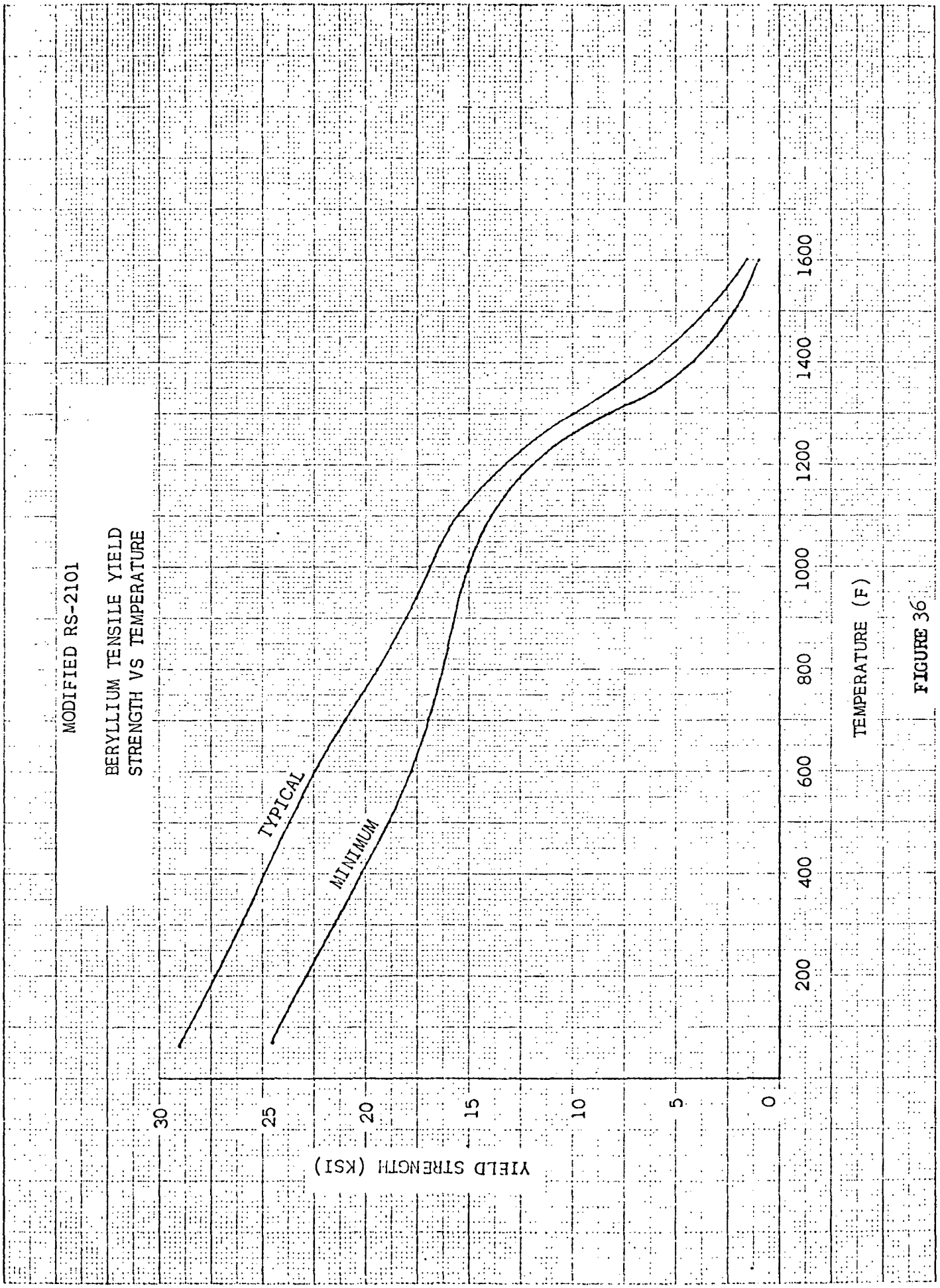
MODIFIED RS-2101
BERYLLIUM TENSILE YIELD
STRENGTH VS TEMPERATURE
TYPICAL
MINIMUM
YIELD STRENGTH (KSI)
30
25
20
15
10
5
0
200
400
600
800
1000
1200
1400
1600
TEMPERATURE (F)

FIGURE 36

N is determined using the following expression derived by Morrow:

$$N = \frac{1}{2} \left(\frac{2 \times e}{\epsilon p} \right)^{1.5}$$

where: e = percent elongation

ϵp = percent plastic strain amplitude

The throat damage is calculated separately for the heatup and cooldown cycles for each engine firing using a weighted average elongation to account for the drastic variation in beryllium elongation (Fig.37). Each complete damage cycle consists of damage sustained during engine firing heatup (1/2 cycle) and during cooldown after engine cutoff (1/2 cycle). The heatup damage is calculated using plastic strain increments of .01%. The cooldown damage for any engine firing duration is calculated using the cutoff plastic strain amplitude acting over the temperature range from cutoff to soakback temperature. The total damage at any run duration is the summation of the heatup and cooldown cycles.

The thrust chamber throat section I.D. and O.D. temperature vs firing time is shown in Fig. 38. Figures 37 and 38 were used to obtain the beryllium transverse percent elongation vs firing time shown in Fig.39. Figure 40 shows the throat I.D. percent plastic strain vs temperature using minimum and typical material tensile yield strength. Figures 37 and 40 are used to plot the throat I.D. percent plastic strain vs firing time shown in Fig.41.

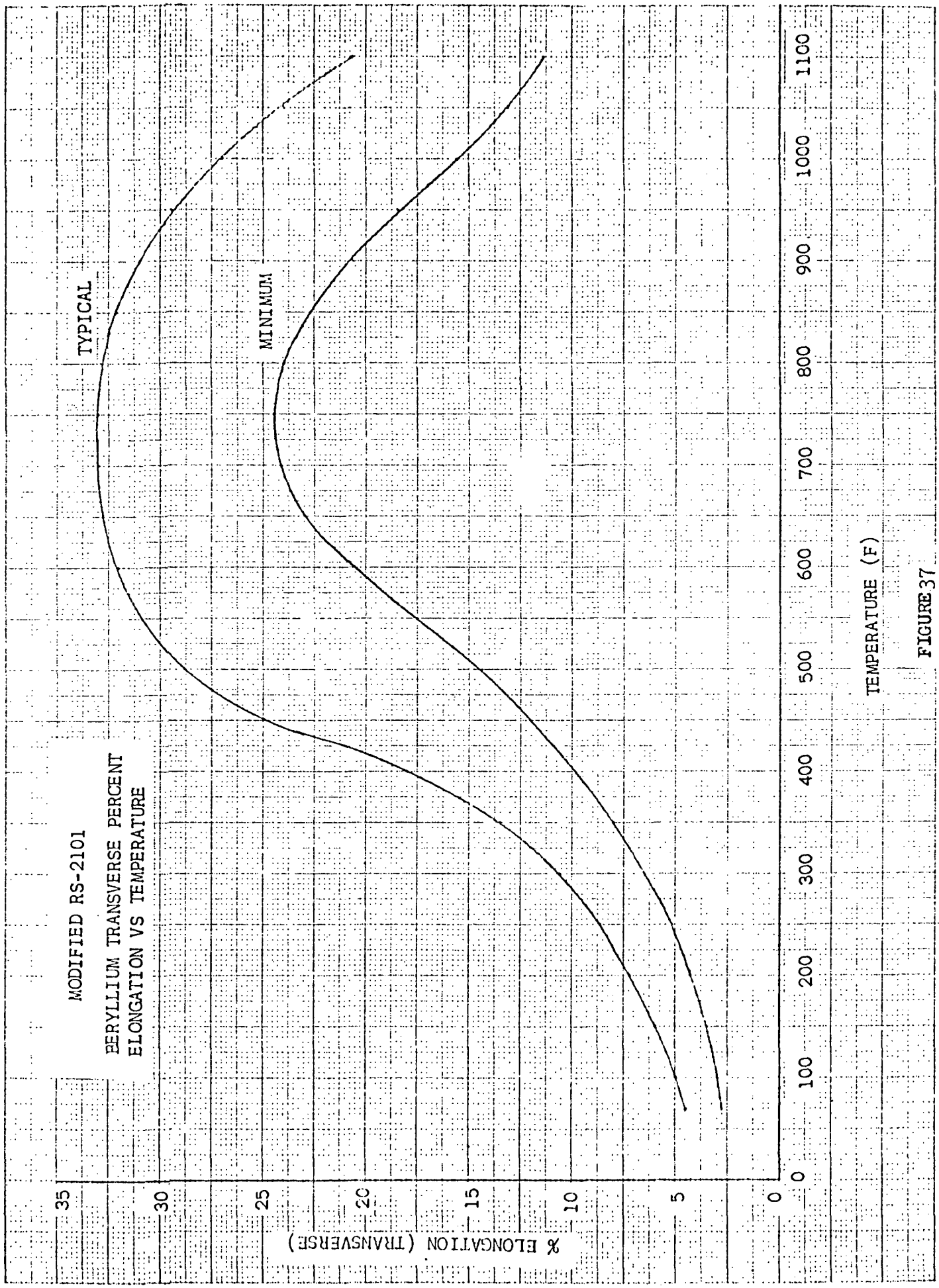
MODIFIED RS-2101
BERYLLIUM TRANSVERSE PERCENT ELONGATION VS TEMPERATURE
TYPICAL
MINIMUM
% ELONGATION (TRANSVERSE)
TEMPERATURE (F)
0
5
10
15
20
25
30
35
0
100
200
300
400
500
600
700
800
900
1000
1100

FIGURE 37

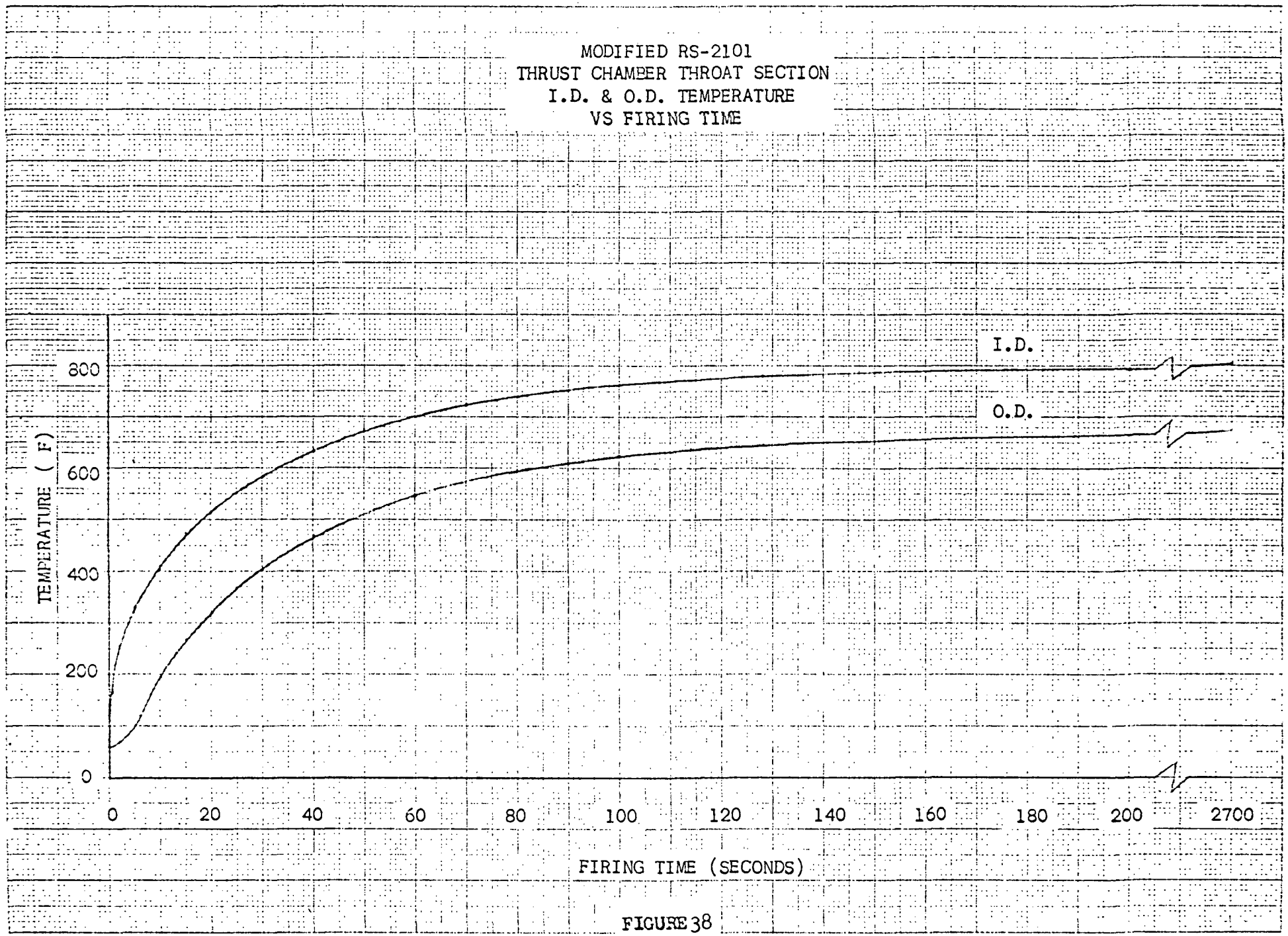

FIGURE 38

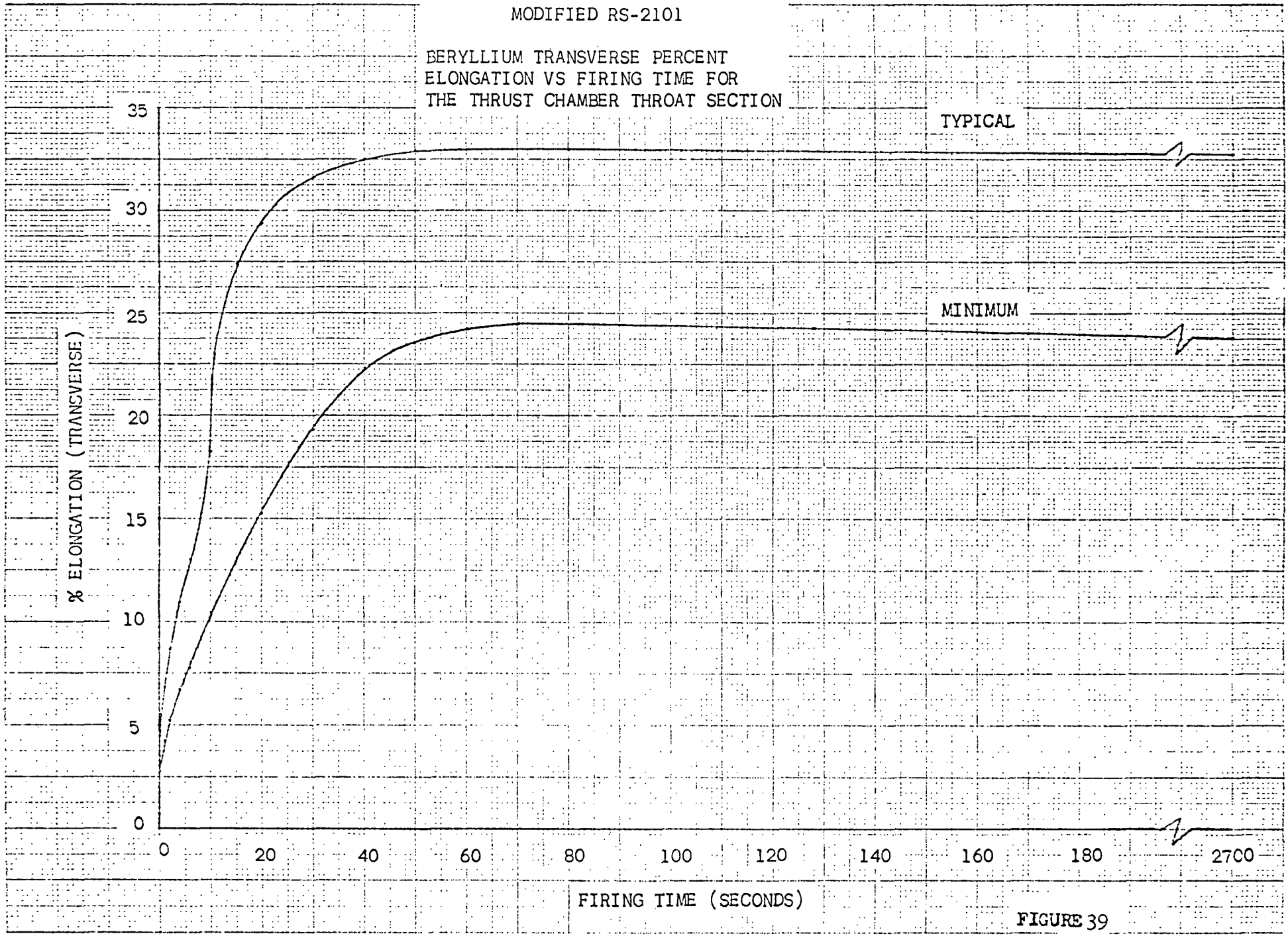
MODIFIED RS-2101
BERYLLIUM TRANSVERSE PERCENT ELONGATION VS FIRING TIME FOR THE THRUST CHAMBER THROAT SECTION
TYPICAL
MINIMUM
% ELONGATION (TRANSVERSE)
35
30
25
20
15
10
5
0
0
20
40
60
80
100
120
140
160
180
2700
FIRING TIME (SECONDS)

FIGURE 39

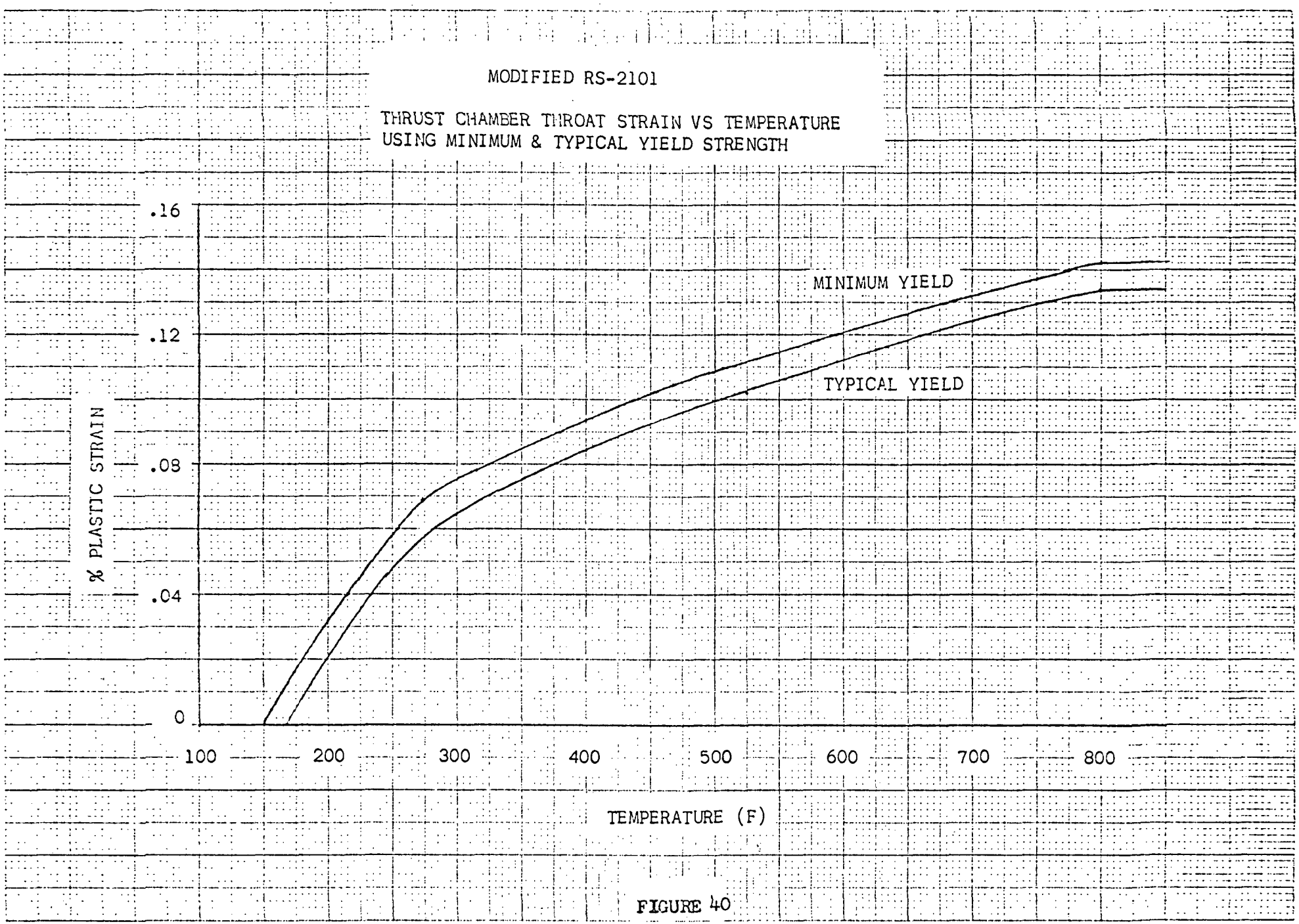

FIGURE 40

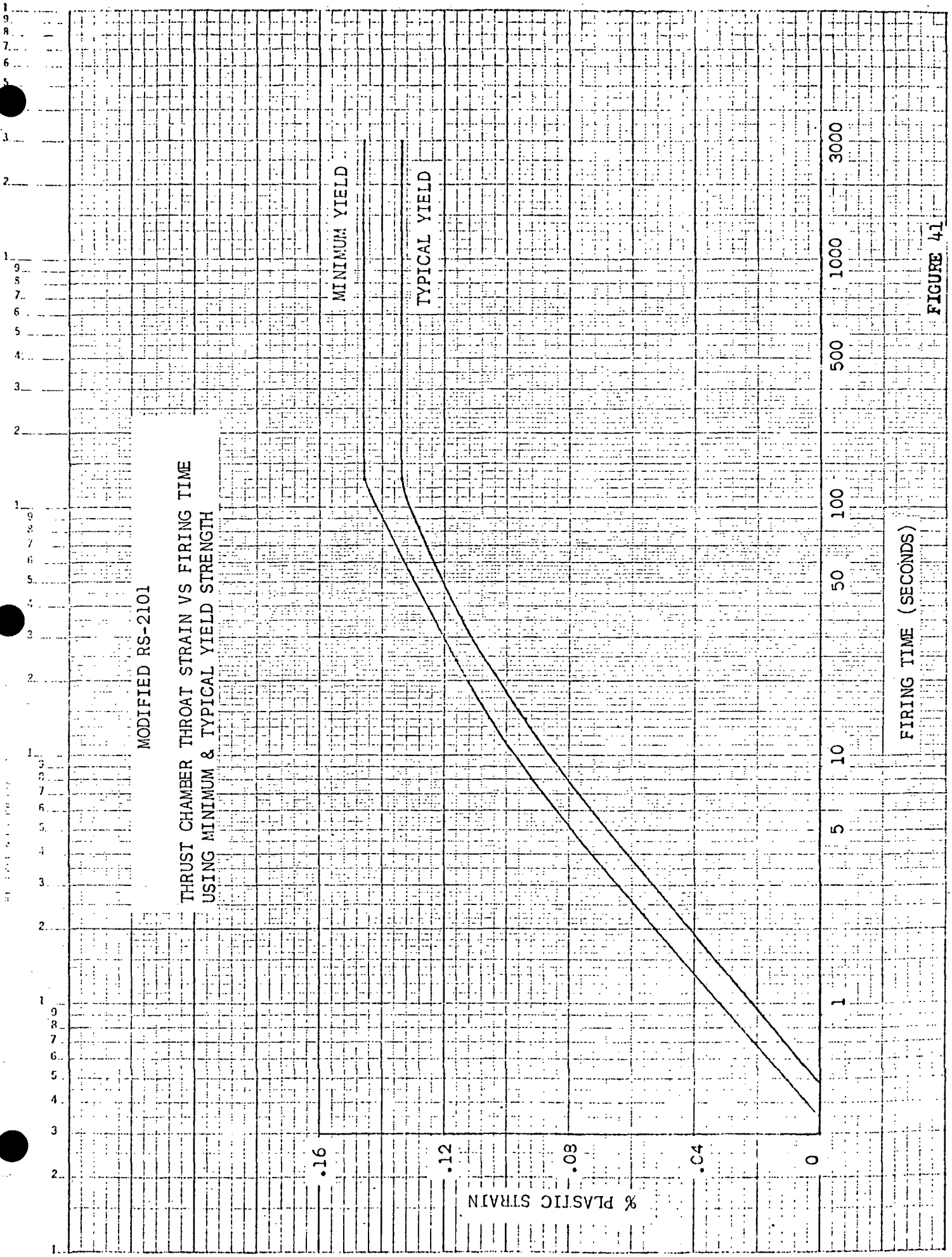
MODIFIED RS-2101
THRUST CHAMBER THROAT STRAIN VS FIRING TIME
USING MINIMUM & TYPICAL YIELD STRENGTH
MINIMUM YIELD
TYPICAL YIELD
% PLASTIC STRAIN
.16
.12
.08
.04
0
FIRING TIME (SECONDS)
1
5
10
50
100
500
1000
3000

FIGURE 41

An example of the analysis procedure for an 8 second firing is presented. The thrust chamber throat section I.D. and O.D. temperature vs firing time is provided in Fig. 42. As shown, the I.D. temperature reaches a maximum of 386F at cutoff (8 seconds) then decays until the I.D. and O.D. temperatures reach 227F, 4.5 seconds after cutoff. The plastic strain at cutoff is .092%.

Table 15 shows the damage increment calculation results using plastic strain increments of .01%. For example, a damage increment of .00011 results when the plastic strain is increased from .04 to .05% when the material elongation range is from 4.6 to 5.0%. The total damage due to the heatup cycle is the summation of the damaged increment column (.00084).

The cooldown cycle damage for the 8 second firing is summarized in Table 16. The weighted average elongation value of 6.83% is obtained by averaging the elongation in 20F temperature increments between the cutoff temperature of 386F and the soakback temperature of 227F. The cutoff plastic strain amplitude (.092%) is used for the cooldown portion of the cycle. Substituting into the damage equation gives a cooldown damage of .00055. The total damage resulting from the 8 second firing is the summation of the heatup and cooldown portions of the cycle (.00139).

The damage analysis is summarized in Fig. 43. As shown, the heatup cycle damage curve approaches .001 after 150 seconds duration, at which time the material elongation is increased to a level where the increment of damage is negligible between 150 and 3000 seconds. The cooldown damage curve peaks at a value of .00065 after 3 seconds duration, then decays to .00016 at 3000 seconds.

MODIFIED RS-2101

THRUST CHAMBER THROAT SECTION I.D. AND O.D. TEMPERATURE VS FIRING TIME FOR AN 8 SECOND ENGINE FIRING

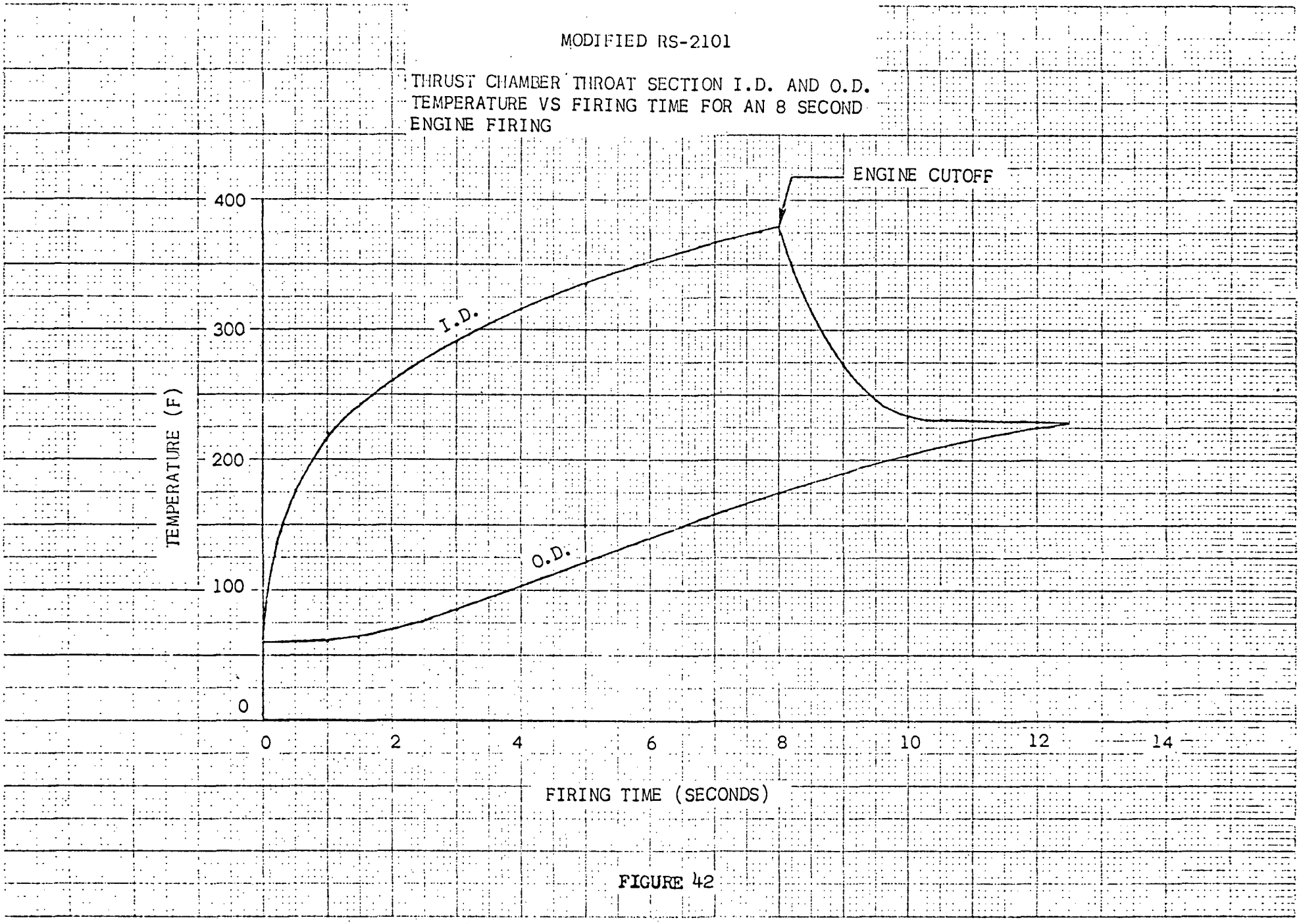

FIGURE 42

HEATUP CYCLE FOR 8 SECOND ENGINE FIRING

PLASTIC STRAIN RANGE (%)	ELONGATION RANGE (%)	DAMAGE INCREMENT
0 - .01	3.5 - 3.7	.00005
.01 - .02	3.7 - 4.0	.00009
.02 - .03	4.0 - 4.3	.00010
.03 - .04	4.3 - 4.6	.00011
.04 - .05	4.6 - 5.0	.00011
.05 - .06	5.0 - 5.4	.00011
.06 - .07	5.4 - 6.0	.00010
.07 - .08	6.0 - 7.3	.00009
.08 - .092	7.3 - 9.2	.00008
		$\sum$ = .00084

TABLE 15

COOLDOWN CYCLE FOR 8 SECOND ENGINE FIRING

CUTOFF TEMPERATURE	=	386 F
SOAKBACK TEMPERATURE	=	227 F
CUTOFF STRAIN AMPLITUDE	=	.092%
WEIGHTED AVERAGE ELONGATION	=	6.83%
COOLDOWN DAMAGE	=	.00055

TOTAL DAMAGE (8 SECOND FIRING)

HEATUP CYCLE	=	.00084
COOLDOWN CYCLE	=	.00055
	$\sum$ =	.00139

TABLE 16

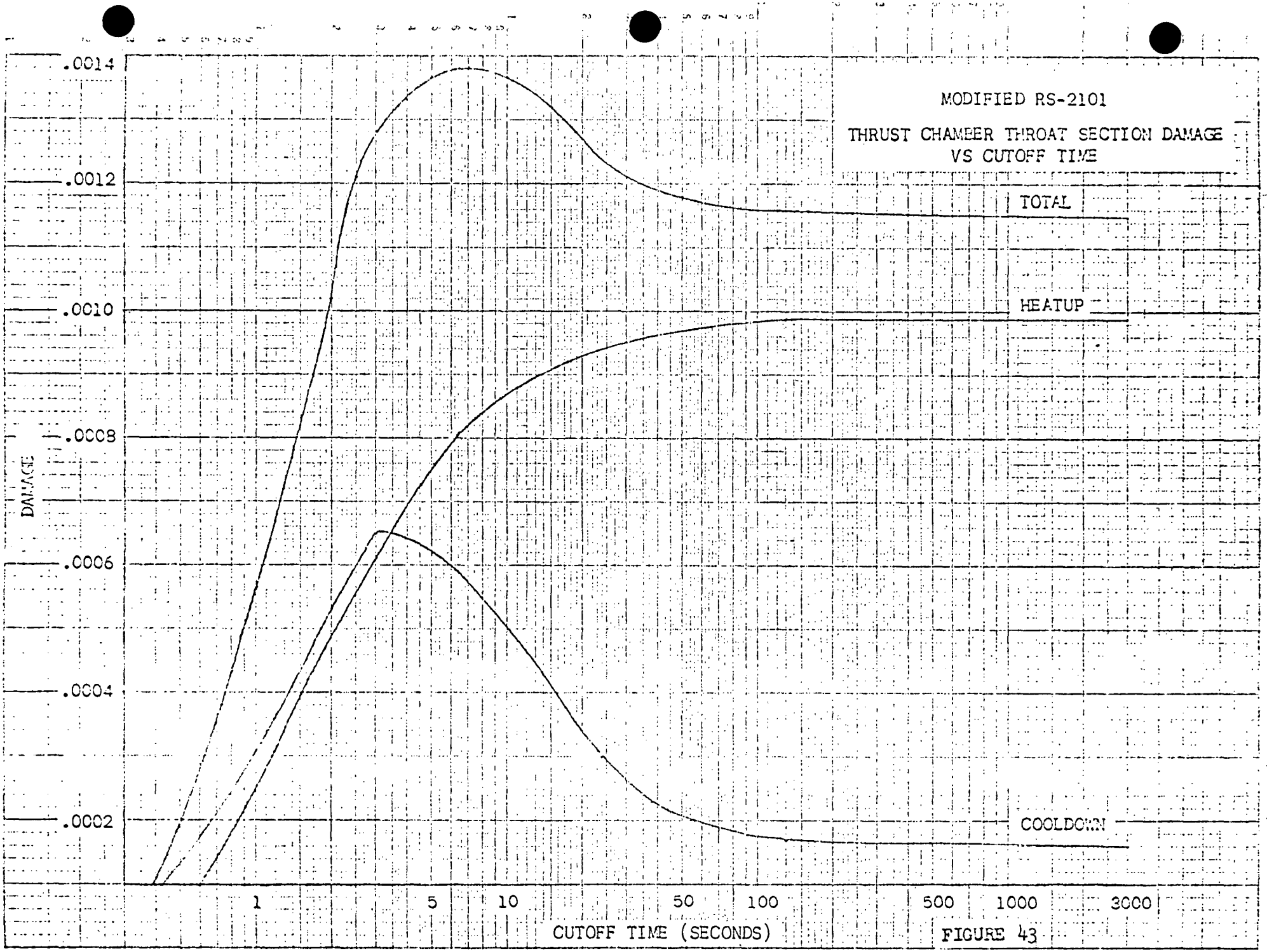
MODIFIED RS-2101
THRUST CHAMBER THROAT SECTION DAMAGE VS CUTOFF TIME
TOTAL
HEATUP
COOLDOWN
DAMAGE
.0014
.0012
.0010
.0008
.0006
.0004
.0002
1
5
10
50
100
500
1000
3000
CUTOFF TIME (SECONDS)

FIGURE 43

Total damage to the throat I.D. for any firing duration is determined by adding the heatup and cooldown damage. This curve shows that the most damaging engine firing occurs between 5 and 10 seconds duration.

Table 17 presents the damage summary for the specified Acceptance Test and MDC requirements, resulting in damage factors of .0068 and .0304, respectively. The total damage of .0372 is the summation of Acceptance and MDC testing. Throat cracking is predicted when this summation equals 1.0. The factor of safety on throat cracking for the modified RS-2101 engine using minimum material properties is approximately equal to 27. This factor of safety increases using typical material properties to approximately 80.

MODIFIED RS-2101

DAMAGE SUMMARY

EVENT	DURATION (SEC)	NUMBER OF CYCLES	DAMAGE
ACCEPTANCE TESTING	10	4	.0056
	2700	1	.0012
			Σ = .0068
MISSION DUTY CYCLE	36	1	.0012
	15	1	.0013
	2700	1	.0012
	128	1	.0012
	24	1	.0012
	14	1	.0013
	8	8	.0111
	3	8	.0110
	.4	8	.0009
			Σ = .0304

TOTAL DAMAGE = .0372

FACTOR OF SAFETY ≈ 27

TABLE 17

Dynamic Analysis

To evaluate the effects of boost and handling vibration on the structural integrity of the RS2101 60 to 1 nozzle extension to thrust chamber joint a dynamic model of the RS2101 engine system was formulated (Figure 44).

Initially, a model of the current MM'71 engine with a 40:1 nozzle extension was obtained and rigid body natural frequencies and mode shapes were matched to experimental data obtained during prequalification testing. As shown in Figure 44, the engine model was supported at the actuator attach points and gimbal ring bearing housing locations. The thrust chamber and nozzle assembly were modeled as a 12 element beam model attached at the injector to a rigid body incorporating mass and inertia properties of the remaining engine components.

As shown in Table 18, the natural frequencies corresponding to experimental results were obtained by varying the support springrates at the gimbal ring bearing attach points. These springrates include estimated stiffness effects of the gimbal ring, thrust mount, and bearings. The X axis springrate, governed primarilly by bending of the gimbal ring was held fixed at 4.3×10^4 lbs/inch while Y and Z axis springrates were varied from 2.8×10^5 lbs/inch to 8.0×10^5 lbs/inch. Considering 3.0×10^5 lbs/inch as a reasonable maximum springrate for a bearing, the third set of springrates listed in Table 18 was selected as most representative of actual conditions.

The 40 to 1 nozzle extension model was replaced by a model of the 60:1 nozzle extension and natural frequencies and mode shapes were obtained for both engine configurations as shown in Table 19.

Current RS2101 T.A. level vibration test requirements were used as inputs to the 40 to 1 engine configuration model to obtain dynamic loads for sinusoidal and random vibration test requirements. Preliminary vibration criteria supplied by JPL were used as inputs for similar analysis of the 60:1 configuration. These vibration requirements are tabulated in Table 20.

The dynamic loads obtained for both engine configurations, assuming 3% model damping, are presented in Tables 21 and 22 for sinusoidal and random vibration requirements respectively.

The maximum dynamic loads at the nozzle to thrust chamber joint occur at the lowest Y and Z axis nozzle extension bending modes for both engine configurations. These maximum dynamic loads are higher for the 60:1 engine configuration by a factor of approximately 2 for sinusoidal vibration and by a factor of approximately 2.7 for random vibration. These higher loads are due to two major factors:

1. Input vibration requirements for the 60:1 configuration engine are higher at the X and Z axis bending mode frequencies than requirements for the 30:1 engine configuration.

2. The 60:1 engine nozzle extension has a higher mass and moment arm than the 40:1 engine nozzle extension.

It is recommended that initial vibration testing of the 60:1 engine configuration be conducted with suitable accelerometer and strain gage instrumentation to verify the analysis results.

PREPARED BY: JMH	ROCKETDYNE A DIVISION OF NORTH AMERICAN AVIATION, INC.	PAGE NO. OF
CHECKED BY:	RS 2101 ENGINE	REPORT NO.
DATE: 5-3-1971	DYNAMIC MODEL	MODEL NO. RS2101

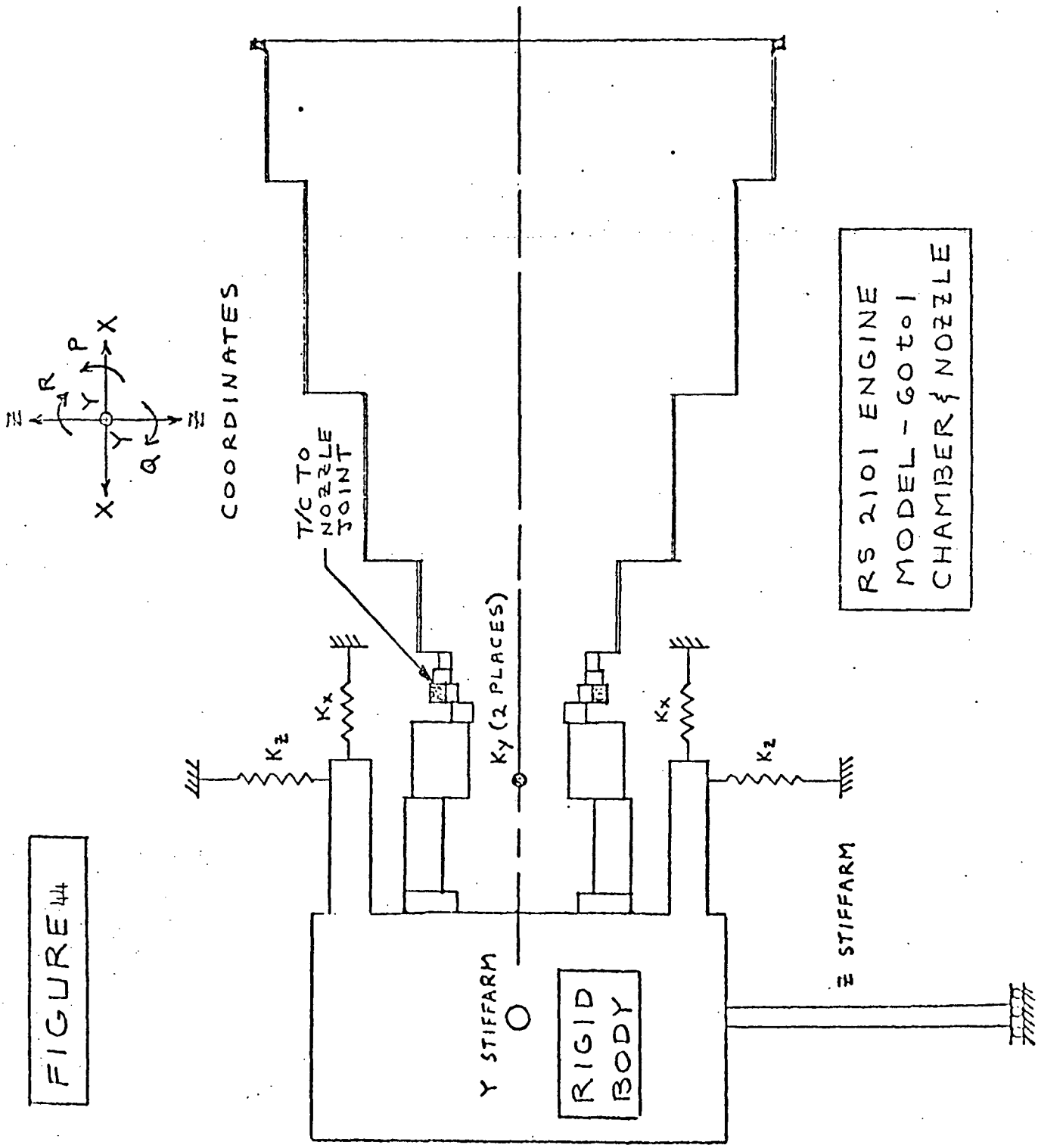

FIGURE 44

RS2101 DYNAMIC MODELS - FIRST 5 NATURAL FREQUENCIES AS FUNCTIONS OF Y AND Z AXIS SPRINGRATES

MODE NO.	SPRING RATES		40 TO 1 NOZZLE MODEL		60 TO 1 NOZZLE MODEL	
	Kv:LBS/IN.	Kz:LBS/IN.	Hz	MODE SHAPE	Hz	MODE SHAPE
1	2.8×10^5	4.0×10^5	158	Y-X RIGID BODY	137	Y RIGID BODY
	3.4×10^5	4.0×10^5	158	X-Y RIGID BODY	140	Y RIGID BODY
	6.0×10^5	3.4×10^5	158.5	X RIGID BODY	152	Y-X RIGID BODY
	8.0×10^5	2.8×10^5	158.6	X RIGID BODY	154	Y-X RIGID BODY
2	2.8×10^5	4.0×10^5	164	Y RIGID BODY	155	X RIGID BODY
	3.4×10^5	4.0×10^5	169	Y RIGID BODY	155	X-Y RIGID BODY
	6.0×10^5	3.4×10^5	182	Y RIGID BODY	156.5	Y-X RIGID BODY
	8.0×10^5	2.8×10^5	188	Y RIGID BODY	160	Y RIGID BODY
3	2.8×10^5	4.0×10^5	224.5	Z RIGID BODY	188	Z RIGID BODY
	3.4×10^5	4.0×10^5	224	Z RIGID BODY	186	Z RIGID BODY
	6.0×10^5	3.4×10^5	225	Z RIGID BODY	186	Z RIGID BODY
	8.0×10^5	2.8×10^5	222.5	Z RIGID BODY	183	Z RIGID BODY
4	2.8×10^5	4.0×10^5	529	BENDING ABOUT Z	493	BENDING ABOUT Z
	3.4×10^5	4.0×10^5	555	BENDING ABOUT Z	511	BENDING ABOUT Z-Y
	6.0×10^5	3.4×10^5	565	BENDING ABOUT Y	525	BENDING ABOUT Y
	8.0×10^5	2.8×10^5	537	BENDING ABOUT Y	504	BENDING ABOUT Y
5	2.8×10^5	4.0×10^5	605	BENDING ABOUT Y	567	BENDING ABOUT Y
	3.4×10^5	4.0×10^5	607	BENDING ABOUT Y	568	BENDING ABOUT Y-Z
	6.0×10^5	3.4×10^5	690	BENDING ABOUT Z	631	BENDING ABOUT Z
	8.0×10^5	2.8×10^5	756	BENDING ABOUT Z	682	BENDING ABOUT Z

COMPARATIVE 40 TO 1 NOZZLE EXPERIMENTAL FREQUENCIES

MODE NO.	FREQUENCY IN HZ	MODE SHAPE
1	157 HZ	RIGID BODY MOTION IN X AXIS
2	197 HZ	RIGID BODY MOTION IN Y AXIS
3	216 HZ	RIGID BODY MOTION IN Z AXIS

TABLE 19

RS2101 ENGINE SYSTEM NATURAL FREQUENCIES AND MODE SHAPES

MODE NO.	60 TO 1 NOZZLE CONFIGURATION		40 TO 1 NOZZLE CONFIGURATION	
	FREQUENCY	MODE DESCRIPTION	FREQUENCY	MODE DESCRIPTION
1	152 HZ	RIGID BODY MOTION IN THE Y-X AXIS	158.5 HZ	RIGID BODY MOTION IN THE X AXIS
2	157 HZ	RIGID BODY MOTION IN THE Y-X AXIS	182 HZ	RIGID BODY MOTION IN THE Y AXIS
3	186 HZ	RIGID BODY MOTION IN THE Z AXIS	225 HZ	RIGID BODY MOTION IN THE Z AXIS
4	525 HZ	BENDING OF NOZZLE ABOUT Y AXIS	565 HZ	BENDING OF NOZZLE ABOUT Y AXIS
5	631 HZ	BENDING OF NOZZLE ABOUT Z AXIS	690 HZ	BENDING OF NOZZLE ABOUT Z AXIS
6	993 HZ	TORSION ABOUT X AXIS AND Y-Z AXIS BENDING	1195 HZ	TORSION ABOUT X AXIS AND Y-Z AXIS BENDING
7	1265 HZ	BENDING OF NOZZLE ABOUT Y AXIS	1380 HZ	BENDING OF NOZZLE ABOUT Y AXIS
8	1300 HZ	BENDING OF NOZZLE ABOUT Z AXIS	1409 HZ	BENDING OF NOZZLE ABOUT Z AXIS
9	1726 HZ	TORSION ABOUT X AXIS	1868 HZ	TORSION ABOUT X AXIS
10	2574 HZ	BENDING OF NOZZLE ABOUT Y AXIS	3150 HZ	BENDING OF NOZZLE ABOUT Y AXIS
11	2575 HZ	BENDING OF NOZZLE ABOUT Z AXIS	3150 HZ	BENDING OF NOZZLE ABOUT Z AXIS

TABLE 20

RS2101 ENGINE SYSTEM VIBRATION TEST REQUIREMENTS

60 TO 1 NOZZLE CONFIGURATION PRELIMINARY JPL VIBRATION CRITERIA	40 TO 1 NOZZLE CONFIGURATION T.A. TEST LEVEL REQUIREMENTS
SINUSOIDAL TEST LEVELS	SINUSOIDAL TEST LEVELS
5 HZ @ 1.28 g PEAK	8 TO 20 HZ @ 2.1 g PEAK
5 TO 20 HZ @ 1.0 INCH D.A.	20 TO 50 HZ @ 17 g PEAK
20 TO 100 HZ @ 11.3 g PEAK	50 TO 120 HZ @ 11.3 g PEAK
100 TO 2000 HZ @ 6.4 g PEAK	120 TO 2000 HZ @ 5.1 g PEAK
RANDOM TEST LEVELS	RANDOM TEST LEVELS
25 HZ @ 0.00016 $(grms)^2$/HZ	30 HZ @ 0.065 $(grms)^2$/HZ
25 TO 50 HZ @ + 24 db/OCTAVE	30 TO 75 HZ @ + 15 db/OCTAVE
50 TO 800 HZ @ 0.1 $(grms)^2$/HZ	75 TO 125 HZ @ 0.63 $(grms)^2$/HZ
800 TO 2000 HZ @ -12 db/OCTAVE	125 TO 400 HZ @ -9.5 db/OCTAVE
2000 HZ @ 0.0026 $(grms)^2$/HZ	400 TO 1000 HZ @ 0.014 $(grms)^2$/HZ
	1000 TO 2000 HZ @ -15 db/OCTAVE
	2000 HZ @ 0.00044 $(grms)^2$/HZ
COMPOSITE LEVEL = 10.0 grms	COMPOSITE LEVEL = 9.2 grms

TABLE 21

RS2101 ENGINE SYSTEM MAXIMUM DYNAMIC LOADS AND RESPONSE FREQUENCIES AT THE THRUST CHAMBER TO NOZZLE EXTENSION JOINT DUE TO SINUSOIDAL VIBRATION INPUTS IN EACH AXIS

60 TO 1 NOZZLE CONFIGURATION

INPUT VIBRATION AXIS	FREQUENCY IN HZ	PEAK DYNAMIC LOADS					
		FX LBS	FY LBS	FZ LBS	MP IN-LBS	MQ IN-LBS	MR IN-LBS
X	153	177	128	48	30	434	1154
X	154	187	137	47	31	417	1219
X	156	195	128	38	28	343	1149
Y	631	0.3	287	46	161	349	2412
Z	525	0.3	72	266	259	2043	596

40 TO 1 NOZZLE CONFIGURATION

INPUT VIBRATION AXIS	FREQUENCY IN HZ	PEAK DYNAMIC LOADS					
		FX LBS	FY LBS	FZ LBS	MP IN-LBS	MQ IN-LBS	MR IN-LBS
X	158.5	114	17	13	4	82	112
X	160	110	18	13	4	82	115
X	181	23	20	8	4	48	128
Y	690	0.4	199	22	50	134	1261
Z	565	1.2	35	187	75	1110	218

TABLE 22

RS2101 ENGINE SYSTEM RMS DYNAMIC LOADS AT THE THRUST CHAMBER TO NOZZLE EXTENSION JOINT DUE TO RANDOM VIBRATION INPUTS IN EACH AXIS

60 TO 1 NOZZLE CONFIGURATION

INPUT VIBRATION AXIS	FREQUENCY RANGE IN HZ	1 σ RMS DYNAMIC LOADS					
		FX LBS	FY LBS	FZ LBS	MP IN-LBS	MQ IN-LBS	MR IN-LBS
X	25 TO 2000	43	22	10	5	83	195
Y	25 TO 2000	3	116	25	136	190	994
Z	25 TO 2000	1	35	98	163	764	295

40 TO 1 NOZZLE CONFIGURATION

INPUT VIBRATION AXIS	FREQUENCY RANGE IN HZ	1 σ RMS DYNAMIC LOADS					
		FX LBS	FY LBS	FZ LBS	MP IN-LBS	MQ IN-LBS	MR IN-LBS
X	30 TO 2000	65	14	9	3	54	89
Y	30 TO 2000	3	57	16	24	104	360
Z	30 TO 2000	2	19	49	27	296	122

Nozzle Thermal Buckling

Studies showed that the 60:1 nozzle defined by Rocketdyne Drawing AP69-216-003-00 did not have optimum thickness to prevent buckling. Therefore, the 60:1 nozzle design was modified by increasing the wall thickness near the attach joint to provide more resistance to thermal buckling. This effort was initiated in light of buckling experienced during the Mariner 71 Program, even though all past buckling occurrences were associated with plugged injector holes. The wall thickness contour selected provides a smooth axial temperature gradient for the nozzle. Figure 45 shows a plot of nozzle wall thickness versus distance from the head end of the thrust chamber for the 60:1, 40:1 and the first buckled 40:1 nozzle (S/N 3871527). The curve for the buckled nozzle represents measured wall thickness while the 40:1 and 60:1 curves represent drawing nominal dimensions.

The expression for the critical membrane buckling force is as follows:

$$F_{cr} = Ket^3$$

Where: K = a function of temperature gradient and a shape factor
E = modulus of elasticity
t = nozzle wall thickness

The product Et^3 is calculated for the 3 nozzles. This product was assigned unity (buckling threshold) for the buckled 40:1 nozzle at the 6.5 inch axial distance station where the buckling occurred. The remaining data for all nozzles were proportioned accordingly.

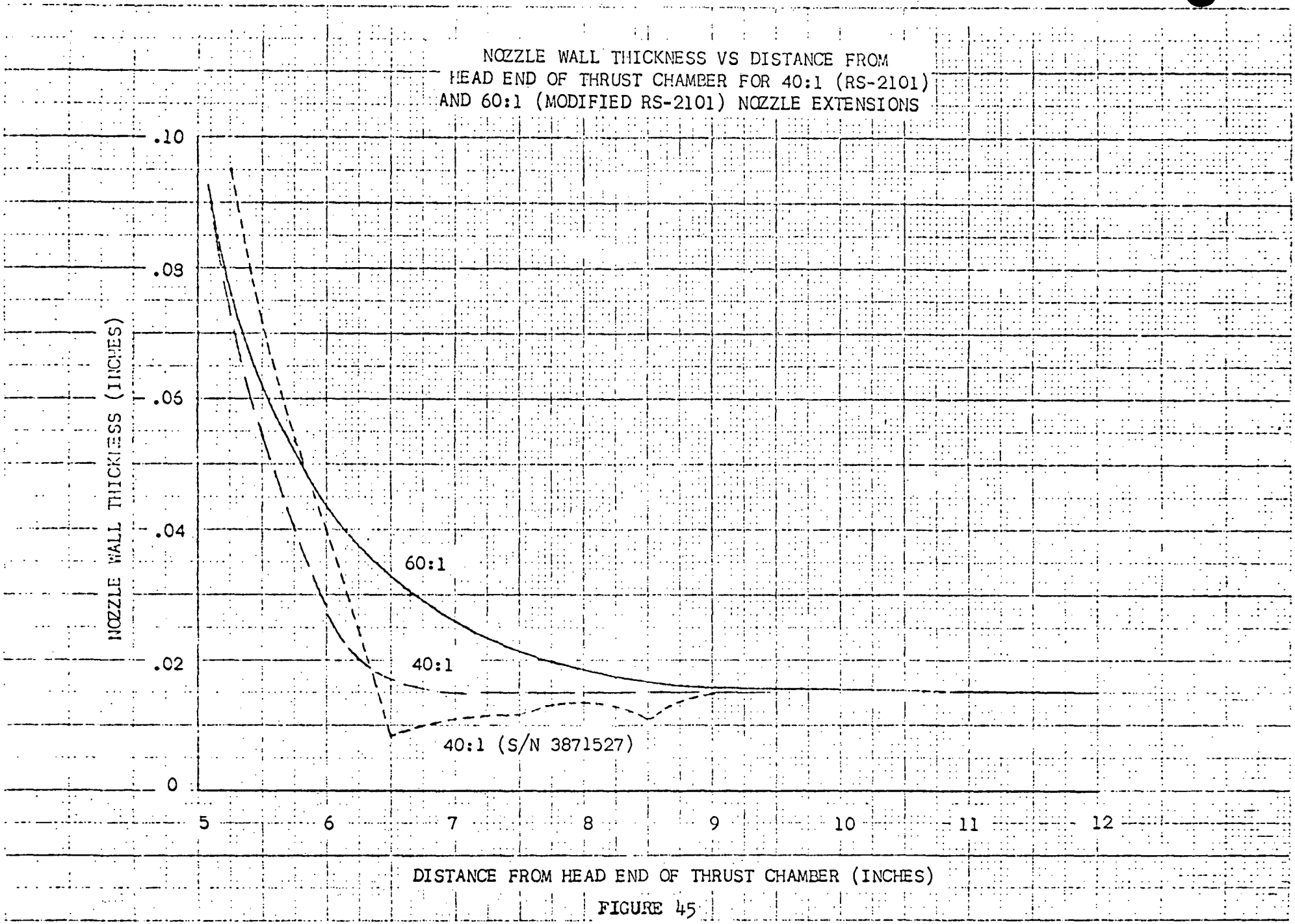
NOZZLE WALL THICKNESS VS DISTANCE FROM
HEAD END OF THRUST CHAMBER FOR 40:1 (RS-2101)
AND 60:1 (MODIFIED RS-2101) NOZZLE EXTENSIONS
NOZZLE WALL THICKNESS (INCHES)
.10
.08
.06
.04
.02
0
60:1
40:1
40:1 (S/N 3871527)
5
6
7
8
9
10
11
12
DISTANCE FROM HEAD END OF THRUST CHAMBER (INCHES)

FIGURE 45

Figures 46, 47, and 48 show the nozzle wall temperature vs distance from the head end of the thrust chamber at several firing time slices for the first buckled nozzle, the 40:1, and 60:1 nozzles, respectively. During heatup the axial temperature gradient is significantly reduced for the 60:1 nozzle. Figure 49 shows the factor of safety on buckling vs distance from the head end of the thrust chamber for the 3 nozzles relative to the buckled 40:1 nozzle. The curve for the buckled nozzle uses measured wall thicknesses while the 40:1 and 60:1 nozzle curves were established using drawing minimum thicknesses.

The 60:1 nozzle is approximately 70 times more resistant to thermal buckling at the 6.5 inch axial distance station than the previously buckled nozzle.

Thrust Chamber To Nozzle Joint

A preliminary analysis has been completed for the thrust chamber-to-nozzle joint and the analysis results are presented in this section.

The applied bending moment at the joint is 2440 in-lbs (Ref.11) or approximately twice the load imposed on the Mariner 71 design. This load increase is due to the combination of a more severe sinusoidal vibration test environment and the nozzle center of mass being located farther aft of the joint for the 60:1 nozzle. A preload must be developed during installation sufficient to prevent joint separation during vibration testing and to preclude yielding the flange fingers during engine operation. To accomplish this, a minor design change of the flange is required and the assembly torquing procedure must be modified.

RS-2101

40:1 NOZZLE (S/N 3871527) WALL THICKNESS TEMPERATURE VS AXIAL DISTANCE FROM HEAD END OF THRUST CHAMBER

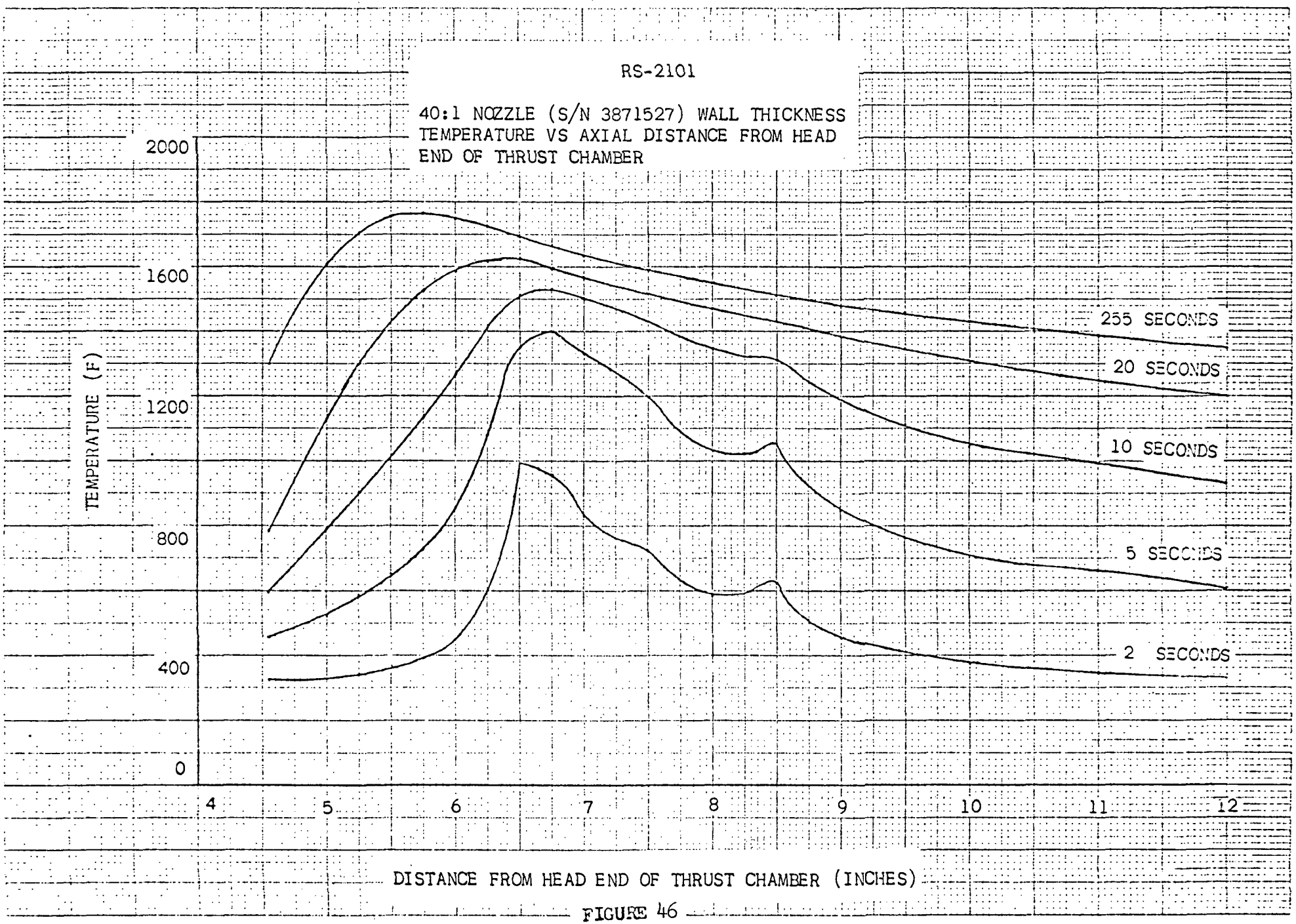

FIGURE 46

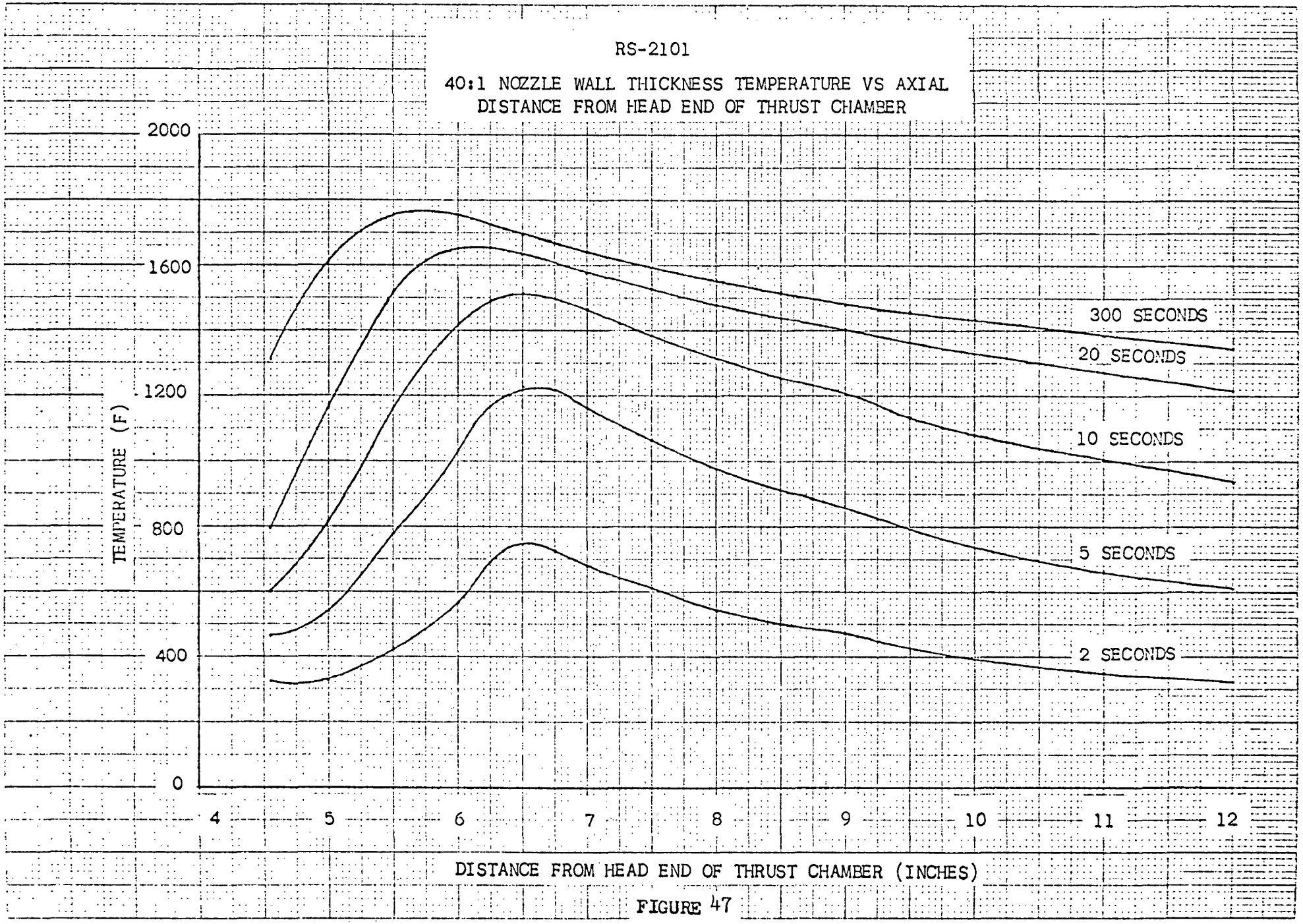

FIGURE 47

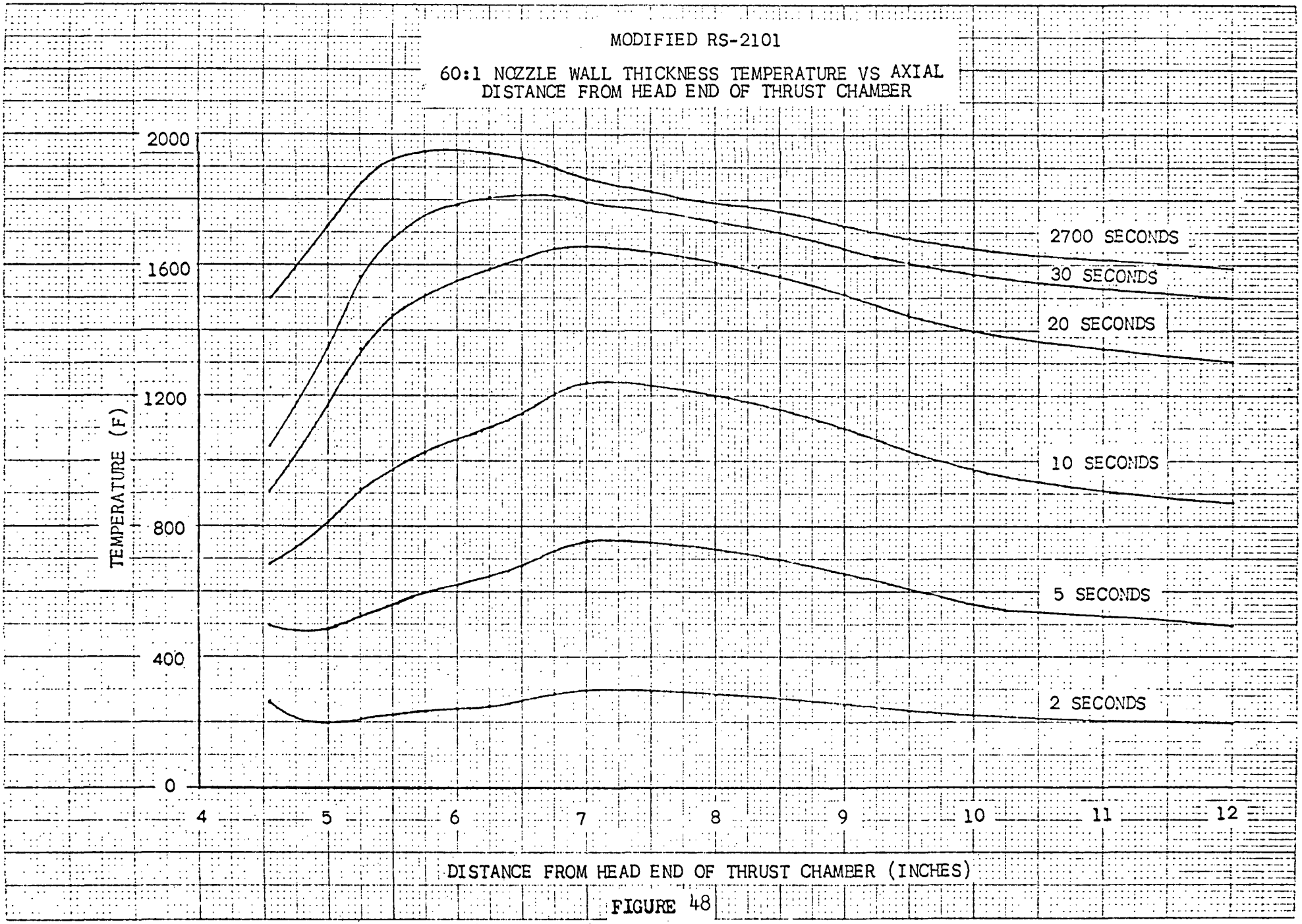

FIGURE 48

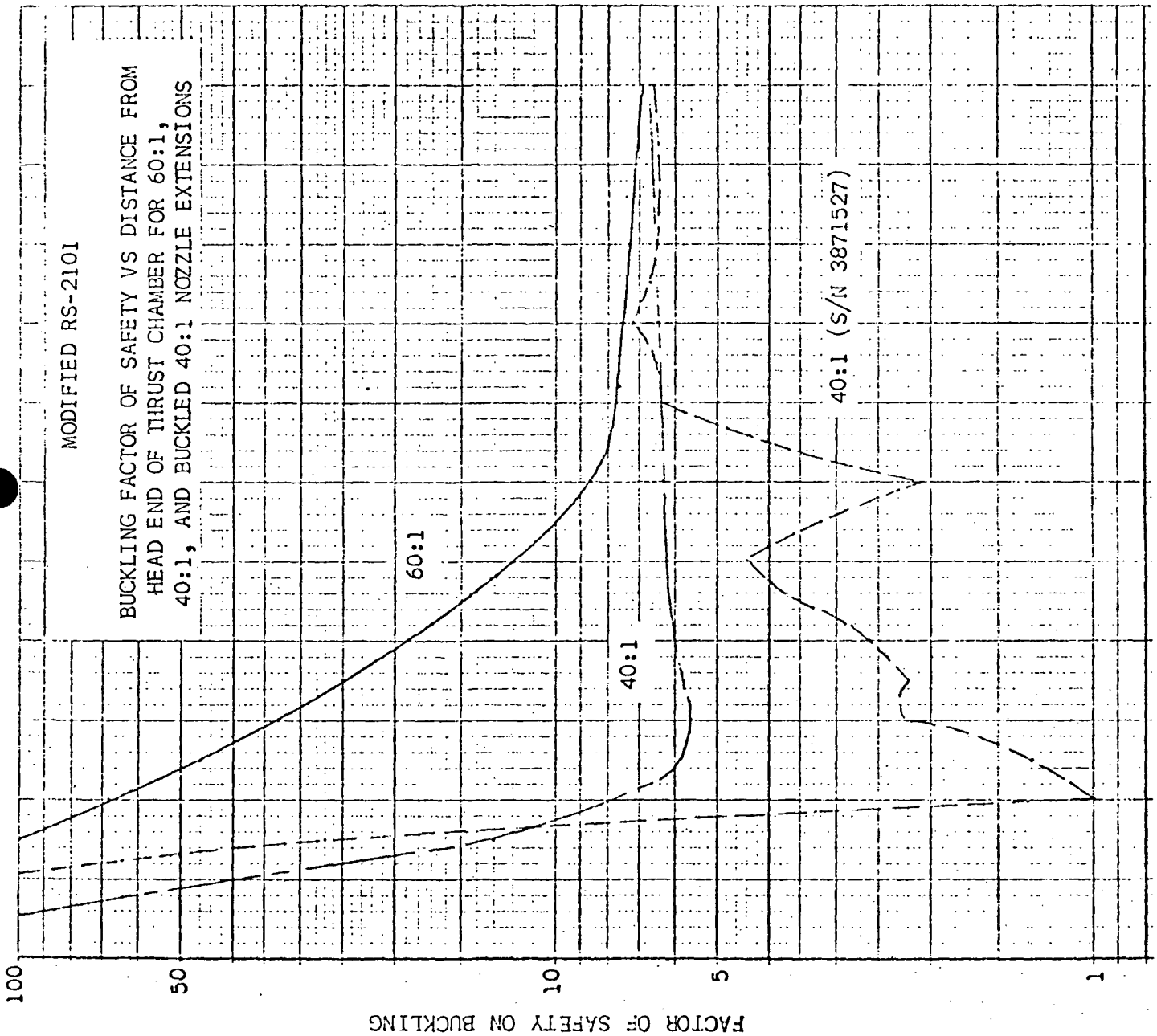
MODIFIED RS-2101
BUCKLING FACTOR OF SAFETY VS DISTANCE FROM HEAD END OF THRUST CHAMBER FOR 60:1, 40:1, AND BUCKLED 40:1 NOZZLE EXTENSIONS
60:1
40:1
40:1 (S/N 3871527)
FACTOR OF SAFETY ON BUCKLING
100
50
10
5
1
6
7
8
9
10
11
DISTANCE FROM HEAD END OF THRUST CHAMBER (INCHES)

FIGURE 49

The recommended flange design change is shown in Fig. 50 . The existing nominal flange thickness of .0575 inch is changed to a tapered thickness of .055 to .065 inch for the horizontal leg and a constant .065 thickness for the vertical leg. This change enables an increased preload to be developed during installation and results in more uniform straining of the total flange section. Fig. 50 also shows the load deflection characteristics of the 2 designs. A minimum required preload of 1830 lbs is required to prevent separation during vibration testing.

The following torquing procedure is recommended for the thrust chamber-to-nozzle joint.

1. Seat parts by torquing the nut to 30 in lbs above the running torque.
2. Mark the relative position of the nut and nozzle.
3. Preform the nut by turning through an angle of 240 $\pm$5 degrees with respect to the nozzle.
4. Mark the relative position of the nut and nozzle.
5. Set the preload by backing off the nut through an angle of 38 $\pm$2 degrees with respect to the nozzle.

The total joint load vs percent strain and load vs nut rotation is shown in Fig. 51 and 52. The nut preforming operation develops a joint load of 3250 lbs and initially yields (less than 0.4 percent) the flange fingers. The 38° nut rotation reduction decreases the joint load to 2440 lbs. The assembly will then exhibit a factor of safety of over 1.3 on joint separation during vibration testing and greater than 1.1 on flange yielding during engine operation.

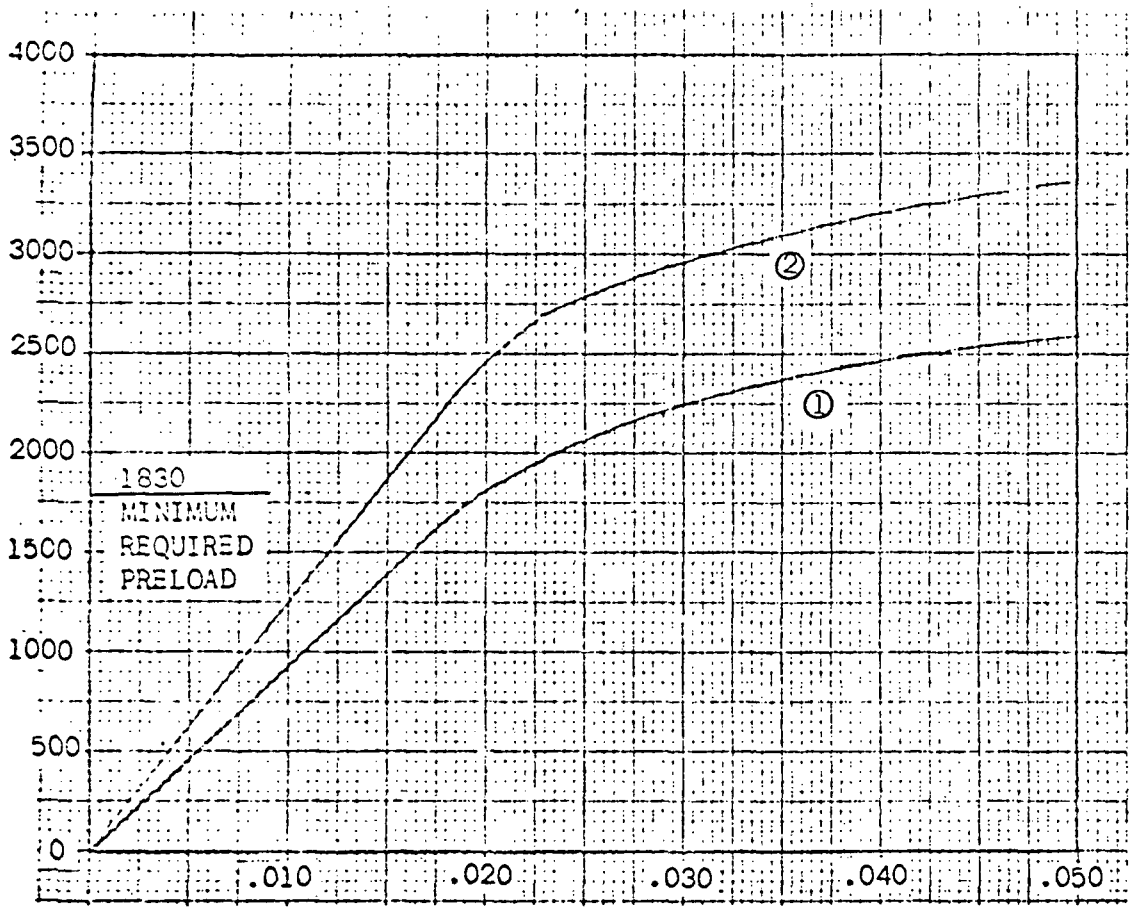

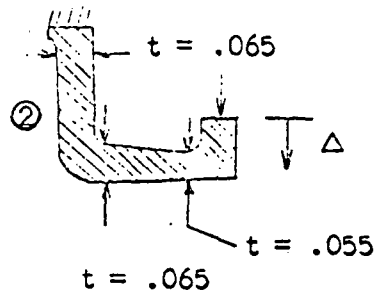

PROPOSED MODIFIED RS-2101 DESIGN

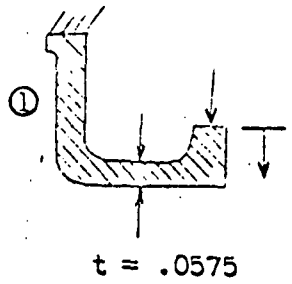

RS-2101 DESIGN

LOAD - DEFLECTION CURVES FOR
RS-2101 NUT P/N RS000607

FIGURE 50

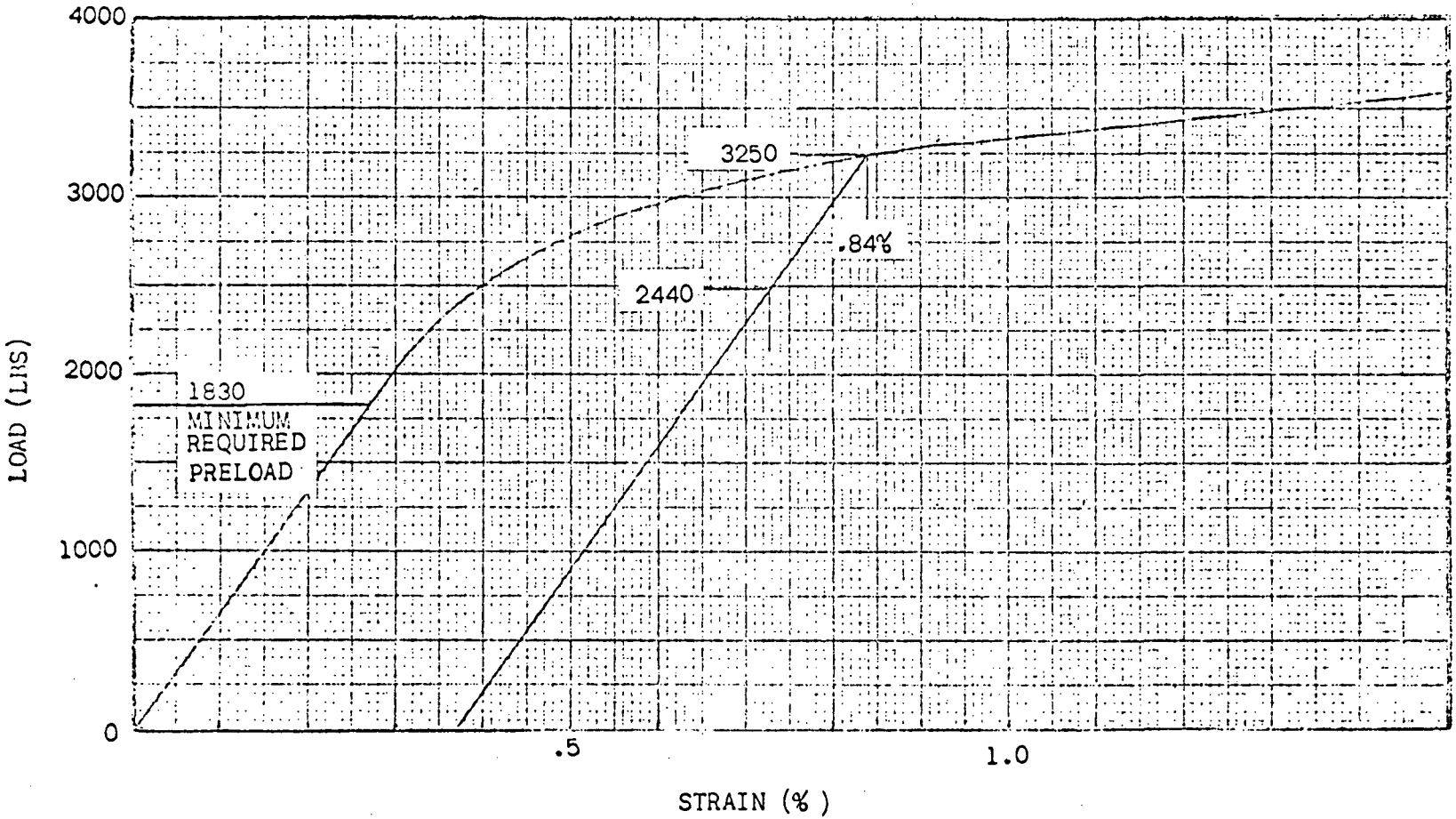

LOAD - STRAIN CURVE WITH FORMING
AND PRELOAD CONDITIONS INDICATED

MODIFIED RS-2101 PROPOSED DESIGN

FIGURE 51

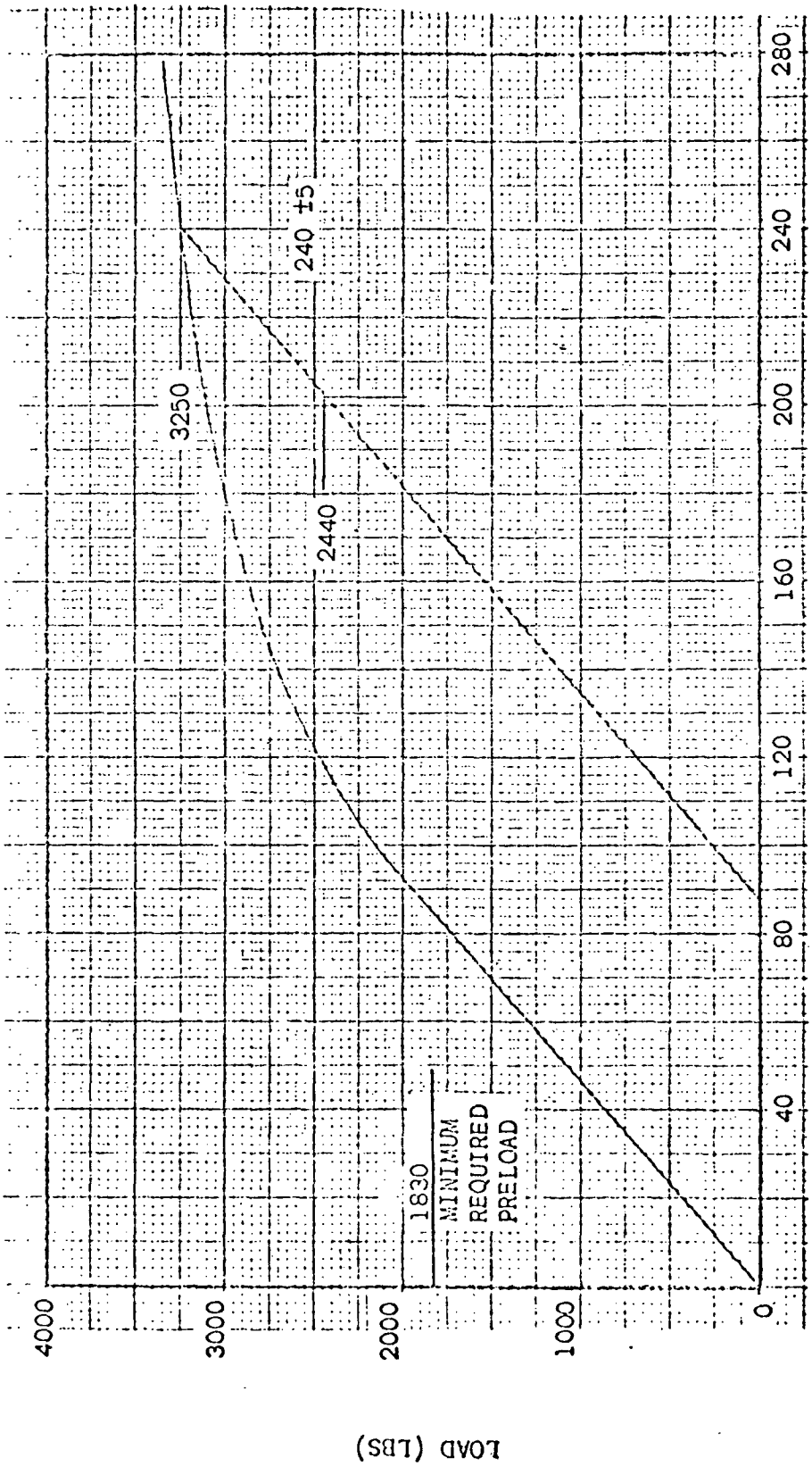

LOAD - ROTATION CURVE WITH FORMING
AND PRELOAD CONDITIONS INDICATED

MODIFIED RS-2101 PROPOSED DESIGN

FIGURE 52

The joint sealing force and flange (finger) yield load vs firing time are shown in Fig. 53. The thermal environment causes the 2440 pound joint installation load to increase to 2590 pounds after 20 seconds firing duration, then decreases to 2440 pounds after 2700 seconds. The factor of safety on flange yielding is 1.23 at 20 seconds and 1.12 at 2700 seconds.

Since the flange fingers never experience yielding after the preforming operation, the joint is capable of withstanding a large number of applied thermal cycles without failure (cracks). The joint thermal cycle life is not a limiting factor for this engine configuration.

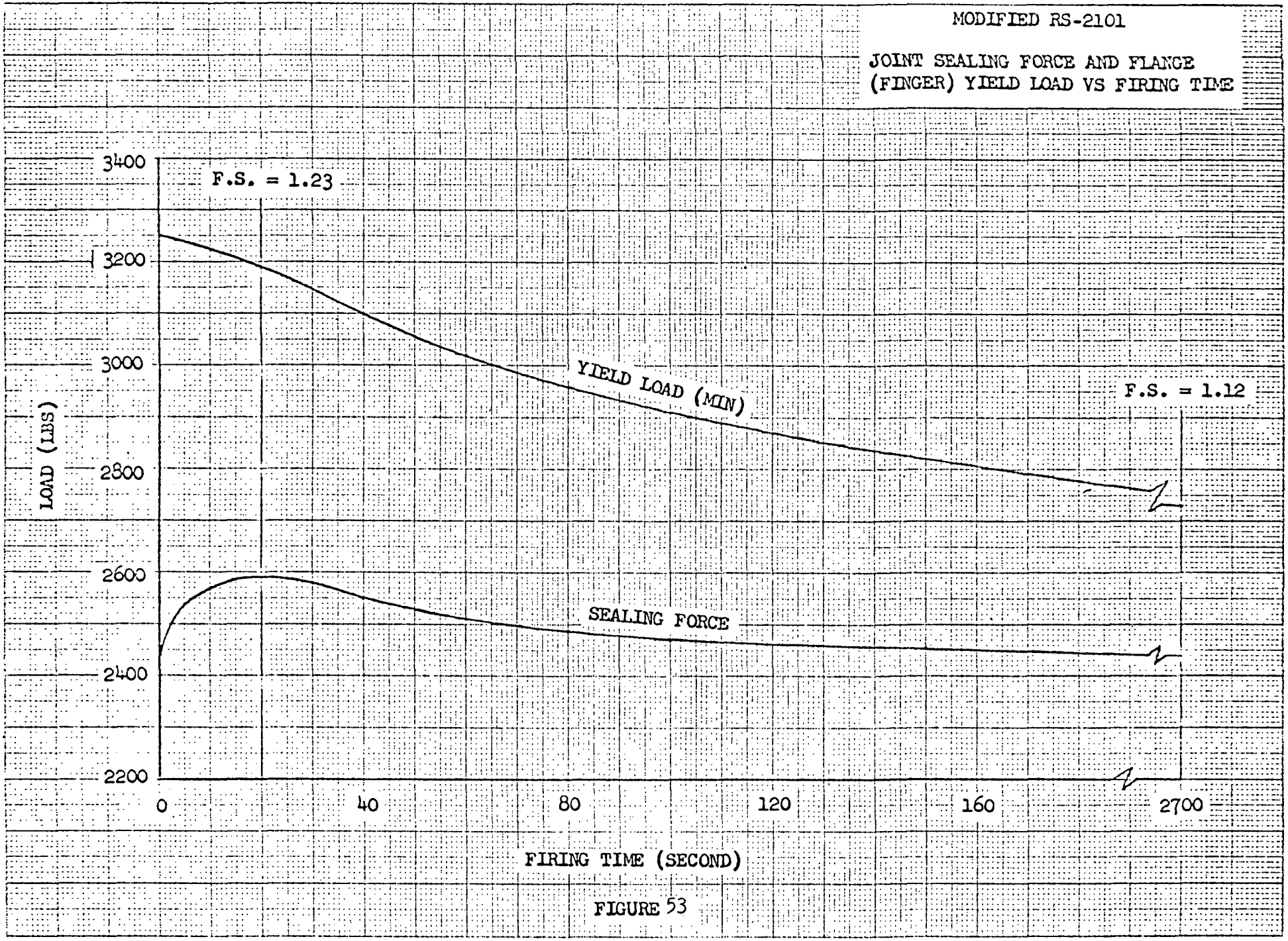

FIGURE 53

Structural Analysis Conclusions

Analysis results indicate the RS2101 engine with the 40:1 nozzle replaced by a 60:1 nozzle is structurally adequate for the defined operational environment provided minor design changes are incorporated for the joint attach hardware. A thermal cycle damage analysis performed for the thrust chamber throat section demonstrates a factor of safety of 27 on throat cracking using minimum material properties. This factor of safety increases to approximately 80 using typical material properties.

The 60:1 nozzle head end wall thickness profile was increased over the 40:1 to attain a smooth axial temperature gradient to increase the resistance to thermal buckling. Due to the thickness change the 60:1 nozzle is approximately 70 times more resistant to buckling than the buckled 40:1 nozzle (S/N 3871527).

The thrust chamber-to-nozzle attach joint flange (fingers) must be increased in thickness to enable a larger preload to be applied to resist the increased loading at the joint interconnection. Incorporation of the design change and a modification to the joint installation procedure will result in a factor of safety of over 1.3 on joint separation during sinusoidal vibration testing and a factor of safety greater than 1.1 on flange yielding during engine operation.

SCHEDULE

ARTICLE 1. STATEMENT OF WORK

(a) The Contractor shall:

(1) Perform thermal analyses on a modified RS-2101 Rocket Engine Configuration. The modified engine configuration shall be identical to the RS-2101 Rocket Engine as represented by Rocketdyne Drawing No. RS000601-001-01 (latest change in effect on date of Contract) except that a 60 to 1 nozzle extension shall replace the present 40 to 1 extension. These analyses shall determine the effects of the new nozzle extension and the extended firing time on engine operation/components. The results of the analyses shall be presented in such a manner as to illustrate the engine thermal characteristics from the initiation of engine firing through the period of maximum soakback temperature with respect to engine firing duration. Discuss observed thermal characteristics which would potentially limit the engine operation during the mission and recommend to JPL engine configuration changes which would resolve such anomalous behavior.

The design criteria for the studies/analyses shall be as defined in Exhibit 1 entitled "Modified RS-2101 Rocket Engine Study Criteria." Particular emphasis shall be placed on the following:

(A) Analyses of the characteristics of heat soakback with special emphasis on the effects of valve inductive heating and extended duration engine firing on the propellant valve seats.

(B) Analyses of the engine thermal stability (interegen) characteristics.

(C) Definition of the engine thermal load to the spacecraft.

(2) Perform design studies and analyses using the RS-2101 Rocket Engine Design defined by Rocketdyne Drawing No. RS000601-001-01 (latest change in effect on date of Contract) to define potential solutions for leakage past the injector-to-thrust chamber seals. The studies shall consider the results of the effort done in support of the failure analyses reporting of the three (3) "V" seal leakage incidents during the Mariner Mars 1971 Type Approval Program. These studies shall include definition of the seals requirements and a trade-off study of available seal candidates. Selection of seals as candidates for further study shall be made while considering such

characteristics as seal(s) configuration, individual sealing characteristics, materials compatibility, seal temperature limitations, sealing surface finish, seal plating requirements, and effect of the seal on engine thermal management. The results of this effort shall be presented as recommendations which, if deemed acceptable, could be implemented and verified during an engine prototype program. These studies/analyses shall place particular emphasis on the following:

(A) Studies of the adequacy of candidate head-end-seals when used with the duty cycle specified in Exhibit 1.

(B) Definition of the compatibility characteristics of candidate seal materials with the injector and combustion chamber materials.

(C) An "Activity Plan" which shall be submitted for JPL approval. The plan shall discuss the particular areas to be studied; outline specific tasks or effort to be accomplished; present the detailed methods or techniques to be used; specify any special equipment, skills or personnel required; and define the sequence of events in schedule form.

(D) A recommendation to JPL for one (1) or more configurations which would not be subject to leakage after the duty cycle specified in Exhibit 1. Potential configuration changes shall include revised seal configurations and seal material changes. Particular emphasis shall be placed upon minimal change to the current RS-2101 engine configuration.

(E) A recommendation to JPL for a leak test procedure for the injector-to-thrust chamber joint which provides a measure of leakage past each and all seals.

(3) Perform an analysis of the structural integrity of the thrust chamber-to-nozzle extension joint when subjected to the vibration spectra presented in Exhibit 1. The design of this joint shall be identical with that of the RS-2101 Rocket Engine as defined by Rocketdyne Drawing No. RS000601-001-01 (latest change in effect on the date of Contract) except for incorporation of a 60 to 1 area ratio nozzle extension as defined by Rocketdyne Drawing No. AP 69-216-003-00 dated 8/4/69. This analysis shall consider the structural limitations imposed upon the joint and the adjacent thrust chamber and nozzle extension during the non-operational (cold) and the operational (long duration firing) environment. The results of the analysis shall be presented in such a manner as to define the structural margin and thermal cycle life capability of this joint design.

(A) In the event of a marginal or inadequate joint design, recommend to JPL joint designs, or modifications to the present design, which will satisfy the thrust chamber-to-nozzle extension structural requirements when subjected to the required vibration environment.

(B) If these studies indicate that the 60:1 nozzle, as defined by Rocketdyne Drawing No. AP 69-216-003-00, does not have optimum thickness to prevent buckling, the Contractor shall submit a revised 60:1 nozzle design.

(4) Provide for an informal final oral review meeting at the Contractor's facility. The final review meeting shall include informal handouts, a brief presentation of the results of the studies/analyses and discussion of the feasibility of implementing any improvements or changes resulting from this effort. Minutes for the meeting may be presented in lieu of and in the format of that month's Monthly Report, as outlined in paragraph (b)(3).

(b) The Contractor shall provide the following documentation:

(1) Prepare and submit a Final Technical Report which presents the results of, and recommendations evolving from, the engine thermal analyses, the injector-to-thrust chamber seal studies and the nozzle extension joint thermal stress analyses. The apparent inter-relationship of these activities dictates the need for a single report; however, for purposes of clarifying the specific impact of an item on engine operation and design, the Contractor may report on portions of each item separately after coordination and prior agreements with JPL. The termal design margin shall be documented in the Final Report to illustrate the nozzle joint attach nut fingers yield stress margin; the nozzle joint sealing force profile before, during and after long duration firing; and thermal cycle life margin of the beryllium throat. The Contractor shall be permitted to use his internal report format for this report.

(A) Submit one (1) copy of the Final Report in preliminary draft form for JPL approval.

(B) Submit one (1) vellum and twenty (20) copies of the Final Report following JPL approval of the preliminary draft.

(2) One (1) reproducible and three (3) copies of all design drawings, specifications and procedures which reflect any changes required by (and to implement) the work described in paragraphs (a)(1) through (a)(3).

(3) Five (5) copies of an Informal Monthly Letter Progress Report which presents a brief narrative summary for each of the three (3) study/analyses work items and presents the status of each item. These reports shall include, but not necessarily be limited to, the following:

(A) Summary.

(B) Technical discussion of work accomplished.

(C) Problems encountered and how resolved.

(D) Recommend/JPL coordinated changes to specific work items.

(E) Status of each of the three (3) work items including slipped schedule dates, reasons for slippage and corrective measures taken.

(4) Seven (7) copies of a Monthly Financial Management Report, NASA Form 533b.

(5) One (1) vellum and three (3) copies of a Seal Activity Plan as outlined in paragraph (a)(2)(C).

(c) The Contractor shall provide for the JPL personnel having technical cognizance over this effort to be apprised by the Contractor, or to be able to apprise themselves, on a continuing basis, of all technical and scientific aspects of the work being performed. Any contemplated recommendations for changes to work items or documentation shall be pre-coordinated with the JPL cognizant Technical Representative. The appointed JPL Technical Representative(s) and authorized alternate(s) shall be designated by letter to the Contractor and shall, in addition to any other rights set forth in the Contract:

(1) Have full and unlimited access to the Contractor's or subcontractor's facility areas wherein the work called for is being performed.

(2) Be provided promptly upon request with data relating to analyses and other technical or scientific matters directly pertaining to the work being performed.

(3) Be notified immediately of any significant problems which arise.

(4) Be provided immediate and complete access to all Contractor internal documentation relating to the technical and scientific aspects of the effort.

(5) Be notified of all Technical meetings of importance and all testing held at the Contractor's facility, a subcontractor's facility or other location. Such notification shall be provided early enough to allow JPL attendance.

(d) JPL will:

(1) Approve, disapprove or recommend changes to the Seal Activity Plan, documentation, and work items (except for the preliminary Draft Final Report) within ten (10) working days after receipt at JPL.

(2) Approve, disapprove or recommend changes to the preliminary Draft Final Report within fifteen (15) working days of receipt at JPL.

(3) Provide spacecraft thermal configuration within ten (10) working days after the date of this Contract.

EXHIBIT 1

MODIFIED RS-2101 ROCKET ENGINE STUDY CRITERIA

(1) Propellant Combination:	Monomethylhydrazine (MMH) and Nitrogen Tetroxide (N_2O_4)
(2) Propellant Mixture Ratio (By Mass):	1.55:1
(3) Vacuum Thrust:	Approximately 300 lb_f at an expansion area ratio of 60:1 with a modified 80% bell nozzle contour
(4) Minimum Steady State Vacuum Specific Impulse:	286 $\frac{lb_f}{lb_m}$ sec
(5) Steady State Vacuum Specific Impulse Design Objective:	300 $\frac{lb_f}{lb_m}$ sec
(6) Chamber Pressure:	Between 110 and 125 psia
(7) Propellants Pressures at Engine Inlet:	$<$250 psia
(8) Mission Duty Cycle:	During a typical mission the engine will be subjected to about 25 starts for a total firing time of about 3500 seconds. There will be one long duration firing of approximately 3000 seconds. Duration of intermediate firings will be from 0.4 to 100 seconds. Between firings the chamber is expected to cool to an equilibrium temperature below 200°F. Thus the objective will be to design an engine which will survive: one (1) mission duty cycle (25 starts with one 3000 second firing) within specified performance limits: and, three (3) mission duty cycles without a catastrophic failure.
(9) Gimbal Requirements:	The engine must be capable of two-axis gimbal operation through an angle of $\pm$ 13°.
(10) Vibration Requirements:	The engine must withstand the sinusoidal, random and acoustic vibration requirements presented on Figure 1, Figure 2 and Table 1 respectively.

(11) Valve Temperature: (Soakback)	The maximum soakback temperature at the valve seat shall not exceed 250°F.
(12) Actuator Temperatures:	The maximum soakback temperature at the engine to actuator attach point shall not exceed 450°F.
(13) Propellant Saturation:	Engine performance shall be assumed to occur with propellants fully saturated with gaseous helium.

PRELIMINARY SINE TEST LEVELS

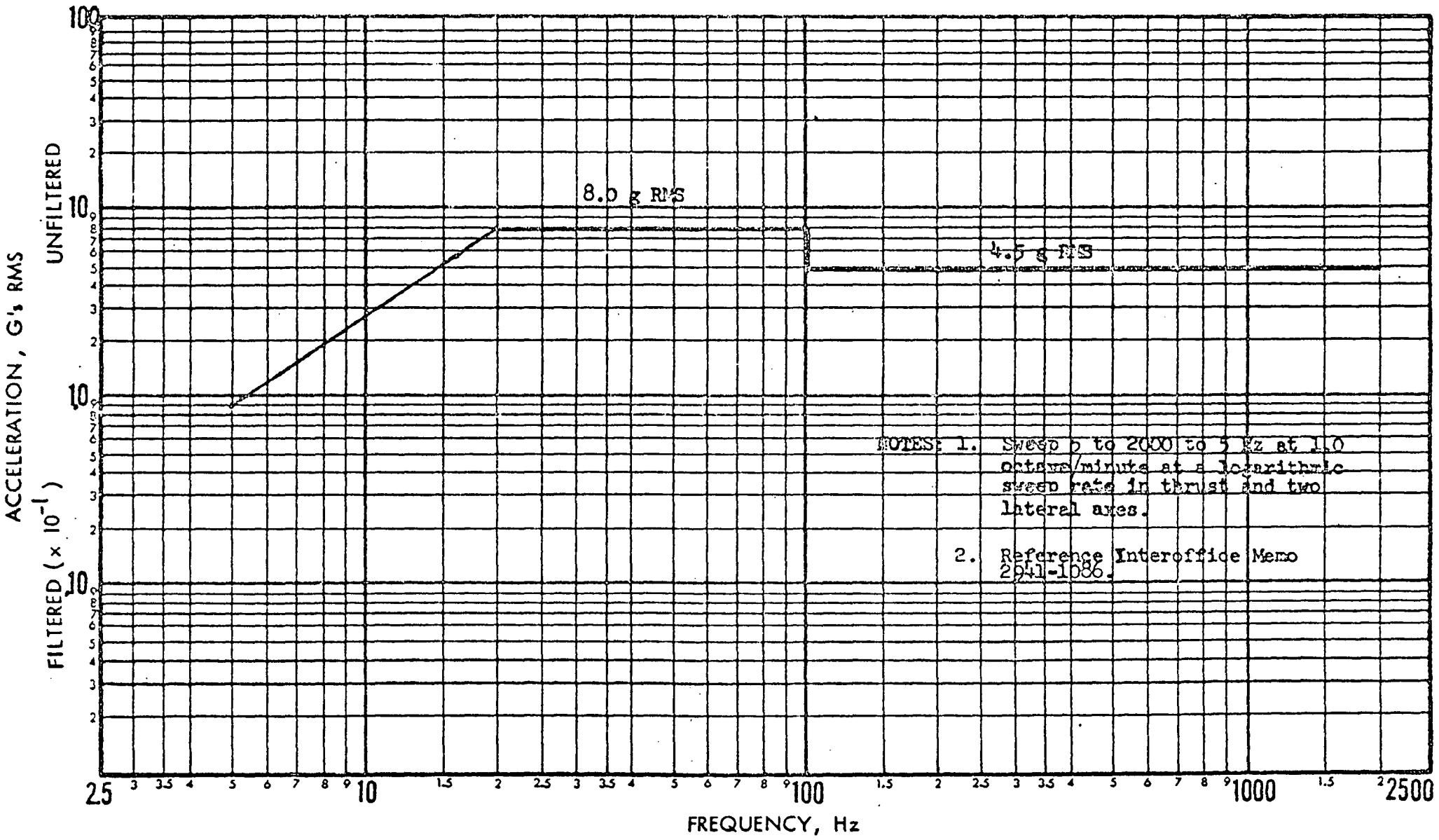

Figure 1

PRELIMINARY RANDOM TEST LEVELS

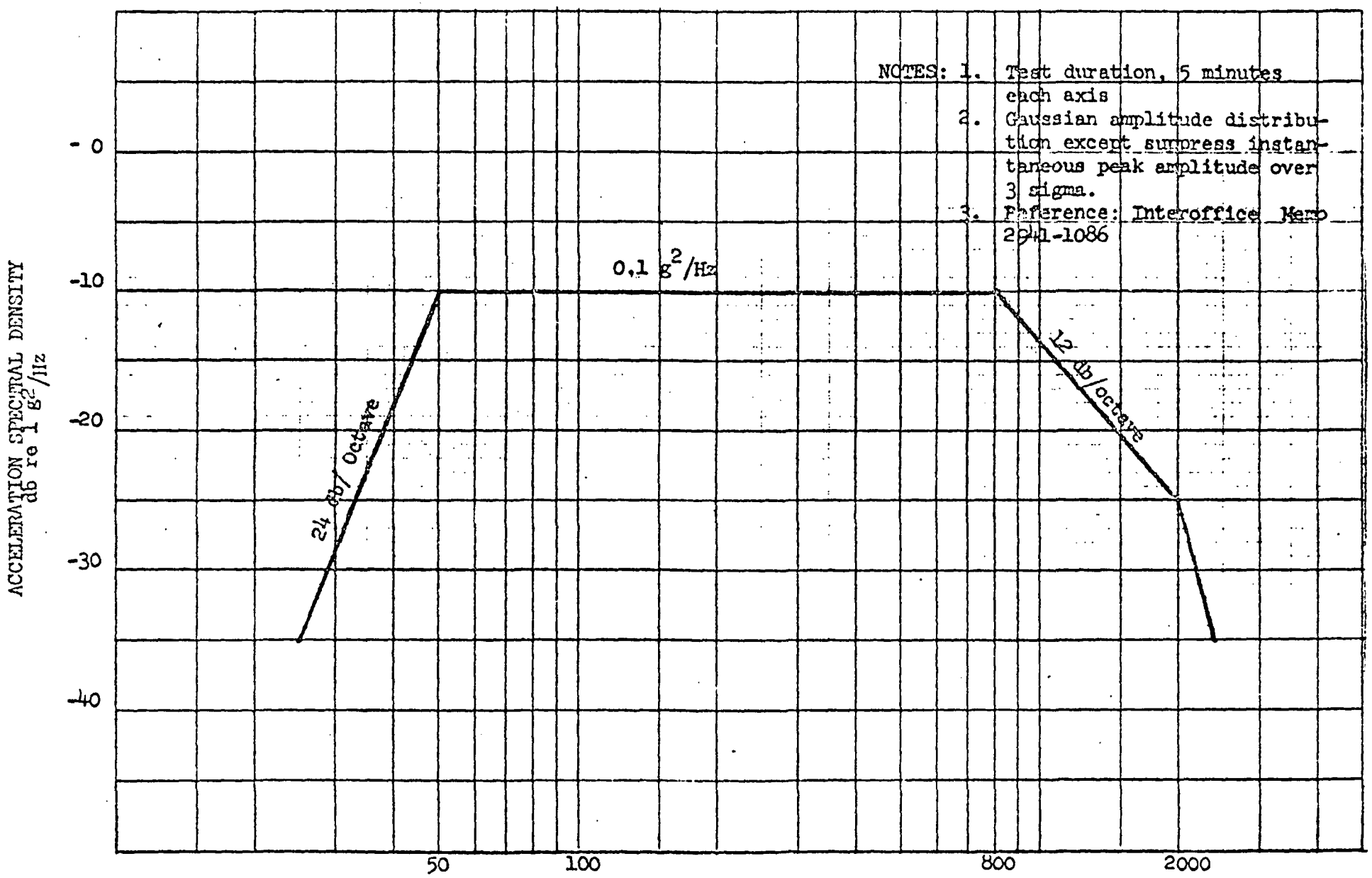

Figure 2

Table 1 Acoustic Test Levels

1/3 Octave Band Center Frequency (Hz)	Sound Pressure Level in 1/3 Octave Bands (db ref 2×10^{-4} dynes/cm^2)
under 50	Roll off rate $\geq$ 12 db
50	133.5
63	134
80	134.5
100	135
125	137
160	139
200	140
250	140.5
315	140
400	138.5
500	137
630	136
800	135
1,000	134
1,250	133
1,600	132
2,000	131
2,500	130
3,150	129
4,000	128
5,000	129
6,300	126
8,000	125
10,000	124
over 10,000	124
Overall	149

Note: Test Duration Shall Be For 5 minutes in a Wideband Acoustic Noise Reverberant Field.

Internal Letter

North American Rockwell

Date 1 April 1971

No SR 1112-4002

TO R. S. Martinez
Address D/596-159, AC04

FROM T. Young
Address D/596-112, AC12

Phone 3241

Subject Modified RS-2101A Rocket Engine Mass Properties Report

Reference (a) SR 0111-4010, "RS-2101A Mass Properties Report", dated 20 April 1970

The mass properties report for the modified RS-2101A Rocket Engine Assembly with a 60:1 extension nozzle is presented in the attached report. Reference (a) is the current RS-2101A Rocket Engine Mass Properties Report with a 40:1 extension nozzle. Based on previous statistical analysis of the RS-2101A engine, the modified engine can be expected to weigh 18.0 $\pm$ .3 lbs.

T. Young
Engine Stress & Weights

TY:ac

Distribution:

D/596-112, AC12
K. H. Acton
J. W. Elliott
G. R. Scheibel

D/596-159, AC04
R. K. Kinningham
W. J. Richtenburg

SR 1112-4002

Modified RS-2101A Engine Assembly (60:1 Nozzle Extension)

Mass Properties Report

22 March 1971

CONTENTS

MASS PROPERTIES REPORT

WEIGHT STATUS

	DESCRIPTION	SPECIFIED WEIGHT BASE	PROCURING ACTIVITY AND GFE CHANGES	REVISED SPECIFIED WEIGHT BASE (3)+(4)	CURRENT STATUS	LAST STATUS SR 0111-4010 DATED 4-20-70	CHANGES FROM LAST TO CURRENT STATUS	BASIS FOR CURRENT DATA			NOTES
								% EST	% CALC	% ACT	
1	2	3	4	5	6	7	8	9	10	11	12
	Rocket Engine Assembly				(17.96)	(17.08)	(+0.88)		(13)	(87)	
	Thrust Chamber				2.78	2.78				100	
	Nozzle Extension				2.40	1.52	+0.86		100		1
	Nozzle Attach Flange				0.14	0.14				100	
	Nozzle Attach Nut				0.25	0.25				100	
	Injector Assembly				2.16	2.16				100	
	Bi-propellant Valve				4.53	4.53				100	
	Thrust Mount				1.88	1.88				100	
	Gimbal Ring				1.96	1.96				100	
	Gimbal Bearing--Bolts (2)				0.27	0.27				100	
	Pivot Assembly--Customer Attach(2)				0.58	0.58				100	
	Pressure Transducer				0.10	0.10				100	
	Miscellaneous & Attach Parts				0.91	0.91				100	

MODEL Modified RS-2101A

REPORT NO. SR 1112-4002

DATE 22 March 1971

MASS PROPERTIES REPORT

CHANGE ANALYSIS

	DESCRIPTION	CUSTOMER WEIGHT CHANGE	CONTRACTOR WEIGHT CHANGE	EXPLANATION	NOTES
1	2	3	4	5	6
	Rocket Engine Assembly		(+0.88)		
	Nozzle Extension		+0.88	Weight change to increase the nozzle expansion area	1
				ration from 40:1 to 60:1. Nozzle extension weight	
				variation due to tolerances was calculated at	
				2.40 ± .56 pounds.	

MODEL Modified RS-2101A

REPORT NO. SR 1112-4002

DATE 22 March 1971

PAGE 2 OF 5

MASS PROPERTIES REPORT

WEIGHT/CG/INERTIA DATA

	DESCRIPTION	NO REQD	CURRENT WEIGHT-(LB)	CENTER OF GRAVITY (INCHES)			MOMENT OF INERTIA ABOUT C.G. (LB IN^2)		
				$\bar{X}$ ARM	$\bar{Y}$ ARM	$\bar{Z}$ ARM	I_x (ROLL)	I_y (PITCH)	I_z (YAW)
1	2	3	4	5	6	7	8	9	10
	Rocket Engine Assembly	1	(17.96)	6.66.	4.88	4.80	120.11	418.92	423.50
	Thrust Chamber	1	2.78	7.08	5.00	5.00	8.72	8.07	8.07
	Nozzle Extension	1	2.40	15.66	5.00	5.00	34.58	62.12	62.12
	Nozzle Attach Flange	1	0.14	9.28	5.00	5.00	0.34	0.17	0.17
	Nozzle Attach Nut	1	0.25	9.63	5.00	5.00	0.67	0.34	0.34
	Injector Assembly	1	2.16	4.45	4.92	5.05	7.52	4.13	4.19
	Bi-propellant Valve	1	4.53	2.25	4.56	4.14	11.23	8.08	7.61
	Thrust Mount	1	1.88	6.44	5.05	4.94	12.35	8.21	8.26
	Gimbal Ring	1	1.96	7.93	5.00	5.00	23.17	12.03	11.54
	Gimbal Bearing--Bolts	2	0.27	7.93	5.00	5.00	2.80	2.80	0.03
	Pivot Assembly--Customer Attach	2	0.58	7.90	5.01	5.00	10.73	0.35	10.55
	Pressure Transducer	1	0.10	3.54	6.08	6.16	0.03	--	0.03
	Miscellaneous & Attach Parts	--	0.91	4.51	4.89	5.07	4.40	3.34	3.41
							Product of	Inertia (About C.G.)	
							P_x	P_y	P_z
							+1.45	+16.36	+8.69

MODEL Modified RS-2101A

REPORT NO. SR 1112-4002

DATE 22 March 1971

PAGE 3 OF 5

	DESCRIPTION	NO. REQD	CURRENT WEIGHT-(LB)	CENTER OF GRAVITY (INCHES)			MOMENT OF INERTIA ABOUT C.G. (LB IN^2)		
				$\bar{X}$ ARM	$\bar{Y}$ ARM	$\bar{Z}$ ARM	I_X (ROLL)	I_Y (PITCH)	I_Z (YAW)
1	2	3	4	5	6	7	8	9	10
	Engine Assembly--Yaw Condition	1	(15.31)	6.44	4.86	4.76	84.89	400.19	396.25
	Thrust Chamber	1	2.78	7.08	5.00	5.00	8.72	8.07	8.07
	Nozzle Extension	1	2.40	15.66	5.00	5.00	34.58	62.12	62.12
	Nozzle Attach Flange	1	0.14	9.28	5.00	5.00	0.34	0.17	0.17
	Nozzle Attach Nut	1	0.25	9.63	5.00	5.00	0.67	0.34	0.34
	Injector Assembly	1	2.16	4.45	4.92	5.05	7.52	4.13	4.19
	Bi-propellant Valve	1	4.53	2.25	4.56	4.14	11.23	8.08	7.61
	Thrust Mount	1	1.88	6.44	5.05	4.94	12.35	8.21	8.26
	Gimbal Bearing--Bolts-Partial	--	0.16	7.93	5.00	4.99	1.64	1.64	0.01
	Pressure Transducer	1	0.10	3.54	6.08	6.16	0.03	----	0.03
	Miscellaneous & Attach Parts	--	0.91	4.51	4.89	5.07	4.40	3.34	3.41

MOMENT OF INERTIA ABOUT GIMBAL AXIS
(Yaw Condition Minimum)

I_{xx} = 86.05 lb-in.^{2} I_{yy} = 435.06 lb-in.^{2} I_{zz} = 430.57 lb-in.^{2}

	Engine Assembly--Pitch Condition	1	(17.55)	6.63	4.88	4.79	112.24	417.84	415.11
	Thrust Chamber	1	2.78	7.08	5.00	5.00	8.72	8.07	8.07
	Nozzle Extension	1	2.40	15.66	5.00	5.00	34.58	62.12	62.12
	Nozzle Attach Flange	1	0.14	9.28	5.00	5.00	0.34	0.17	0.17
	Nozzle Attach Nut	1	0.25	9.63	5.00	5.00	0.67	0.34	0.34
	Injector Assembly	1	2.16	4.45	4.92	5.05	7.52	4.13	4.19
	Bi-propellant Valve	1	4.53	2.25	4.56	4.14	11.23	8.08	7.61
	Thrust Mount	1	1.88	6.44	5.05	4.94	12.35	8.21	8.26
	Gimbal Ring	1	1.96	7.93	5.00	5.00	23.17	12.03	11.54
	Gimbal Bearing--Bolts	2	0.27	7.93	5.00	5.00	2.80	2.80	0.03
	Pivot Assembly--Partial	--	0.17	7.93	5.01	5.00	2.89	0.01	2.89
	Pressure Transducer	1	0.10	3.54	6.08	6.16	0.03	--	0.03
	Miscellaneous & Attach Parts	--	0.91	4.51	4.89	5.07	4.40	3.34	3.41

MOMENT OF INERTIA ABOUT GIMBAL AXES
(Pitch Condition Maximum)

I_{xx}= 113.27 lb-in.^{2} I_{yy} = 448.27 lb-in.^{2} I_{zz} = 445.02 lb-in.^{2}

ENGINE REFERENCE AXES